

# Targeting antibody secreting B cells as a novel therapeutic approach to treat allergic diseases

vorgelegt von

Master of Science (Biotechnology)

Kiran Kumar Mudnakudu Nagaraju

Mysore, India

Von der Fakultät II - Mathematik und Naturwissenschaften

der Technischen Universität Berlin

zur Erlangung des akademischen Grades

Doktor der Naturwissenschaften

**Dr. rer. nat.**

genehmigte Dissertation

Promotionsausschuss:

Vorsitzender: Prof. Dr. rer. nat. Thomas Friedrich

Gutachterin: Prof. Dr. med. Margitta Worm (Charité Mitte)

Gutachter: Prof. Dr. rer. nat. Roderich Süßmuth

Tag der wissenschaftlichen Aussprache: 08 July 2014

Berlin 2014

D 83

## Table of Contents

<b>1. ABBREVIATIONS.....</b>	<b>1</b>
<b>1. ABSTRACT.....</b>	<b>5</b>
<b>2. ZUSAMMENFASSUNG.....</b>	<b>6</b>
<b>3. INTRODUCTION.....</b>	<b>7</b>
<b>3.1. Allergy and Atopy.....</b>	<b>7</b>
3.1.1. <i>Epidemiology</i> .....	7
3.1.2. <i>Type-1 hypersensitivity reaction</i> .....	7
<b>3.2. Atopic Dermatitis.....</b>	<b>9</b>
3.2.1. <i>Epidemiology</i> .....	9
3.2.2. <i>Skin barrier</i> .....	9
3.2.3. <i>Pathophysiology of atopic dermatitis</i> .....	10
3.2.4. <i>Therapeutic approaches in atopic dermatitis</i> .....	12
3.2.5. <i>Mouse models of atopic dermatitis</i> .....	13
<b>3.3. Food Allergy.....</b>	<b>14</b>
3.3.1. <i>Epidemiology</i> .....	14
3.3.2. <i>Oral tolerance</i> .....	14
3.3.3. <i>Pathophysiology of food allergy</i> .....	14
3.3.4. <i>Therapeutic approaches in food allergy</i> .....	15
3.3.5. <i>Mouse models of food allergy</i> .....	16
<b>3.4. Proteasome and Bortezomib.....</b>	<b>18</b>
3.4.1. <i>Proteasome</i> .....	18
3.4.2. <i>Bortezomib and its therapeutic implications</i> .....	20
<b>4. OBJECTIVES.....</b>	<b>21</b>
<b>5. MATERIALS AND METHODS.....</b>	<b>22</b>
<b>5.1. MATERIALS.....</b>	<b>22</b>
5.1.1. <i>Antibodies</i> .....	22
5.1.2. <i>Buffers and solutions</i> .....	24
5.1.3. <i>Reagents</i> .....	26
5.1.4. <i>Lab ware</i> .....	27
5.1.5. <i>Technical equipment</i> .....	28
5.1.6. <i>Software</i> .....	29
<b>5.2. METHODS.....</b>	<b>30</b>
<b>5.2.1. Animal experiments.....</b>	<b>30</b>
5.2.1.1. <i>Animal work</i> .....	30
5.2.1.2. <i>Mouse model of allergen-induced eczema</i> .....	30
5.2.1.3. <i>Assessment of atopic eczema symptoms</i> .....	31
5.2.1.4. <i>Mouse model of hazelnut-induced intestinal anaphylaxis</i> .....	31
5.2.1.5. <i>Assessment of hazelnut-induced intestinal anaphylactic symptoms</i> .....	33
5.2.2. <i>Preparation of hazelnut extract</i> .....	33
5.2.3. <i>Cell and/or organ culture methods</i> .....	33

5.2.3.1. Mouse splenocyte and lymph node cell isolation.....	33
5.2.3.2. Skin biopsy culture.....	34
5.2.3.3. Culture conditions.....	34
<b>5.2.4. Immunological methods.....</b>	<b>34</b>
5.2.4.1. Enzyme-linked immunosorbent assay (ELISA).....	34
5.2.4.2. Murine immunoglobulin ELISA.....	35
5.2.4.3. Enzyme-linked immunospot (ELISpot).....	36
5.2.4.4. Western blot.....	37
5.2.4.5. Principles of flow cytometry.....	37
5.2.4.6. Flow cytometric analysis of T- and B-cells.....	38
5.2.4.7. Flow cytometric analysis of plasma cells.....	38
<b>5.2.5. Immunohistochemistry.....</b>	<b>39</b>
5.2.5.1. Staining of cellular infiltrates in the lesional skin of atopic eczema mouse.....	39
5.2.5.2. Staining of cellular infiltrates in the jejunum of food allergy mouse.....	39
5.2.5.3. Histological analyses.....	40
<b>5.2.6. Molecular biology methods.....</b>	<b>40</b>
5.2.6.1. RNA isolation from murine skin and jejunum.....	40
5.2.6.2. cDNA synthesis.....	40
5.2.6.3. Real-time PCR/quantitative PCR.....	41
<b>5.2.7. Statistical analyses.....</b>	<b>42</b>
<b>6. RESULTS.....</b>	<b>43</b>
6.1. Clinical severity remained unchanged upon bortezomib treatment in an atopic eczema mouse.....	43
6.2. Establishment of oral-induced intestinal anaphylaxis in mice.....	43
6.3. Comparative analysis of IgE/binding patterns from human and mouse serum.....	46
6.4 Bortezomib treatment ameliorates hazelnut-induced intestinal anaphylaxis in mice.....	48
6.5. Reduction of plasma cells by proteasome inhibitor in AD and FA murine models.....	48
6.6. Reduction of humoral immune response upon bortezomib treatment.....	51
6.7. T- and B- cell subsets upon treatment with bortezomib.....	54
6.8. Interference with the local inflammatory cells.....	56
6.9. Altered expression of genes in intestinal jejunum of FA mouse upon bortezomib treatment.....	59
6.10. Abolished skin barrier gene expression.....	60
<b>7. DISSCUSSION.....</b>	<b>62</b>
7.1. Bortezomib strongly interferes with immune response without affecting skin eczema in AD mouse.....	62
7.2. Bortezomib treatment ameliorates hazelnut allergen-induced intestinal anaphylaxis in mice.....	66
<b>8. BIBILOGRAPHY.....</b>	<b>71</b>
<b>9. ACKNOWLEDGEMENT.....</b>	<b>85</b>
<b>10. PUBLICATIONS.....</b>	<b>86</b>

**1. ABBREVIATIONS**

AD	Atopic Dermatitis
AE	atopic eczema
Ag	antigen
alum	aluminium hydroxide and magnesium hydroxide
AMP	antimicrobial peptide
anti	antibody
AP	alkaline phosphatase
APC	allophycocyanin or antigen presenting cell
ASC's	antibody secreting cells
AU	arbitrary units
BALB/c	a mouse strain
BCL6	B cell lymphoma 6
BLIMP1	B lymphocyte-induced maturation protein 1
bio	biotinylated
bp	base pair (only with numbers)
BSA	bovine serum albumin
Bz	bortezomib
CCL	CC chemokine ligand
CCR	CC chemokine receptor
CCS	charcoal stripped fetal calf serum
CD	cluster of differentiation
cDNA	complementary DNA
CE	cornified envelope
CSR	class switch recombination
CT/CP	threshold cycle value/crossing point
d	day(s); deoxy; distilled (as in dH <sub>2</sub> O)
DC	dendritic cell
DMF	<i>N,N</i> -dimethylformamide
DMSO	dimethylsulfoxide
DNA	deoxyribonucleic acid

DNase	deoxyribonuclease
ds	double-stranded (as dsDNA)
e.c.	epicutaneous
EDTA	ethylenediaminetetraacetic acid
ELISA	enzyme-linked immunosorbent assay
ELISpot	enzyme-linked immunospot
ER	endoplasmic reticulum
FA	Food allergy
FACS	fluorescence-activated cell sorting
FCS	fetal calf serum
FcεR	receptor for IgE (FcεRI high affinity/ FcεRII (CD23) low affinity)
FITC	fluorescein isothiocyanate
FL	fluorescence
FO	follicular zone
FSC	forward scatter channel
<i>g</i>	acceleration of gravity
h	hour (only with numbers)
HE	hematoxylin and eosin
HN	hazelnut
HPRT	hypoxanthine-guanine phosphoribosyltransferase
HRP	horseradish peroxidase
IFN	interferon (e.g., IFN- $\gamma$ )
Ig	immunoglobulin (also IgA, IgD, IgE, IgG, IgM)
i.g.	intra-gastrical
I $\kappa$ B	inhibitor of NF- $\kappa$ B
IL	interleukin (e.g., IL-4, IL-33)
i.p.	intra-peritoneal
i.v.	intra-venous
kb	kilobase (only with numbers)
Kd	distribution coefficient; dissociation constant; kilo-dalton
kg	kilogram
L	ligand

LAGeSo	State Office of Health and Social Affairs
LU	laboratory unit
mAb	monoclonal antibody
MACS	magnetic-activated cell sorting
MAPK	mitogen-activated protein kinase
MFI	median fluorescence intensity
mg	milligram (only with numbers)
MHC	major histocompatibility complex
min	minute (only with numbers)
ml	milliliter (only with numbers)
MP	milk powder
mRNA	messenger RNA
MZ	marginal zone
n	number in study or group
n.d.	not detectable
n.s.	not significant
NF- $\kappa$ B	nuclear factor $\kappa$ B
N-terminus	amino terminus or NH <sub>2</sub> -terminus
OVA	ovalbumin
PBMC	peripheral blood mononuclear cell
PBS	phosphate-buffered saline
PBS-T	PBS with Tween20
PC	plasma cells
PCR	polymerase chain reaction
PE	phycoerythrin
PerCP	peridinin-chlorophyll proteins
PI	propidium iodide; proteasome inhibitor; proteasome inhibition
<i>p</i> NPP	<i>para</i> -nitrophenylphosphate
qPCR	quantitative PCR
r	recombinant (e.g., rIL4)
RBC	red blood cell

RNA	ribonucleic acid
RNase	ribonuclease
RT	room temperature; reverse transcriptase
s	second (use only with numbers)
<i>S. aureus</i>	<i>Staphylococcus aureus</i>
s.c.	subcutaneous
SEM	standard error of the mean
SSC	side scatter channel
TBS	Tris-buffered saline
TBS-T	TBS with Tween 20
TGF	transforming growth factor
TH cell	T helper cell
TLR	Toll-like receptor
TMB	3,3',5,5'-tetramethylbenzidine
TNF	tumor necrosis factor (e.g., TNF $\alpha$ )
TNP	trinitrophenyl
Treg	regulatory T cell
Tris	tris(hydroxymethyl)aminomethane
TSLP	thymic stromal lymphopoietin
UV	ultraviolet
wk	week (only with numbers)
$\beta$ -ME	$\beta$ -mercaptoethanol
$\mu$ g	microgram (only with numbers)
$\mu$ l	microliter (only with numbers)
7-ADD	7-amino-actinomycin D

## 1. ABSTRACT

Allergic diseases, which encompass atopic dermatitis and food allergy, are steadily increasing and characterised by a deviated immune response towards harmless antigens. The underlying pathophysiology is complex. Plasma cells secrete immunoglobulins of which IgE play a central role in immediate allergy. Proteasome inhibitors have been shown to target plasma cells and thereby eliminate immunoglobulins.

The objective of this thesis is to deplete plasma cells by proteasomal inhibition and to examine the consequences on the systemic and local immune response in murine models of allergy. Two different allergen-driven mouse models of allergy were applied, which display allergic symptoms caused by a deviated immune response. One of the models involves the skin and the other one the gastrointestinal mucosa as sites of the allergic response. The administration of the proteasomal inhibitor bortezomib *in vivo* in a mouse with allergen-induced atopic eczema led to a profound reduction of plasma cells thereby inhibiting the systemic IgE response but also IgG1 and IgA, although to a much lesser extent. Skin homing T cells were also largely reduced, but without improving the clinical severity. In contrast, in the newly established food allergy model intestinal anaphylactic symptoms in mice were alleviated and accordingly B cell subsets including plasma cells, but also systemic IgE and to some magnitude IgG1 were also significantly reduced after proteasomal inhibition.

In conclusion, bortezomib treatment leads to a strong reduction of plasma cells and consecutively the humoral immune response in both allergy models. The data indicates a different pathophysiological role of IgE in the two allergy models. In the skin, the local inflammatory response plays a major role to mount the eczematous skin reaction, whereas IgE-dependent mast cell activation seems to play a central role in the gastrointestinal mediated allergy. Taken together, the results demonstrate that targeting antibody-secreting B cells by bortezomib as a new therapeutic approach to treat gastrointestinal, but most likely not skin related allergic diseases.

## **2. ZUSAMMENFASSUNG**

Allergische Erkrankungen haben in den letzten Jahrzehnten stetig zugenommen. Sie können sich an verschiedenen Organsystemen manifestieren, zu den häufigsten gehören die atopische Dermatitis und die Nahrungsmittelallergie. Allergien sind charakterisiert durch eine immunologisch vermittelte Überempfindlichkeit gegenüber harmlosen Antigenen. Die zugrunde liegende Pathophysiologie ist komplex und umfasst zahlreiche Effektorzellen und Moleküle. Plasmazellen produzieren Immunglobulin E, welches eine zentrale Rolle bei der Typ I Allergie spielt. Eine Möglichkeit Plasmazellen zu eliminieren, besteht über die Anwendung von Proteaseinhibitoren, somit könnten auch Immunglobuline eliminiert werden.

Ziel der vorgelegten Arbeit ist es Plasmazellen durch Hemmung des Proteasoms zu beeinflussen und die systemischen und lokalen Auswirkungen auf die allergische Immunantwort in Mausmodellen zu untersuchen. Zwei Allergiemodelle mit Manifestation an der Haut und des Gastrointestinaltraktes wurden untersucht.

Die Ergebnisse zeigen, dass nach Verabreichung des Proteasominhibitors Bortezomib in einem mit Allergen abhängig auftretendem Hautekzem Plasmazellen vermindert wurden und die systemische IgE aber auch IgG1- und IgA-Antwort reduziert war. Darüber hinaus waren T-Zellen in der Haut vermindert, jedoch fand sich kein Einfluss auf den klinischen Ausprägungsgrad.

Dagegen wurde in einem im Rahmen dieser Arbeit neu etablierten Nahrungsmittelallergiemodell nach Gabe von Bortezomib sowohl die klinischen Symptome als auch die B-Zellsubpopulationen einschließlich Plasmazellen und die systemische Immunantwort reduziert.

Zusammenfassend zeigen die vorgelegten Daten, dass durch eine Hemmung des Proteasoms Plasmazellen stark reduziert werden und in der Folge die humorale Immunantwort vermindert ist. Während in der Haut nach der Behandlung mit Bortezomib keine klinischen Veränderungen trotz der verminderten humoralen Immunantwort messbar waren, konnte in dem gastrointestinalen Allergiemodell nicht nur ein signifikanter Rückgang der humoralen Immunantwort sondern auch der klinischen Symptome beobachtet werden.

Schließlich zeigen die Ergebnisse, dass durch Elimination Antikörper produzierender B-Zellen allergische Erkrankungen, die sich am Gastrointestinaltrakt abspielen, wie die Nahrungsmittelallergie, jedoch nicht das atopische Ekzem beeinflussen lassen.

### 3. INTRODUCTION

#### 3.1. Allergy and Atopy

The term ‘*allergy*’ (meaning- *allos*, other, *ergon*, reaction) was introduced in 18<sup>th</sup> century by Clemens von Pirquet (1906), an Viennese pediatrician<sup>1</sup>. In 1923, Coca and Cooke defined the term ‘*atopy*’ (meaning *ἀτοπία* - special, unusual, extraordinary)<sup>2</sup>. They described this phenomenon of hypersensitivity marked by immediate wheal reactions in the skin and its association with allergic manifestations such as asthma, hay fever and eczema<sup>2</sup>. In spite of the fact that knowledge about ‘*eczema*’ and ‘*allergy*’ was limited until 19<sup>th</sup> century, only in the recent few decades there has been a strong increase in the number of publications on allergic diseases due to its rising incidences and prevalence.

##### 3.1.1. Epidemiology

Atopy refers to a state of ‘hyperallergic’ and/or IgE-mediated hypersensitivity reaction<sup>3</sup>. Over the past several years, incidence of atopic diseases such as atopic dermatitis, allergic rhinitis, allergic asthma and food allergy have been increasing<sup>3</sup>. The development of specific IgE against environmental and/or food allergens have been shown to be a characteristic feature of atopic diseases<sup>3,4</sup>. In addition, genetic<sup>5,6</sup>, epigenetic<sup>7,8</sup>, microbial burden<sup>9</sup>, nutrition<sup>10</sup>, immunological and barrier defects<sup>11</sup> are contributing factors for the increase of allergic diseases in industrialized nations. Today, up to 20 to 25% of the general population are affected<sup>12,13</sup>. Atopic diseases start often early in childhood of an individual and tend to persist for a longer time in their life<sup>14</sup>. Reports so far suggest that atopic diseases start with food allergy and atopic eczema in children progressing to allergic asthma or rhinitis in adults– a phenomenon entitled as the “atopic march”<sup>12,14</sup>.

##### 3.1.2. Type-1 hypersensitivity reaction

In general, allergy refers to a hypersensitivity disorder of the immune system<sup>3</sup>. For instance, various harmless substances (known as antigens or allergens) in the environment can cause allergic reactions<sup>3,15</sup>. Allergens are categorized into two subgroups; Type-1 allergens are non-infectious proteins that bind to IgE molecule and induce T<sub>H</sub>2 cell mediated immune responses causing allergic rhinitis, systemic reactions (anaphylaxis), food allergies and allergic asthma<sup>3</sup>. Type 2 allergens are non-infectious environmental small molecules that cause T-cell dependent immune responses leading to local inflammation, without the involvement of IgE (in case of contact dermatitis)<sup>3</sup>.

Type-1 hypersensitivity involves the immediate, and late-phase reaction<sup>3,16</sup>. The immediate reaction occurs minutes after allergen exposure and includes the release of vasoactive amines and lipid mediators<sup>3,16</sup>. During the late-phase reaction leukotrienes and cytokines are released. It occurs 2-4 h after the initial allergen exposure<sup>3,16</sup>. The latter reaction recruits a variety of immune cells including T cells, eosinophils, basophils and leukocytes. Repeated re-exposure to the same allergen in the previously sensitized allergic individuals promotes chronic inflammation<sup>3,16</sup>.

The pathophysiology of a type-I allergic reaction involves a sensitisation and elicitation phase (Figure 1<sup>17</sup>). During the sensitization phase, the allergen induces specific T-cell clonal expansion in periphery. Upon re-exposure to the same allergen latter on allergen specific CD4<sup>+</sup> T<sub>H</sub>2 cells produce IL-4 and IL-13<sup>3,16,17,18</sup> (Figure 1a). These cytokines induces class switching to the epsilon (ε) heavy chain<sup>19</sup>. This class switched IgE memory B-cells secretes specific antibodies against allergens (Figure 1b).

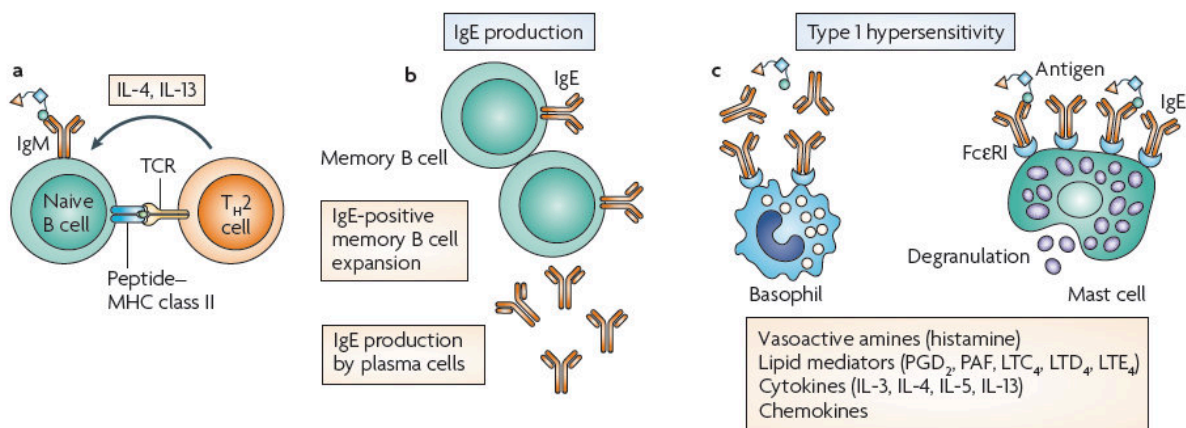


**Figure 1 Sensitisation and elicitation of the IgE dependent immune response (detailed explanation in the text and the permission has been obtained to reuse this figure)<sup>17</sup>.**

These antibody-secreting B-cells migrate to the bone marrow and/or lymphoid tissues, where IgE is continuously produced<sup>17,18,19</sup>. Circulating IgE binds to mast cells and basophils through FcεR1. Upon allergen re-exposure, cross linking of IgE by allergens on the surface of mast cells<sup>3,16,17,18,19</sup> and/or blood basophils in periphery via FcεR1α receptor (Figure 1c) leads to degranulation and release of pre-stored and newly formed inflammatory mediators. These are histamine, serotonin, PAF (platelet-activating factors), leukotriene (LTC<sub>4</sub> and LTD<sub>4</sub>), prostaglandins, heparin, proteases, cytokines and chemokines, which elicit the allergic reaction<sup>3,16,17,18,19</sup>.

## **3.2. Atopic Dermatitis**

### ***3.2.1. Epidemiology***

Atopic dermatitis (AD) is a chronic relapsing, eczematous skin disease that is characterized by erythema, edema, excoriations, xerosis and marked pruritis<sup>20</sup>. Frequently AD starts early in childhood (early-onset AD) and is often associated with food allergy and asthma<sup>20,21</sup>. Environmental factors and modern life style has been much debated to play a role in the development of AD<sup>21</sup>. There has been an increase of the AD prevalence in the last decades, affecting 10-20% of children and 1-3% of adults worldwide<sup>20,22</sup>. AD is classified into the extrinsic and intrinsic type, of which 70-80% are extrinsic AD<sup>23-25</sup>. In this type, patients show an increased IgE level in the serum to environmental or food allergens<sup>24,25</sup>, whereas the remaining 20-30% belong to the intrinsic AD type possessing low or no serum IgE antibodies<sup>24</sup>.

### ***3.2.2. Skin barrier***

The skin acts as an important barrier in regulating the entry of microbes and environmental allergens<sup>20,26</sup>. The cornified layer (stratum corneum) represents the outermost layer of the epidermal barrier consisting of dead cells, corneocytes and the cornified envelope (Figure 2<sup>26</sup>). The cornified envelope controls the physical barrier integrity by cross-linking matrix associated lipids and structural proteins (like loricrin, involucrin, pro-filaggrin, small proline-rich proteins and S100A) which are necessary to reduce water loss but also the penetration of allergens and microbes into the skin<sup>26</sup>. Below the cornified envelope upper granular, granular, spinous, basal and basal lamina layers constitute the epidermis of the skin (Figure 2)<sup>26</sup>. These layers are characterized by the expression of barrier proteins like transglutaminases (type-1,-2,-3,-5)<sup>26,27</sup>, keratin (type-1,-2,-5,-9,-10,-14)<sup>26</sup>, desmoglein (type-1,-2,-3,-4)<sup>26</sup> and many others<sup>26</sup>. These and other proteins are cross-linked along with transglutaminases to form the cornified envelope<sup>26</sup>.

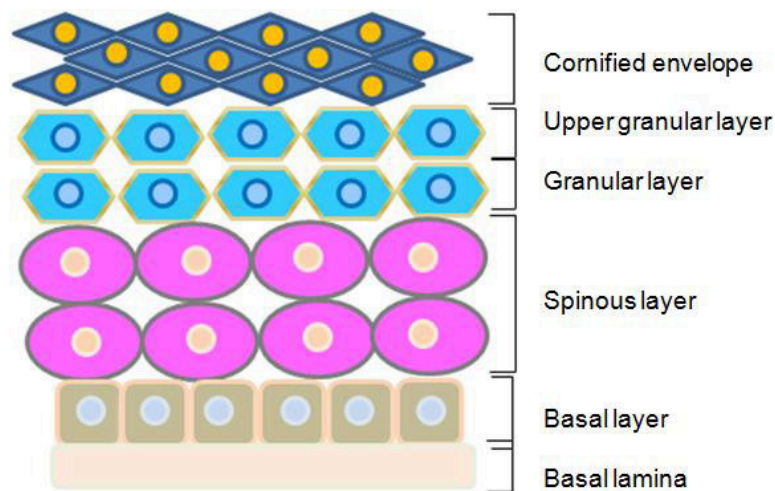


**Figure 2 Epidermal differentiation of the skin (detailed explanation in the text and the figure is modified<sup>26</sup>)**

### ***3.2.3. Pathophysiology of atopic dermatitis***

The understanding of the (immune) etiology of AD is still not completely unravelled, especially with regards to the chronological sequence of the pathophysiological molecular events<sup>28,29</sup>. It's been controversial whether the disease arises rather from a misguided immune system or is due to constitutive defects in the skin itself or both<sup>20-22,28,29</sup>. Overall, AD is associated with multiple mutations in genes regulating skin barrier, innate and adaptive immune response<sup>30</sup>.

AD patients can have defects in the skin barrier (Figure 3)<sup>30</sup>, which leads to increased water loss and penetration of chemical pollutants, allergens and microbes<sup>20-22,28-30</sup>. In addition, the local immune reaction of the skin (Figure 3)<sup>30</sup> is associated with the ability to respond appropriately to bacteria, fungi and other microbes<sup>22,30</sup>. Recent reports suggest that defects in the skin barrier promote the development of skin inflammation in AD patients<sup>31-33</sup>. The inflammation in AD skin leads to transepidermal water loss<sup>29</sup> followed by a defective terminal keratinocyte differentiation. This leads to a reduction of ceramides<sup>34</sup>, filaggrin (FLG)<sup>35</sup> and antimicrobial peptides (AMP)<sup>36</sup> in the AD skin. Recently, a loss-of-function mutation of the FLG gene has been shown as a predisposing factor in the development of AD (in case of extrinsic type)<sup>35,37-42</sup>. FLG gene deficiency has shown to increase dryness of the skin of AD patients<sup>41</sup>. A number of cytokines such as interleukin (IL) -4, -13, -25 and TNF have been reported to reduce filaggrin expression in AD skin<sup>43-45</sup>. Apart from FLG deficiency, mice with claudin1 (CLDN1, a key tight junction protein) deficiency died within a day due to increased dehydration as a consequence of following the increased epidermal

permeability and transepidermal water loss<sup>46</sup>. Also the other barrier proteins have been described to be altered in AD patients<sup>30,36,47,48</sup>. In human AD patients, profiling of CLDN-1 and CLDN-23 expression was strikingly reduced in non-lesional skin of extrinsic AD<sup>47</sup>. Other studies have shown that loricrin and involucrin are decreased in the AD skin<sup>48</sup>. Finally, also a reduced expression of antimicrobial peptides such as S100 proteins, defensins and cathelicidins has been reported in AD patients<sup>30,36</sup> (Figure 3).

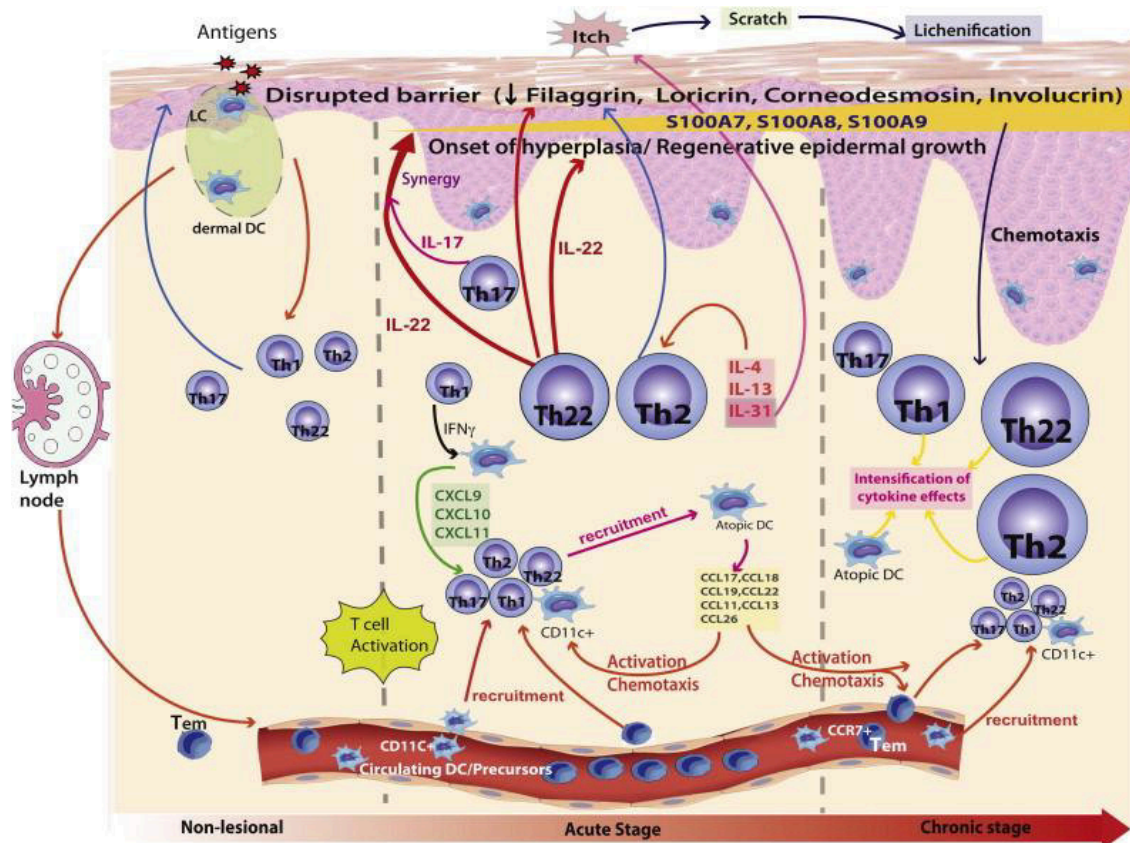


**Figure 3** Interplay between the disturbed skin barrier and the T-cell dominated skin inflammation<sup>30</sup> (detailed explanation in the text and obtained permission to reuse this figure here).

Apart from skin barrier defects studies proved that highly diversified interactions of many immune cells are a hallmark of AD. T-cells are of major significance for the disease development (Figure 3)<sup>30</sup>. Based on a number of experimental and clinical observations, AD lesions mostly show a pronounced T-cell infiltration<sup>21,22,30</sup>. Evidence from both mouse and human studies suggests that CD4<sup>+</sup> effector T cells are primarily important for the development of AD<sup>20-22,49</sup>. AD patients often have a predisposition to develop a T<sub>H</sub>2- as opposed to a T<sub>H</sub>1-(or Treg) response<sup>21,22,30</sup>. Such polarization of T cells into the T<sub>H</sub>2

phenotype has been observed in acute AD skin lesion which is characterized by cytokines IL-4, -5 and -13. A T<sub>H</sub>1 cell dominated immune response is observed in chronic AD skin inflammation<sup>20-22,30,50</sup>. Several other reports indicate that also other T-cell phenotypes such as T-regulatory (T-regs), T<sub>H</sub>17, T<sub>H</sub>9 as well as T<sub>H</sub>22 cells are involved in the AD pathogenesis<sup>30,51</sup>, but their exact role in the AD inflammation is still controversial. The central role of T-cells is further supported by findings showing that T-cell-deficient (SCID) mice do not develop AD, but become capable to develop AD after adoptive transfer of human PBMC<sup>52,53</sup>. Correspondingly, T-cell directed therapies (for example with the calcineurin inhibitor tacrolimus) have shown excellent therapeutic results<sup>54,55</sup>.

Although T cells are numerically more pronounced in the skin lesions of AD patients, B cell infiltrates can also be detected<sup>56-59</sup>. Recently, it has also been reported that B cell driven CD19 expression contributes to a greater extent to AD pathogenesis<sup>59</sup>. However, overall the knowledge about the role of B cells for the generation and maintenance of AD is still not well understood.

### ***3.2.4. Therapeutic approaches of atopic dermatitis***

AD is a chronic inflammatory skin disorder and current therapies aim to suppress clinical symptoms due to severe inflammation<sup>60</sup>. Currently there is no available treatment to cure AD. The treatment approaches of AD in clinics consist several anti-inflammatory strategies including phototherapy, topical and systemic treatment, corticosteroids and calcineurin inhibitors<sup>60</sup>. These therapeutic drugs provide a temporary relief, but do not serve a long term treatment option to cure this condition<sup>60</sup>. Novel approaches for AD therapy in humans are considered to target defects in skin barrier, adaptive and innate immunity.

Depletion of B cells using rituximab (anti-CD20 antibody) in AD patients showed an immediate decrease of inflammation in the lesional skin<sup>57</sup>. In this study B cell numbers were slightly reduced in the skin and to a much higher extent in the blood, followed by decrease in activated T cells along with reduced IL-5 and -13 cytokine secretion<sup>57</sup>. Another treatment possibility is to reduce and/or abolish IgE, as 80% of AD patients show higher total and specific IgE levels<sup>61</sup>. The anti-IgE (omalizumab) treatment in AD patients revealed a reduction of FcεR1 expression from blood and skin cells as well as decreased serum free IgE<sup>61</sup>. Also, numbers of IgE<sup>+</sup> bearing dendritic cells in the skin were reduced<sup>62</sup>. Several reports rather speak against the therapeutic effect of omalizumab in AD treatment due to limited clinical efficacy and its potential side effects which includes anaphylaxis, headache, viral infection and urticaria<sup>62</sup>.

### 3.2.5. Mouse models of atopic dermatitis

Several mouse models have been used to better understand the pathogenesis of AD. Features of murine AD models can be grouped into three main types: (1) applying sensitizers/antigens epicutaneously (e.c.); (2) knockout/transgenic mice that lacks/overexpress specific genes; and (3) spontaneous development of AD-like lesions in genetically defined mice<sup>49</sup>.

As mouse model 1 has also been used in this thesis, it will be described in more detail in the following paragraph. In this model, AD is induced by skin injury and e.c. ovalbumin (OVA, chicken allergen) sensitization in a Balb/c or C57BL/6 mouse strain<sup>63</sup>. The repeated epicutaneous allergen sensitization induces skin inflammation followed by scratching, dermal and epidermal thickening, accumulation of CD4<sup>+</sup> T cells and eosinophils, followed by upregulation of T<sub>H</sub>2 cytokines IL-4, -5, and -13<sup>63</sup>. In addition, the expression of eotaxin, chemokine receptor 3 (CCR3, enhances eosinophil migration to the skin), and CCR4 (increases CD4<sup>+</sup> T cell infiltrates in the skin) in the inflammatory skin is enhanced<sup>63</sup>. OVA-specific IgE, IgG1 and IgG2a levels are increased in the serum and *in vitro* re-stimulation of splenocytes with OVA show increased levels of IL-4, -5, -13 and IFN- $\gamma$ <sup>63</sup>.

Also, mice deficient in IL-4, -5, -10, -17, IFN- $\gamma$ , CCR3 and CCR4 have been tested for their role in inducing skin inflammation in the e.c. sensitization model<sup>49,64-66</sup>. Interestingly, IL-4<sup>-/-</sup> and -5<sup>-/-</sup> mice display a decreased eosinophil migration into the OVA-sensitized skin<sup>49</sup>. IFN- $\gamma$ <sup>-/-</sup> mice show a reduction in the dermal thickening in the lesional skin of OVA-sensitized mice<sup>67</sup>. Laouini et al. (2003)<sup>65</sup> further demonstrated that IL-10<sup>-/-</sup> mice show a reduction of the infiltration of eosinophils as well as a decreased expression of eotaxin, IL-4 and -5 mRNA in the lesional skin. In addition, eosinophil infiltration into the inflammatory skin of e.c. sensitized mice was abolished in CCR3<sup>-/-</sup> mice<sup>66</sup> whereas CD4<sup>+</sup> T cells migration was severely impaired in lesional skin of CCR4<sup>-/-</sup> mice<sup>66</sup>. Similar to OVA e.c. sensitization model, recombinant house dust mite allergen (Der p8)<sup>68</sup> and the superantigen staphylococcal enterotoxin B (SEB)<sup>69</sup> was epicutaneously applied in murine models which displayed characteristic features of AD symptoms.

Transgenic mice (Tg) models over-expressing IL-4<sup>70</sup>, IL-31<sup>71</sup>, thymic stromal lymphopoietin (TSLP)<sup>72</sup>, caspase-1<sup>73</sup>, and IL-18<sup>73-75</sup> have also been used to study their relevant role in inducing skin inflammation in AD. Skin of IL-4Tg<sup>70</sup> and IL-31Tg<sup>71</sup> mice spontaneously develop pruritus and chronic dermatitis, followed by dense T cells infiltration. TSLPTg<sup>72</sup> mice on Balb/c background express skin-specific TSLP (regulated by kertain-5 promoter) and show similar characteristic features to that of IL-4Tg mice<sup>70</sup>. Furthermore, caspase-1-

transgenic (CASPI1Tg)<sup>73</sup> and IL-18Tg mice<sup>74,75</sup> show AD symptoms, followed by elevated plasma histamine and increased migration of neutrophils in the skin including T<sub>H</sub>2 immune response in the spleen.

Overall all these murine AD models have contributed to a better understanding of complex disease.

### **3.3. Food Allergy**

#### ***3.3.1. Epidemiology***

Food allergy has developed in the recent decades to an increasing health problem in industrialized countries, affecting 6% of children and 1-3% of adults<sup>76,77</sup>. The major eight foods causing allergies stated by World Health Organization (WHO) and Food Agricultural Organization (FAO) include hazelnut, peanut, egg, milk, fish, shellfish, soy and celery<sup>78</sup>.

#### ***3.3.2. Oral tolerance***

Food antigens that pass through the gut system can be defended by the innate and adaptive immunity, which are governed by numerous genes<sup>79</sup>. A person normally consumes about 100 kg protein/year, which passes through the intestine of a single individual. Normally these food proteins cause no harmful immune response, a phenomenon known as oral tolerance<sup>80-82</sup>. Tolerance is characterized by anergy or apoptosis of antigen-specific T cells and the release of immunosuppressive cytokines (IL-10, TGF- $\beta$ ) by T-regulatory cells (T-regs)<sup>82</sup>. The former mechanism occurs at very high doses of antigen and seems to be crucial for various foods administered to physiological amounts<sup>83</sup>.

Two types of defence mechanisms are active, 1. immune exclusion – secretory IgA (sIgA) combats the migration of microorganisms through the epithelium and 2. immunosuppression through the release of anti-inflammatory cytokines<sup>79</sup>. These homeostatic conditions are necessary to avoid the adverse reactions to food allergens and to establish oral tolerance<sup>79,80,82</sup>.

#### ***3.3.3. Pathophysiology of food allergy***

A classical reaction to innocuous food antigens (or allergenic proteins) lacks homeostatic balance and has been associated with the hypersensitivity reaction in sensitized individuals<sup>76,77</sup>. Food allergens have specific structural characteristics, which consist of metal ions or carbohydrates at their catalytic site, also form aggregates in combination with lipids as well as show resistance to proteolytic digestion and heat denaturation<sup>78,83</sup>. The detailed

mechanism of food-induced type-1 hypersensitivity is explained in section 3.1.3 (page no. 9-10, paragraph 2).

The mediators released during the effector phase of allergic response causes a variable range of local as well as systemic symptoms and in severe cases, particularly with respect to anaphylactic shock may lead to the death of an individual<sup>76,77,84</sup>. However, the mild form of symptoms are more frequent and include one or more of the following characteristics: vomiting, diarrhea, difficulty in breathing, swelling of the face and throat, urticaria and oral allergy syndrome<sup>3,18,76,77,84</sup>.

#### ***3.3.4. Therapeutic approaches of food allergy***

Food allergy is often manifested by an abnormal humoral immune response causing mild to severe reactions<sup>76,77,85</sup>. Until now, there is no available remedy to treat and/or provide long term remission from FA. Hence, development of new therapies is needed. Allergen specific immunotherapy (SIT) with single food allergens as well as systemic treatment with specific and non-specific agents has been shown to be a possible approach to treat FA<sup>17,77</sup>. SIT aims to desensitize or induce tolerance to allergen exposure<sup>17,77</sup>. Protocols to desensitize through oral immunotherapy (OIT) and/or sublingual immunotherapy (SLIT) have been described<sup>17,77</sup>. The mechanisms of such protocols are not fully understood<sup>17</sup>. It is assumed that altered T cell responses to specific allergens and/or the enhancement of T-reg cells, a reduction of IgE bound to FcεR1 on mast cells or basophils, but also diminished effector cell responses including B cells and/or eosinophils are involved<sup>17</sup>. OIT with peanut (PN) leads to a decrease of PN specific-IgE and an increase of IgG4 and accordingly a decrease of basophil activation<sup>86</sup>. Although OIT and SLIT induce tolerance, its safety in general has not been clearly addressed<sup>77</sup>. Another treatment approach involves the usage of modified recombinant food proteins as vaccines<sup>88</sup>. These engineered food proteins are constructed with the aim to modify the binding capacity of IgE to antigens without affecting T cell response, mast cells and/or basophils. The proteins/allergens from fish, peanuts and apple have been engineered<sup>88</sup>. *In vitro* studies revealed that T cells from peanut allergic donors showed reduced proliferation capacity upon stimulation with recombinant peanut allergens (Ara h 1, 2, 3) and that IgE reactivity decreased significantly compared to the positive control<sup>89,90</sup>. Treatment of these modified recombinant peanut proteins (produced from heat-killed E.coli) in a peanut allergy mice model showed protection against anaphylaxis<sup>91</sup>. This study exhibited a significant decrease of IgE and T<sub>H</sub>2 cytokines<sup>91</sup>. Likewise various treatment approaches including peptide immunotherapy, immunostimulatory sequence-conjugated protein

immunotherapy and plasmid DNA immunotherapy in a murine model of peanut allergy showed clinical improvement as the outcome<sup>92-94</sup>. All these study used modified peanut Ara h 2 major allergen *in vivo*.

Also, non-specific therapies have been used in the treatment of food allergy<sup>95-101</sup>. Most cases of food allergy patients show an increase of IgE levels. Hence, anti-IgE therapy was designed as a potential treatment approach to suppress allergic symptoms. Several humanized monoclonal antibodies are available for clinical studies that identify and bind to fragment crystal (Fc) portion of the IgE molecule<sup>17,95-97</sup>. Omalizumab (anti-IgE, a recombinant DNA-derived humanized IgG1k monoclonal antibody) and another clone of anti-IgE TNX-901 antibodies have been used for the treatment of food allergy<sup>96,97</sup>.

Another treatment approach is Chinese herbal medicine (FAHF-2). This medicine has been shown positive results *in vitro*, but also in a mouse model of food allergy<sup>98-101</sup>. Although all these above mentioned approaches have provided some basic understanding of therapeutic possibilities, there has been still no proper remedy to treat food allergy<sup>77</sup>. Thus, there is a high need to investigate further approaches to treat food allergic diseases<sup>77</sup>.

### ***3.3.5. Mouse models of food allergy***

Due to its high risk of causing severe allergic reactions in humans, mouse models have been experimentally tested to address molecular events in the disease progression and its therapeutic targets to combat the allergic symptoms<sup>102</sup>. The evidence from literature suggests that food induced allergy mouse models closely mimic human food allergy<sup>103</sup>. There are other several major benefits to use mouse as a model animal to understand food allergy<sup>103</sup> i.e., 1. characterize specific inbred mouse strains, 2. genetic modification (by knockout/transgenic approach), 3. target specific approach (by using drugs, antibodies or cytokines therapeutically). So far several inbred mouse strains such as, BALB/c, C57/BL6, C3H/HeJ, and DBA/2 have been used to study food allergy<sup>103,104</sup>. However, BALB/c and C3H/HeJ mouse strains in common spontaneously developed systemic IgE and/or IgG1-mediated antibody response to allergens, which displayed typical T<sub>H</sub>2 skewing compared to other strains<sup>105</sup>. Also, using adjuvants [alum<sup>105</sup> or cholera toxin<sup>106</sup> (CT) or staphylococcal enterotoxin B<sup>107</sup> (SEB)] via intraperitoneal (i.p.), intragastric (i.g.), oral, nasal, and cutaneous routes are used to promote the T<sub>H</sub>2 response in these mice. The most common foods that often used *in-vivo* in mouse models are chicken's egg (ovalbumin), cow's milk, peanuts and/or tree nuts<sup>104</sup>.

To establish a unique food antigen-induced intestinal systemic anaphylaxis in mouse, comparable to human situation, has been difficult due to different mouse strains, allergen dose, and immunological response<sup>105-107</sup>. Nevertheless, the protocols described so far require systemic sensitization with allergen plus adjuvant (alum by i.p. route and SEB/CT via i.g. route) followed by repetitive antigen exposure via i.g. route<sup>105-108</sup>. These mice develop intestinal anaphylaxis, followed by elevated IgE response, mast cell hyperplasia, increase in eosinophils and cytokine changes in the jejunum including diarrhea as a common characteristic feature, similar to human food allergy<sup>105-108</sup>. Published data confirm that IgE and mast-cell are required for the onset of diarrhea in these models<sup>105-108</sup>. Further, typical T<sub>H</sub>2 dominated immune responses have been shown to be important in food allergy, with IL-4 and IL-13 as prominent cytokines<sup>105-110</sup>. Adoptive transfer of activated CD4<sup>+</sup> T cells from alum/OVA sensitized mice to naive/biologically similar Balb/c mice show increased diarrhea<sup>111</sup>. Further, IL-9 mediated mastocytosis in the gut of food allergic mice predisposes to disease outcome<sup>112</sup>. Recently, basophils (via IgG1) have been shown to induce anaphylaxis in mice through the release of PAF, suggesting another pathway apart from the alternative or classical pathway<sup>113</sup>. Germ free mice develop spontaneous food allergy to antigen ingestion suggesting importance of the gut microbiota<sup>114,115</sup>. Mice with disruptions in TLR4 signaling (TLR4 = toll-like receptor 4) as well as treatment with antibiotics on the other hand show an increased tendency to oral sensitization<sup>116,117</sup>.

However, although allergen-alum sensitized mouse model have been widely accepted, the use of allergen with CT or SEB (as adjuvants) are also commonly used<sup>104,106,107</sup>. Li et al.<sup>118</sup> sensitized C3H/HeJ mice with cow's milk (CM) antigen with CT followed by protein challenge with higher doses. This study showed that i.g. sensitization followed by i.g. antigen challenge in mice lead to systemic anaphylaxis including respiratory discomfort<sup>118</sup>. These mice developed CM-specific IgE, elevated histamine level and an increase in the classical T<sub>H</sub>2 cytokine response<sup>118</sup>. Further experiments by Morafo et al.<sup>106</sup> using peanut proteins in Balb/c and C3H/HeJ murine strains demonstrate that anaphylactic symptoms occur in the C3H/HeJ mouse strain, but not in the Balb/c suggesting strain specific responses<sup>106</sup>. The C3H/HeJ mouse typically develops an increased migration of eosinophils and mast cells to the gut, followed by an increase of T-lymphocytes at the site of inflammation<sup>106</sup>. Further, mice deficient in mast cells, B cells and CD40-L show a complete abolishment of intestinal anaphylaxis<sup>119</sup>. In contrast, FcεR1-knockout mice display less systemic anaphylaxis in peanut challenged mice, but fail to provide evidence of involvement of the classical pathway<sup>119</sup>. Furthermore, biopsies obtained from allergen sensitized mast cell-deficient mice show using

the Ussing chamber that changes in the chloride ion transport across the intestinal tissues depend on mast cells<sup>120,121</sup>.

However, allergic diarrhea was more pronounced in the mice without Payer's patches<sup>115,122</sup>. Here, anti-IL-7 $\alpha$  was injected in the offspring mice during the gestation period to abolish Payer's patches<sup>115,122</sup>. Additionally, antigen-specific IL-10 production has been shown to be localized in Payer's patches in the gut, and that upon transferring isolated IL-10-producing CD4<sup>+</sup> CD25<sup>+</sup> T-reg cells to allergic mice abolished allergic diarrhea symptoms<sup>122</sup>. Additional experiment proved that inhibiting IL-10 production or T-regs in the Payer's patches intact mice resulted in allergic diarrhea<sup>122</sup>. These results show that Payer's patches are important sites for the development of allergic inflammation in the intestine<sup>115,122</sup>.

### **3.4. Proteasome and Bortezomib**

#### **3.4.1. Proteasome**

The proteasome is an ATP-dependent protein complex, which degrades selectively unneeded or damaged proteins<sup>123</sup>. Proteasomes are mainly present inside all eukaryotes, archaea and in few bacteria<sup>123</sup>. Two main pathways catalyze the protein degradation; 1. ubiquitin-dependent and 2. ubiquitin-independent<sup>124</sup>. The ubiquitin-dependent proteasomal degradation depends on the covalent attachment of polyubiquitin chains to a target protein, which is catalyzed by specific enzymes known as ubiquitin ligases whereas the ubiquitin-independent degradation involves specific co-factors that are bound to the protein substrate<sup>124</sup>. The molecular size of eukaryotic 26S proteasome is approximately 2.4 MDa, with multiple subunits of approximately 700 kDa one catalytic 20S proteasome (known as 20S core particle) and approximately 900 kDa two 19S regulatory particle (also known as PA700)<sup>125,126</sup>. The structure of the 26S proteasome is depicted in the Figure 4<sup>126</sup>. The 20S subunit consists of active proteolytic sites for protein degradation whereas the 19S subunit contains ATPase active sites and ubiquitin binding sites for recognizing and transferring polyubiquitinated proteins to the catalytic core for proteolysis<sup>126</sup>. The 20S core particle is a barrel like-structure composed of  $\alpha$  and  $\beta$ - subunits, which are stacked together to form a cylindrical structure of 2 $\alpha$  and 2 $\beta$  rings<sup>126</sup>. Each ring consists of 7 different subunits<sup>123-126</sup>. The  $\alpha$ -rings act as an entry site of the unfolded proteins whereas  $\beta$ -rings function as proteolytic chamber for enzymatic activity. The catalytically active  $\beta$ -subunit consists of  $\beta$ 1,  $\beta$ 2 and  $\beta$ 5 subunits, which are responsible for caspase-like, trypsin-like and chymotrypsin-like, proteolytic activity respectively<sup>124-126</sup>.

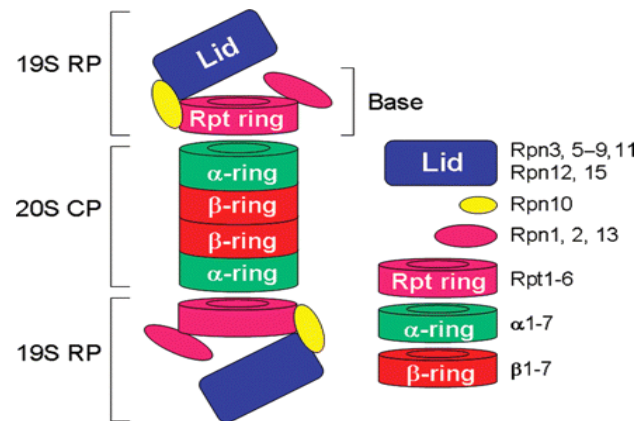


**Figure 4 Structure of 26S proteasome. (detailed explanation in the text and permission obtained to reuse this figure here)<sup>126</sup>**

The 19S regulatory unit holds 6 ATPase and nearly 8 non-ATPase subunits. These subunits regulate proteins entering the 20S unit. Their main functional role is to regulate de-ubiquitination, and to unfold and translocate proteins<sup>124-126</sup>.

Every eukaryotic cell contains proteasomes, which are present in the cytoplasm, but also in the nuclei. Their expression levels are highly variable, which depend on the proliferative status of a cell<sup>127,128</sup>. Proteasomes that are present within the cytoplasm appear to be closely associated with cytoskeletal elements, the centrosomes and the outer surface of the endoplasmic reticulum (ER). Within the nucleus, proteasomes are present in the nucleoplasm<sup>127,128</sup>. Due to its ability to degrade targeted proteins, the proteasome has the capacity to control several biological processes inside the cell and unidirectionally catalyze specific reactions<sup>127,128</sup>. Other functional roles of proteasomes include the control of the cell cycle, apoptosis, metabolism, signal transduction, DNA repair and chromatin remodelling<sup>127,128</sup>. Moreover proteasome function is also important for controlling immune responses and inflammatory processes<sup>127,128</sup>.

Plasma cells (PCs) are non-proliferative and end-stage B cells<sup>129</sup>. PCs depend on proteasomes to secrete antibodies (at the rate of greater than 3,000 molecules per second)<sup>130</sup>. But also the differentiation and survival of PCs depends on the degree of unfolded protein response (UPR) due to aggregation of unneeded proteins within the endoplasmic reticulum (ER)<sup>131-133</sup>. Therefore, selective inhibition of a proteasome activates terminal UPR and causes extensive ER stress, which leads PCs to undergo apoptosis by enhancing the proapoptotic active protein-Chop as well as stimulating caspases<sup>131-133</sup>. During apoptotic process, inhibition of the proteasome blocks IκB protein degradation, which in turn impedes downstream activation of NF-κB<sup>131-133</sup>. Thus, proteasomes regulate PCs survival<sup>130</sup>.

### 3.4.2. Bortezomib and its therapeutic implications

Proteasomes are crucial for cell function in eukaryotes<sup>123-127</sup>. Their primary task is to clear abnormal, mutated and/or degraded proteins<sup>123-127</sup>. Therefore, the manipulation of this machinery has been shown to be of potential research interest for treatment of cancer and inflammatory diseases<sup>129,130,134</sup>. There are numerous specific natural and synthetic inhibitors available today<sup>135</sup>. These inhibitors bind to the catalytic site of a proteasome either reversibly or irreversibly and block its active function<sup>135</sup>. One of such reversible proteasome inhibitor is bortezomib (Bz; Velcade, Millennium Pharmaceuticals, Inc., Cambridge, MA), a dipeptide boronic acid derivative<sup>135</sup>. Its structure consists of pyrazinoic acid, phenylalanine and leucine with boronic acid (Figure 5)<sup>135</sup>. The molecular weight is C<sub>19</sub>H<sub>25</sub>BN<sub>4</sub>O<sub>4</sub> and its chemical IUPAC name is [3-methyl-1-(3-phenyl-2-pyrazin-2-ylcarbonylamino-propanoyl) amino-butyl] boronic acid<sup>135</sup>.

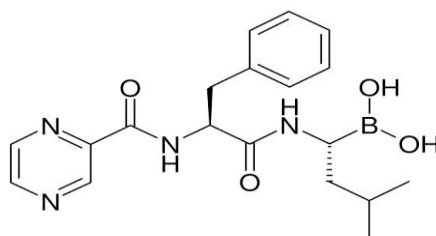


**Figure 5 Structure of bortezomib (detailed explanation in the text)<sup>135</sup>**

The function of an effective proteasome inhibitor depends on its specificity, kinetics, interaction, stability and availability<sup>135</sup>. The reversible proteasome inhibitor Bz has been approved for the treatment of mantle cell lymphoma and multiple myeloma (a malignant PC disorder) in humans<sup>136-138</sup>. The mechanism behind the selective inhibition process is not completely known yet, but it seems partly it acts on PCs by stabilizing regulatory proteins [e.g. I $\kappa$ B, p21, and p53]<sup>137</sup>. Moreover, this inhibition might be directly coupled to the protein synthesis rate<sup>138</sup>. In fact the immense protein synthesis and the highly associated endoplasmic reticular stress are the key components of every antibody-producing PCs<sup>139</sup>. Hence these observations paved the way to examine normal, untransformed PCs in the case of multiple myeloma as well as autoimmunity for their sensitivity towards Bz<sup>139</sup>. Data suggest that during terminal differentiation of PCs, their proteasomal capacity decreases reaching saturation of the ubiquitin-proteasome system (UPS) earlier than other cells<sup>140</sup>. Apart from cancer related studies, the application of Bz have been recently extended to test its significance in autoimmune disease murine models like SLE (lupus), arthritis and myasthenia gravis<sup>129,141,142</sup>, but also in allergy mouse model of asthma<sup>143</sup>.

#### **4. OBJECTIVES**

This thesis aimed to investigate the consequences of plasma cell elimination and abolishment of the humoral immune response in skin and mucosal allergy mouse models.

The first part of the thesis work employed an allergen-triggered eczema mouse model -

1. To explore if bortezomib might have a therapeutic potential for treating inflammatory skin diseases
2. To further help unravel whether atopic eczema is, at least in part, mediated by IgE (as there is some contradiction in this regard in the literature)
3. To delineate if IgE, the allergy-driving Ig isotype, is downregulated by Bz
4. To find if total Ig and specific IgE reduction is associated with other immune changes and skin changes in this model

The second part of the experimental approach was focussed on a mouse model of food-induced intestinal anaphylaxis -

1. To establish an hazelnut-induced intestinal anaphylaxis mouse model which is associated with a specific humoral immune response and which dependent on an allergen relevant in humans
2. To characterise clinical and immunological parameters in this model
3. To evaluate the clinical and immunological efficacy of bortezomib in the established mouse model
4. To describe the cellular inflammatory response in the model

## 5. MATERIALS AND METHODS

### 5.1. MATERIALS

#### 5.1.1. Antibodies

Antibody	Clone	Manufacturer
Anti-chicken egg albumin (OVA)	OVA-14	Sigma-Aldrich
Anti-mouse CD3 FITC	145-2C11	eBioscience
Anti-mouse CD4 PE	GK1.5	DRFZ
Anti-mouse CD8 APC	53-6.7	BD Pharmingen
Anti-mouse CD21/35 FITC	7G6	BD Pharmingen
Anti-mouse CD23 PE	B3B4	BD Pharmingen
Anti-mouse CD19 APC	1D3	BD Pharmingen
Anti-mouse CD44 PE-Cy7	IM7	eBioscience
Anti-mouse CD62L A405	MEL14	DRFZ
Anti-mouse CD138 PE	281-2	BD Pharmingen
Anti-mouse CD45 R (B220) PE-Cy5	RA3-6B2	BD Pharmingen
Anti-mouse IgA, biotin	1040-01	Southern Biotech
Anti-mouse IgE	R35-72	BD Pharmingen
Anti-mouse IgE, biotin	EM95.3	DRFZ
Anti-mouse IgG1, biotin	A85-1	BD Pharmingen
Anti-mouse IgG1 APC	X56	BD Pharmingen
Anti-mouse IgG2a, biotin	R19-15	BD Pharmingen
Anti-mouse <i>Kappa</i> pacblue	187.1	DRFZ
Anti-rat IgG, biotin	IHC	BD Pharmingen
Bio-conjugated OVA		DRFZ

#### 5.1.2. Buffers and solutions

Buffer/Solution	Composition	Manufacturer
50x Tris-acetate-EDTA (TAE) buffer		Gibco, Invitrogen
1x Tris-EDTA (TE), pH 8.0	10 mM Tris 1 mM EDTA	

Buffer/Solution	Composition	Manufacturer
AEC-DMF buffer (pH 5.0)	64 mM CH <sub>3</sub> COONa 45 mM CH <sub>3</sub> COOH	
Blocking buffers	3% BSA/1x PBS 2% BSA/1x TBS 3% MP/1x PBS	
Coating buffer, pH 9.6	34.8 mM NaHCO <sub>3</sub> 154 mM NaCl 15.1 mM Na <sub>2</sub> CO <sub>3</sub>	
DermaLife K Complete Medium	6mM L-Glutamine 0.4% Extract P <sup>TM</sup> 1.0 μM (-)-Epinephrine-(+)-Bitartrate 0.5 ng/mL rh TGF-α 100ng/mL Hydrocortisone Hemisuccinate 5 μg/mL rh Insulin 5 μg/mL Apo-Transferrin	
FACS buffer	1% BSA or FCS/1x PBS	
Loading buffer, pH 8.0	1x TE 40% glycerine 0.25% bromphenol blue	Sigma-Aldrich Sigma-Aldrich
Medium complete	500 ml Advanced RPMI 1640 25 ml CCS 4 mM L-glutamine 100 U/ml penicillin 100 μg/ml streptomycin	Gibco, Invitrogen Biochrom AG Biochrom AG Biochrom AG Biochrom AG
PBS, pH 7.4	137 mM NaCl 2.7 mM KCl 10 mM Na <sub>2</sub> HPO <sub>4</sub>	

Buffer/Solution	Composition	Manufacturer
Sodium carbonate buffer, pH 9.6	1.8 mM KH <sub>2</sub> PO <sub>4</sub> 28.6 mM NaHCO <sub>3</sub>	
Substrate buffer, pH 9.8	15.1 mM Na <sub>2</sub> CO <sub>3</sub> 1 M diethanolamine	
TBS, pH 7.4	0.5 mM MgCl <sub>2</sub> 100 mM Tris-Base	
TMB buffer, pH 5.0	154 mM NaCl 0.05 M Na <sub>2</sub> HPO <sub>4</sub> 0.02 M citric acid	

### 5.1.3. Reagents

Reagent	Specification	Manufacturer
3,3',5,5'-tetramethylbenzidine (TMB)		Sigma-Aldrich
3-amino-9-ethylcarbazole dihydrochloride	20 mg per tablet	Sigma-Aldrich
Acetic acid, CH <sub>3</sub> COOH	≥ 99.7%	Sigma-Aldrich
Advanced RPMI 1640		Invitrogen
Agarose LE Agarose		Biozym scientific GmbH
Albumin from chicken egg white (OVA)	Grade V	Sigma-Aldrich
Antibody diluent (Dako REAL™)		DAKO Diagnostika
Avidin/biotin blocking Kit		Vector
Bortezomib®		Charite central pharmacy
Bovine serum albumin (BSA)	Fraction V, pH 7.0	Serva
Charcoal stripped FCS (CCS)	S3113, heat-inactivated	Biochrom AG
Citric acid, C <sub>6</sub> H <sub>8</sub> O <sub>7</sub>	≥ 99%	Merck
Detection System (Dako REAL™)	K 5005, AP/RED	DAKO Diagnostika
Diethanolamine, (HOCH <sub>2</sub> CH <sub>2</sub> ) <sub>2</sub> NH	≥ 98%	Sigma-Aldrich
Disodium carbonate, Na <sub>2</sub> CO <sub>3</sub>		Merck
Disodium hydrogen phosphate, Na <sub>2</sub> HPO <sub>4</sub>		Merck
Dimethylsulfoxide (DMSO)	Hybri-Max™	Sigma-Aldrich

Reagent	Specification	Manufacturer
DNAse		Macherey-Nagel
Dry milk powder (MP)	blotting grade, powdered	Carl ROTH®
Dulbecco's phosphate-buffered saline (PBS), without Ca <sup>2+</sup> /Mg <sup>2+</sup>		PAA
Ethanol, CH <sub>3</sub> CH <sub>2</sub> OH	absolute	Merck
Ethidium bromide solution	10 mg/ml	Gibco/Invitrogen
Ethylenediaminetetraacetic acid (EDTA)	≥ 99%, anhydrous	Sigma-Aldrich
Extra Avidine Peroxidase		Sigma-Aldrich
FACS Flow		BD Pharmingen
FastStart DNA Master SYBR® Green		Roche
Fetal calf serum (FCS)	0314G, heat-inactivated	Biochrom AG
Ficoll	sterile, d = 1.077 g/mL	PAA
Goat serum normal	DakoCytomation, X097	DAKO Diagnostika
Heparan sulfate		Rotexmedica GmbH
Hydrochloric acid, HCl	≥ 37%	Merck
Hydrogen peroxide, H <sub>2</sub> O <sub>2</sub>	≥ 30%	Merck
Imject® Alum (Al(OH) <sub>3</sub> , Mg(OH) <sub>2</sub> )	40 mg/ml	Thermo Fisher Scientific
Isoflurane (Forane)	≥ 99.9% w/w	Abott
Kaiser's glycerol gelantine		Merck
L-glutamine 200 mM		Biochrom
Magnesium chloride, MgCl <sub>2</sub> *6H <sub>2</sub> O		Merck
<i>N,N</i> -dimethylformamide (DMF)	≥ 99%	Sigma-Aldrich
NucleoSpin® RNA II Kit		Macherey-Nagel
Papanicolaou, Harris' Hematoxylin solution		Merck
<i>para</i> -nitrophenylphosphate ( <i>p</i> NPP)		Sigma-Aldrich
Penicillin/streptomycin	10000 U/ml, µg/ml	Biochrom AG
Potassium chloride, KCl		Merck
Potassium dihydrogen phosphate, KH <sub>2</sub> PO <sub>4</sub>		Merck
Propidium iodide		Sigma-Aldrich
ProTaq Tris, pH 7.6		BIOCYC
Proteinase K		Macherey-Nagel

Reagent	Specification	Manufacturer
Quick-Load <sup>®</sup> 100 bp DNA Ladder		New England BioLabs <sup>®</sup>
Red blood cell (RBC) lysis buffer		eBioscience
RNeasy Mini Kit		Quiagen
Sodium acetate, CH <sub>3</sub> COONa		Merck
Sodium bicarbonate, NaHCO <sub>3</sub>		Merck
Sodium chloride, NaCl		Merck
Streptavidin-alkaline phosphatase (AP)		ZYMED
Streptavidin-horseradish peroxidase (HRP)		R&D Systems <sup>®</sup>
Sulfuric acid, H <sub>2</sub> SO <sub>4</sub>	≥ 96%	Merck
TaqMan <sup>®</sup> Reverse Transcription Reagents		Applied Biosystems
Toluidine blue		Merck
Tris(hydroxymethyl)aminomethane (Tris-Base)		Sigma-Aldrich
Tween20		Sigma-Aldrich
β-Mercaptoethanol	14.3 M, ≥ 98%	Sigma-Aldrich

#### 5.1.4. Lab ware

Labware	Specification	Manufacturer
12-, 24-, 48-, 96-well plates	multiwell suspension culture	Greiner Bio-One
autoMACS <sup>®</sup> columns		Miltenyi Biotec
Biopsy punch, sterile	4 mm diameter	Stiefel
Blade for Cryostat		Feather
Cell strainers	40 μm, 100 μm	BD Falcon
Cohesive bandage	Peha-haft <sup>®</sup> , 6 cm width	Hartmann
Coverslips		Menzel-Gläser
Cryo-spray	cryogenic spray	Bio Optica
Disposable wet razor		Wilkinson
ELISA plates	Immuno 96 MicroWell <sup>™</sup> Solid Plates, MaxiSorp <sup>™</sup>	Nunc
Filter paper discs	7.5 mm	Epitest Ltd Oy

Labware	Specification	Manufacturer
Finn chambers <sup>®</sup>		Epitest Ltd Oy
Hypodermic needle, sterile	Sterican	Braun
LightCycler <sup>®</sup> capillaries	20 µl	Roche
LS/LD columns		Miltenyi Biotec
Microscope slide	Superfrost <sup>™</sup> Plus R.	Langenbrinck
Mortar and pestle		Carl ROTH <sup>®</sup>
MultiScreenHTS IP	hydrophobic PVDF, 0.45 µm	Millipore
Petri dishes		Greiner Bio-One
Pre-Separation Filters	30 µm	Miltenyi Biotec
Shredder columns for tissue samples		Quiagen
Syringes, sterile 1, 2, 5, 10, 20, 50 ml		Braun
Tissue freezing medium	Tissue-Tek <sup>®</sup> O.C.T <sup>™</sup> Compound	Sakura Finetek
Vinyl specimen mold		Sakura Finetek

Pipettes, reaction tubes, pipette tips and further standard labware were obtained from Eppendorf, Sarstedt, BD Falcon and Kimberly-Clark.

#### 5.1.5. Technical equipment

Equipment	Model	Manufacturer
Analytical balances		Sartorius AG
CASY <sup>®</sup> Technology Cell Counter	Casy 1, Model TT	Roche Innovatis AG
Centrifuges	Varifuge RF	Heraeus Holding
	Megafuge 1.0R	Heraeus Holding
Clean bench	HeraSafe	Heraeus Holding
Cryostat	Chryotome FSE	Thermo Fisher Scientific
Digital camera	EOS20D	Canon
Electrical pipetting aid	Pipetus	Hirschmann Laborgeräte
ELISPOT Analyzer	CTL-ImmunoSpot <sup>®</sup> S4	C.T.L Cellular Technology
Flow cytometer/FACS	MACSQuant <sup>®</sup> Analyzer	Miltenyi Biotec
Freezer (-20°C)/Fridge (4°C)	TKF380	EUREKA
Freezer (-80°C)	HeraFreeze	Heraeus Holding

<b>Equipment</b>	<b>Model</b>	<b>Manufacturer</b>
Gel chamber		Bio-Rad Laboratories
Heating block	Thermomixer 5436	Eppendorf
Hot plate	nuova II	Thermolyne
Incubator	Heracell <sup>®</sup>	Heraeus Holding
Magnetic stirrer	Magnetmix 2070	Hecht-Assistent
Microscope and camera	AxioPlan 2	Carl Zeiss AG
	AxioCam HRC	Carl Zeiss AG
pH electrode		neoLab GmbH
pH meter	MV 870	Digital Präcitronic
Pipetts	10µl, 100µl, 200µl, 1000µl	Eppendorf, Brandt
Plate reader	MRX Microplate Reader	Dynex Technologies GmbH
Plate washer	TECAN	
Power supply	Power Pac300	Bio-Rad Laboratories
Shaker	IKA-Vibrax-VXR	IKA <sup>®</sup> Werke GmbH & Co. KG
Spectrophotometer	NanoDrop 1000	Thermo Fisher Scientific
Table top centrifuge	5417 C	Eppendorf
Table top centrifuge	5417 R	Eppendorf
Thermal cyclers	LightCycler <sup>®</sup> 1.5	Roche
	Px2	Thermo Electron Corporation
Vortex mixer	Reax 2000	Heidolph
Water bath	U3	Julabo

#### 5.1.6. Software

<b>Software</b>	<b>Release</b>	<b>Developer</b>
AxioVision	4.6.3	Carl Zeiss AG
CASY <sup>®</sup> measure	1.5	Schärfe System
Excel 2003, 2007		Microsoft Corporation
FlowJo	7.6.1	Tree Star, Inc.

<b>Software</b>	<b>Release</b>	<b>Developer</b>
Immunocapture	6.0 C.T.L	Cellular Technology
ImmunoSpot	v4.0.13 C.T.L	Cellular Technology
LightCycler <sup>®</sup> Software	Version 3	Roche
Prism	5.00	GraphPad
Revelation	G3.2	Dynex Technologies GmbH

## 5.2. METHODS

### 5.2.1 Animal experiments

#### 5.2.1.1. Animal work

Female BALB/c mice (8-10 weeks old) were obtained from Janvier, *Le Genest-Saint- Isle*, France. To conduct animal experiments, approval was taken from the Local State Office of Health and Social Affairs (LAGeSo), Germany (with registration numbers G0359/09 and G0091/09). Mice were kept within an accredited animal facility at the Charite-Universitätsmedizin (Berlin, Germany) and maintained under specific pathogen-free conditions at constant room temperature ( $21 \pm 1^\circ\text{C}$ ), relative humidity ( $45 \pm 5\%$ ) and 12 h light–dark cycle. All mice were provided with regular diet and water.

#### 5.2.1.2. Mouse model of allergen-induced eczema

Skin inflammation was induced in Balb/c mice by an epicutaneous (e.p.) allergen application by patch test method, as described previously<sup>144</sup>. Mice were sensitized i.p. on days 1, 14 and 21 with 10  $\mu\text{g}$  ovalbumin (OVA, which is the major allergen in egg, its molecular weight of glycoprotein is approximately 45kDa<sup>145</sup>) plus 1.5 mg alum (combination of aluminium hydroxide and magnesium hydroxide) in a total volume of 0.1 ml in PBS (Figure 6). Alum was used as an adjuvant to induce the adaptive immune reaction<sup>146</sup>. The skin of the mice was shaved at the belly and 100  $\mu\text{g}$  OVA with 1.5 mg alum in 20  $\mu\text{l}$  of total volume was applied e.c. using a sterile patch and dressed with elastic cohesive bandage for fixing the patch. Each mouse was then subjected to a total of 3 one week exposures to the same skin site, with renewal of the patch after third day and a two-week interval between each application. After the second patch period, proteasome inhibitor bortezomib (0.75 mg per kg body weight<sup>129</sup>) or PBS as a control on day 52 was injected into the vein<sup>147</sup>. On day 71, mice were sacrificed by cervical dislocation. Blood was collected using a micro-lancet via *vena facialis* at different time points as indicated in the experimental plan. Eczema outcome was photographed and documented. Skin biopsies were immediately snap frozen in the liquid nitrogen for RNA isolation and a biopsy punch was embedded in an O.C.T medium followed by slow freezing in liquid nitrogen for immunohistochemistry. Spleen, bone marrow, axillary and inguinal lymph nodes were removed and stored in PBS for isolation of lymphocytes on ice.

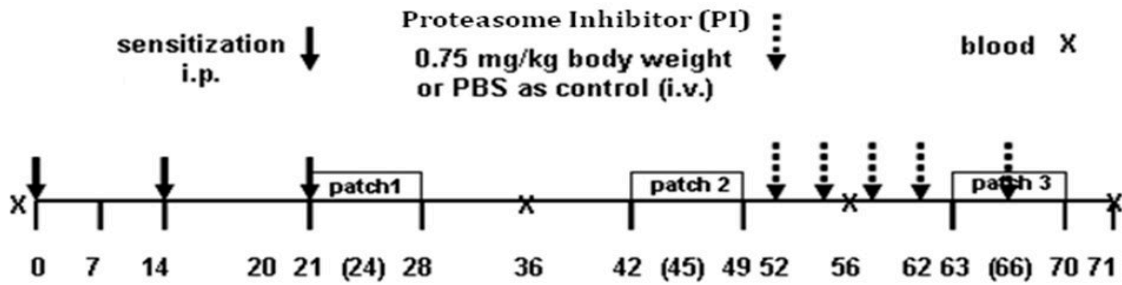


**Figure 6 Experimental design.** Allergen-induced eczema mouse model<sup>147</sup>.

### 5.2.1.3. Assessment of atopic eczema symptoms

The severity of OVA-induced eczematous skin lesions was evaluated by a skin scoring system, which considers typical features of human AD<sup>144</sup>. The eczema symptoms include erythema, edema/papules, oozing/crusts, dryness, and extension as described earlier<sup>144</sup>. The parameters were investigated blindly by 6 independent evaluators and were graded into: 0, no eczema; 1, mild eczema; 2, intermediate eczema; 3, severe eczema. Skin score is calculated by the sum from these factors. The overall score was considered as an index of skin eczema severity<sup>144</sup>.

### 5.2.1.4. Mouse model of hazelnut-induced intestinal anaphylaxis

Mice were intraperitoneally sensitized on days 1, 14 and 21 with 20  $\mu$ g of European Hazelnut (HN) (Greer Laboratories, Lenoir, NC, USA) or PBS and 2.5 mg alum (Figure 7A). After sensitization, mice were orally administered with 250  $\mu$ l containing 12.5 mg of HN, starting from day 28<sup>th</sup>, followed by three times a week (every other day). Each mouse received 10 oral challenges until the end of the experiment and was sacrificed on day 55 (Figure 7A).

In the second model (Figure 7B), mice were intragastrically sensitized with 500 and 1500  $\mu$ g European HN (Greer Laboratories) together with 10  $\mu$ g *staphylococcal enterotoxin B* (SEB) as adjuvant<sup>148</sup> in 150  $\mu$ l total volume, every week and then, challenged twice on days 57 and 64 with 50 mg of HN and sacrificed on day 64.

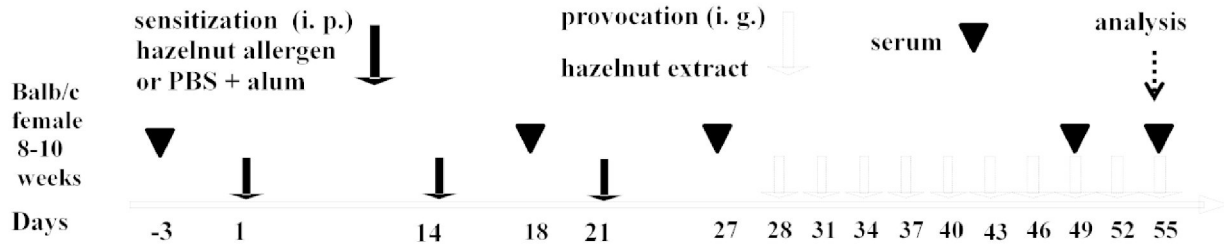


**Figure 7A Experimental setup.** HN-induced intestinal anaphylaxis protocol 1

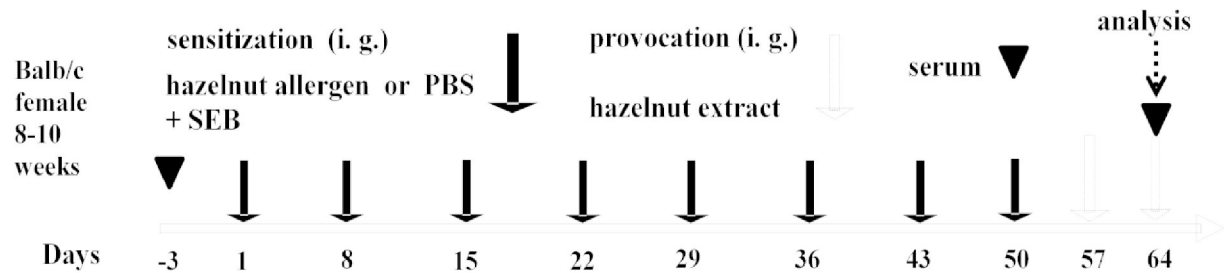


**Figure 7B Experimental setup.** HN-induced intestinal anaphylaxis protocol 2.

Using the established HN induced intestinal anaphylaxis (protocol 1, Figure 7A), bortezomib (Bz, 0.75 mg per kg body weight<sup>129</sup>) or PBS as a control was administered intravenously *via* tail vein, twice weekly, starting from day 36 (Figure 8). A fresh vial of Bz was used for each time interval, because of its short half-life. At the end of the experiment mice were sacrificed.

Blood was withdrawn *via vena facialis* at different time intervals within 1 to 2 hours after the challenge as indicated by the arrows in the respective experimental protocol (Figure 7A, 7B and 8) for separating the serum. A small piece of intestinal jejunum biopsy weighing approximately 1 to 2 mg was immediately snap frozen in the liquid nitrogen for RNA isolation and a biopsy was stored in 10% formalin for paraffin sections. Spleen and mesenteric lymph nodes were removed and stored in PBS for lymphocyte isolation on ice.

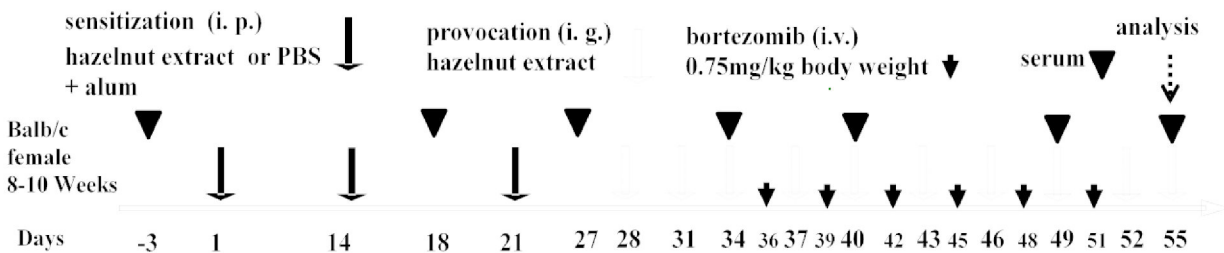


**Figure 7: Experimental regime.** Application of bortezomib in a mouse model of hazelnut induced intestinal anaphylaxis.

### **5.2.1.5. Assessment of hazelnut-induced intestinal anaphylactic symptoms**

The clinical severity of the mice was assessed by monitoring mice up to an hour after the challenge as described previously<sup>148,149</sup>. The clinical severity symptom scores were recorded and include: 0, without any symptoms; 1, intense scratching and rubbing around the body (head, nose and tail); 2, diarrhea, and/or lowered activity with higher respiratory rate; 3, wheezing, and/or difficulty in respiration; 4, without any activity in the cage after shock and convulsion; 5, death. Rectal temperature measurements for intestinal anaphylaxis were performed immediately before (time 0) and at different time points for up to 1 h after hazelnut challenge.

### **5.2.2. Preparation of hazelnut extract**

A 100 g hazelnut packet was grounded to powdery form using liquid nitrogen and blender. Afterwards the extracts were defatted with acetone three times and completely air dried. HN proteins were extracted in PBS and precipitated with 80%  $(\text{NH}_4)_2\text{SO}_4$  for 2 hr at 4°C. The precipitate was centrifuged at 10,000 g for 1 hour. The pellet obtained was dissolved in 1x PBS and dialysed against 1x PBS at 4°C to completely remove the  $(\text{NH}_4)_2\text{SO}_4$ . After dialysis, the HN extract was filtered through 0.2  $\mu\text{m}$  filters, freeze dried at -70°C and lyophilized. The HN protein concentration was measured by Bradford protein assay<sup>150</sup>.

### **5.2.3. Cell and/or organ culture methods**

#### **5.2.3.1. Mouse splenocyte and lymph node cell isolation**

Spleen from each BALB/c mouse was removed with sterile surgical instrument and placed in 1x phosphate buffered saline (PBS) at 4°C. Each spleen was kept on a sterile 100  $\mu\text{m}$  nylon mesh cell strainer in a petri-dish and mashed gently with a 5 ml syringe plunger. The mashed spleen solution was collected into ice-cold 1x PBS/2 mM ethylenediaminetetraacetic acid (EDTA). The procedure was repeated to dissolve remaining clumps and/or any imbedded material. The cell clumps were then resuspended in a chilled 1x PBS/2 mM EDTA tube to obtain single cell suspension and passed on to a 50 ml falcon tube using 40  $\mu\text{m}$  size cell strainer. After repeated washing steps with 1x PBS/2 mM EDTA, the suspension containing splenocytes was centrifuged with a speed of 340 g for 10 min at 4°C. After centrifugation, the supernatant was discarded carefully without disturbing the cell pellet. The pellet containing splenocytes was resuspended cautiously and red blood cells (RBC) were lysed in a 2.5 ml RBC lysis buffer for 5 minutes on

ice. To stop the reaction, tubes were filled with 30 ml ice cold 1x PBS/2 mM EDTA and cold centrifuged for 10 min at 340 g. The supernatant was discarded and the cell pellet was once again resuspended in 30 ml 1x PBS/2 mM EDTA. The cells were counted using CASY®-Technology instrument. At the end, required cell numbers for the flow cytometry analysis were taken in the advanced RPMI (1640) culture medium [supplemented with 4 mM L-glutamine, 50 U/ml penicillin, 50 µg/ml streptomycin and 5% heat inactivated charcoal stripped fetal calf serum (CCS)].

#### **5.2.3.2. Skin biopsy culture**

The belly area of the naïve Balb/c mice skin was wet shaved after sacrificing by cervical dislocation and 5 mm punch skin biopsies were obtained. Several biopsy punches were washed in 5ml of DermaLife K Complete Medium (a hydrocortisone free medium) for 30 minutes. These skin biopsies (*ex vivo*) were plated in 96-well-cell culture plate. Each well was treated with Bz at the concentrations of 0, 10, 50 and 100 nM either in the presence or absence of IL-1 $\beta$  (20 ng/mL) and incubated for 24 h to mimic an inflammatory microenvironment with an increased protein turnover<sup>151</sup>. The incubated skin samples were snap frozen using liquid nitrogen and stored at -80°C until RNA isolation. All experiments were repeated 5 times.

#### **5.2.3.3. Culture conditions**

All cell cultures were carried out at 37°C and 5% CO<sub>2</sub> in a humidified atmosphere.

#### **5.2.4. Immunological methods**

##### **5.2.4.1. Enzyme-linked immunosorbent assay (ELISA)**

ELISA is a specific and highly sensitive immunoassay for quantification of antigens or antibodies in a solution, usually cell free medium. This technique has been used to measure the concentrations of the immunoglobulins subtypes which are secreted by B-cells during the allergic manifestation. In principle antibodies or antigens are coated onto the microtiter plates to capture specific antibodies of interest. To this bound analyte, a secondary antibody tagged to an enzyme, usually biotinylated or alkaline phosphatase in this case, was incubated. Detection was carried out by using enzyme conjugated streptavidin followed by adding substrate for the development of colored reaction, which is measured by spectrophotometry.

### 5.2.4.2. Murine immunoglobulin ELISA

ELISA technique was used to measure total, OVA- and HN-specific immunoglobulins. Total and OVA specific IgE, IgG1, IgA, IgM and IgG2a from the sera of AD mouse model<sup>60</sup> as well as HN-specific IgE, IgG1 and IgA from sera of HN-induced intestinal anaphylaxis model were measured. The concentrations of OVA-specific as well as HN-specific antibodies were estimated by comparison to a standard curve prepared from pooled sera from OVA-sensitized and HN-sensitized mice. Data are expressed as laboratory units per milliliter (LU/ml). OVA-14 (OVA-specific mouse IgG1) was used as standard for OVA-IgG<sub>1</sub>. To measure total immunoglobulins, maxisorp plates were coated with anti-mouse antibodies and stored at 4°C, overnight. After blocking unspecific binding, detection was performed using biotinylated and/or alkaline phosphate secondary antibodies followed by streptavidin-conjugated HRP or streptavidin-conjugated AP, respectively. The colorimetric reaction of TMB or pNPP substrate was measured at 450 and 405 nm, respectively after adding 1 M sulfuric acid. Standard curve was determined to each ELISA's. Refer tables 1, 2 and 3 for further details.

Immunoglobulin ELISA	Blocking reagent	Coating antibody	Standard	Secondary antibody
IgE	PBS/3% milk	rat anti-mouse IgE R35-72, BD	mouse IgE, κ BD	anti-IgE-Bio EM95.3, DRFZ
IgG1	PBS/3% BSA	goat anti-mouse IgG1 1070-01, Southern Biotech	mouse IgG1, κ BD	anti-IgG-AP, 1030-04, Southern Biotech
IgA	PBS/3% BSA	goat anti-mouse IgA, 1040-01, Southern Biotech	mouse IgA, κ S107 Southern Biotech	anti-IgA-AP, 1040-04, Southern Biotech
IgM	PBS/3% BSA	goat anti-mouse IgM, 1020-01, Southern Biotech	mouse IgM PP50, Chemicon	anti-IgM-AP, 1020-04, Southern Biotech
IgG2c	PBS/3% BSA	goat anti-mouse IgG2c, Bethyl	mouse IgG2c reference serum	anti-IgG2c-HRP Bethyl

**Table 1 Specific antibodies and substances used for the measurement of total immunoglobulins.**

Immunoglobulin ELISA	Blocking reagent	Coating	Standard	Secondary antibody
IgE	PBS/3% BSA	rat anti-mouse IgE R35-72, BD	Serum pool	OVA-Bio EM 95.3, DRFZ
IgG1	PBS/3% milk powder	OVA	OVA 14 IgG1 Sigma	anti-IgG1-Bio A85, BD
IgA	PBS/3% milk powder	OVA	Serum pool	anti-IgA-Bio 1040-08, SouthernBiotech
IgM	PBS/3% BSA	OVA	Serum pool	anti-IgM-AP 1020-04, SouthernBiotech
IgG2c	PBS/3% BSA	OVA	Serum pool	anti-IgG2c-HRP Bethyl

**Table 2 Specific antibodies and substances used for the measurement of OVA specific immunoglobulins**

Immunoglobulin ELISA	Blocking reagent	Coating	Standard	Secondary antibody
IgE	PBS/3% BSA	HN	Serum pool	anti-IgE-Bio EM 95.3, DRFZ
IgG1	PBS/3% milk powder	HN	OVA 14 IgG1 Sigma	anti-IgG1-Bio A85, BD
IgA	PBS/3% milk powder	HN	Serum pool	anti-IgA-Bio 1040-08, SouthernBiotech

**Table 3 Specific antibodies and substances used for the measurement of HN specific immunoglobulins**

### 5.2.4.3. Enzyme-linked immunospot (ELISpot)

ELISpot assays were used to measure the frequency of specific antibody-secreting cells. After wetting thoroughly with ethanol for few seconds, multiscreen<sub>HTS</sub>-IP 96 well plates with PVDF membranes were coated with 10 µg OVA per well in a total volume of 100 µl sodium carbonate buffer, overnight at 4°C. Blocking of wells were performed using RPMI-1640/10% FCS and PBS/3% BSA (1:1 dilution) for 1 h at 37°C in CO<sub>2</sub> incubator. To analyze IgE, IgG1 and IgA antibody secreting cells (ASCs), serial dilutions of splenocytes and bone marrow cells (starting with 5 x 10<sup>6</sup>, 1 x 10<sup>6</sup> and 5 x 10<sup>6</sup>) were plated and incubated overnight at 37°C in CO<sub>2</sub> incubator. After washing the cells thoroughly in 1xPBS/0.5% tween-20, plates were re-incubated with

biotinylated secondary-antibody [anti-murine IgE-biotin (EM 95.3), anti-murine IgG1-biotin (A85-1, BD) and anti-murine IgA-biotin (1040-08, southern biotech)], respectively. Then, streptavidin-HRP was incubated for 1h at RT followed by development of the reaction by peroxidase substrate 3,3'-amino-9-ethyl-carbazole/n, n-dimethylformamide. The reaction was stopped by running water and ASC's appearing as red spots were analyzed with the C.T.L ImmunoSpot S4 Analyzer.

#### **5.2.4.4. Western blot**

10 µg HN protein extract was denatured in sample buffer containing β-mercaptoethanol for 5 min at 95°C. The denatured protein was loaded onto the sodium dodecyl sulfate polyacrylamide gel electrophoresis (SDS-PAGE) to resolve proteins based on their relative molecular weight. The stacking gel (6% tris glycine SDS-polyacrylamide gel) as well as resolving gel (12 % tris glycine SDS-polyacrylamide gel) was used for electrophoresis. The separated proteins were then transferred onto a polyvinylidene fluoride (PVDF) membrane using the western-blot transfer unit. After blocking the membranes with 5% milk powder/PBS for an hour, 1:10 diluted serum obtained from HN allergic human and HN-sensitized mice were incubated overnight at 4°C. Control serum (PBS mice) was incubated as well. Membranes were washed again and incubated with secondary antibodies (anti-mouse or anti-human IgE) for an hour at RT. After washing the membranes again, the specific bands were detected using the chemiluminescent ECL plus detection reagent (contains HRP- substrate luminol).

#### **5.2.4.5. Principles of flow cytometry**

Flow cytometry is a technique to evaluate simultaneously multiple physical characteristics of a single cell. The principle behind this measurement depends on light scattering, light excitation and emission of fluorescence to fluorochromes conjugated to a single cell or particles. Each cell or a particle size range from 0.5 to 50 µm in diameter. Lasers are commonly used as light source in flow cytometry. The population of single cell suspension tagged to fluorochrome is injected into the centre of the sheath flow. Single cells pass one by one through a beam of interrogation point in which appropriate light excitation source, usually laser, intersects the cells. The emitted light in all direction is detected by photomultiplier tubes which are controlled by optical filters that separate specific wavelength bands (also known as fluorescence channels).

Physical parameters such as the size of a cell are roughly measured by forward light scatter (FSC) whereas the cell's internal granularity is measured by side scatter channel (SSC). This parameter can resolve certain target cell populations which are conjugated by fluorochrome dyes to differentiate between surface and internal staining. It can as well differentiate between live cells and/or debris.

#### **5.2.4.6. Flow cytometric analysis of T- and B-cells**

Single-cell suspensions were prepared from spleen and lymph nodes (mesenteric, axillary and inguinal) from AD and FA mouse experiments.  $2 \times 10^6$  cells were washed with 1% BSA in 1x PBS and centrifuged at 340g for 10 min at 4°C. Supernatant was removed and the unspecific binding was blocked with anti Fc $\gamma$ -receptor (2.4G). Cells were then stained with fluorochrome-conjugated monoclonal antibodies against mouse for 15 min at 4°C. T cell panel analyses were performed with antibodies against mouse CD3 $\epsilon$  (145-2C11), CD4 (GK1.5), CD8 (53-7), CD44 (IM7), CD62L (MEL14) and the B cell panel with anti-mouse CD19 (ID3), CD21/CD35 (7G6), CD23 (B3B4). Gating strategy for T cell composition involves CD3 $^+$  CD4 $^+$  and/or CD3 $^+$  CD8 $^+$ . Further these cells were sub-gated to differentiate between CD62L (marker for naive T cells) and CD44 (marker for memory T cells compartment). B cells were gated on CD19 $^+$  and their subsets were further analysed for CD21/CD35 and CD23 expression. Dead cells were excluded using 1  $\mu$ M 7- aminoactinomycin D (7-ADD). All the analysis of the data was performed using FLOWJO software.

#### **5.2.4.7. Flow cytometric analysis of plasma cells**

About  $1 \times 10^7$  splenocytes were washed with 1% BSA in 1x PBS and centrifuged at 340g for 10 min at 4°C. The cells surface was blocked with anti Fc $\gamma$ -receptor (2.4G) and the flow cytometry analysis was performed by staining for surface markers with anti-mouse B220 (RA3.6B2) and anti-mouse CD138 (281-2) including 7-ADD to exclude dead cells. After washing the unbound antibodies, cells were fixed with 2% paraformaldehyde for 10 min at 4°C. The cells were washed in 0.5% saponin/FACS buffer and intracellular staining was performed with anti-mouse IgG1 (X56) and OVA in 0.5% saponin/FACS buffer for 30 min at 4°C. In another experiment intracellular staining was also performed using anti-kappa-lambda along with anti- mouse IgG1. One thousand fold unlabelled excess OVA were used to check the specificity of OVA binding. After the last washing step, the flow cytometry analysis for plasma cell staining was examined.

Here, 7-ADD<sup>neg</sup> B220<sup>low</sup> IgG1<sup>hi</sup> CD138<sup>+</sup> and OVA<sup>+</sup> cells were considered as OVA specific IgG1<sup>+</sup> plasma cells. Another marker was considered for staining plasma cells 7-ADD<sup>neg</sup> B220<sup>low</sup> IgG1<sup>hi</sup> CD138<sup>+</sup> and kappa-lambda<sup>+</sup> in HN-induced intestinal anaphylaxis mouse model.

### **5.2.5. Immunohistochemistry**

Embedded skin samples were cut into 5 µm sections using cryotome at -24 or -28°C. These thin sections were transferred onto glass slides and stored at -80°C until further use. Similarly, 1-2 µm sections of formalin-fixed, paraffin-embedded tissue were cut and kept at RT until further analysis.

#### **5.2.5.1. Staining of cellular infiltrates in the lesional skin of atopic eczema mouse**

Cryo-sections were rehydrated with 1x TBS prior to staining protocol. Slides were blocked with 5% normal goat serum in 1x TBS for 20 min followed by incubation for 1 h with rat anti-mouse CD4 (RM4-5, 1:30 dilution), CD8 (53-6.7, 1:30 dilution) or CD11c (HL3, 1:100 dilution). After incubation, slides were washed in 1x TBS and incubated with biotinylated polyclonal goat anti-rat IgG. Dako REAL<sup>TM</sup> detection system Alkaline Phosphatase/RED kit method was used for the development and papanicolaou dye as counter staining. Mast cells were stained with 0.1% toluidine blue. Negative controls either without primary or secondary antibodies or substrate were run in parallel. All the slides were mounted with gelatin.

#### **5.2.5.2. Staining of cellular infiltrates in the jejunum of food allergy mouse**

Slides containing sections were deparaffinized, and subjected to a heat induced epitope retrieval step. Afterwards, these slides were rinsed in cool running water and washed in Tris-buffered saline (pH 7.4). Endogenous peroxidase was blocked using Dako REAL<sup>TM</sup> Peroxidase Blocking-Solution prior to incubation with goat anti-mouse CD3ε antibody (M-20) and anti-mouse B220 antibodies for 30 minutes at room temperature, rinsed and incubated again for 30 minutes at RT with biotinylated rabbit anti-goat secondary antibody followed by incubation for 30 minutes at RT with alkaline phosphatase labelled streptavidin (Dako). Alkaline phosphatase was revealed by Fast Red as chromogen for 20 minutes at RT. Nuclei were counterstained with hematoxylin. Eosinophils were detected by Sirius red whereas mast cells were stained by chloroacetate esterase method. All the slides were mounted with gelatin.

### 5.2.5.3. Histological analyses

For cryo-sections, cells were analyzed by using Axiovision measuring-tools on the AxioPlan light microscope at x100 magnification and expressed as cells per square millimeter. Images from paraffin embedded sections were acquired using a AxioImager Z1 microscope. Positive cells were quantified in 5 high power fields (1 hpf = 0.237 mm<sup>2</sup>). All immunohistochemical evaluations were performed in a blinded manner.

### 5.2.6. Molecular biology methods

The gene expression analysis was performed in skin of AD as well as jejunum of FA mice. RNA was isolated from the frozen tissues, followed by complementary DNA (cDNA) synthesis and analysis by quantitative PCR (qPCR).

#### 5.2.6.1. RNA isolation from murine skin and jejunum

RNA extraction was performed from frozen tissues of the skin of AD and jejunum of FA mice using Precellys<sup>®</sup>24 Homogeniser followed by Nucleospin<sup>®</sup> RNA II – kit according to manufacturer's instructions. Accordingly, 500 µl of lysis buffer containing 1% β-mercaptoethanol was added to skin and jejunum samples and subjected to homogenization. Homogenized samples were pipetted into shredded columns and centrifuged at 11,000g for 3 min. The supernatant was retained and proteinase K was added to digest the proteins at 55°C for 10min. After digestion, the solution was passed onto the RNA binding column and centrifuged at 8,000 g for 1min. Supernatant was discarded and DNA was digested with DNAase enzyme for 15 at RT. After performing several washing steps and centrifugations, RNA was eluted from column with 50 µl RNAase-free-water. RNA concentration was measured by Nanodrop UV-Vis spectrophotometer at 260 nm. RNA quality was checked on the 1% agarose gel. Remaining RNA was stored at -80°C until analysis.

#### 5.2.6.2. cDNA synthesis

Reverse transcriptase-PCR with TaqMan<sup>®</sup> Reverse Transcription Reagents was used for synthesizing cDNA. This reagents contains a recombinant Moloney Murine Leukemia Virus Reverse Transcriptase, random hexamers and oligo d(T)<sub>16</sub>. Total RNA (1–2 µg) in a total volume of 7.7 µl along with 12.3 µl reaction mix was used to transcribe cDNA (Table 4). The steps

involved to transcribe cDNA using Thermal cycler are given in the table 5. The synthesized cDNA samples were stored at -20°C.

Component	Sample vlume	Final concentration
10x TaqMan RT Puffer	2.0 µl	1x
25 mM MgCl <sub>2</sub> (or prediluted)	4.4 µl	3-6 mM
2 mM dNTPs Mixture (each)	4.0 µl	500 µM (each)
50 µM Random Hexamers	0.5 µl	1.25 µM
50 µM Oligo d(T)16	0.5 µl	1.25 µM
20 U/µl RNase Inhibitor	0.4 µl	0.4 U/µl
50 U/µl MultiScribe Reverse Transcriptase	0.5 µl	1.25 U/µl

**Table 4 Reaction mix of transcriptase reagents.**

Step	Temperature	Time
RNA-primer template binding	25°C	10 min
Reverse transcription	48°C	40 min
Reverse transcriptase inactivation	95°C	05 min

**Table 5 Transcribed cDNA synthesis program.**

### 5.2.6.3. Real-time PCR/quantitative PCR

Routine and widely used fluorescence-based real-time polymerase chain reaction (real-time PCR/qPCR) is a technique for quantifying, analysing and characterizing gene amplification with higher sensitivity. qPCR was performed with the LightCycler<sup>®</sup> Fast Start DNA Master SYBR Green I and according to the manufacturer's instructions. Here, the bound high affinity SYBR Green fluorescence dye binds to double stranded DNA forming a PCR product, which is visualized by real time detection method. Oligonucleotide primers were designed for qPCR quantification using Primer3 software<sup>152</sup> as described elsewhere<sup>153</sup> and synthesized by TIB MOLBIOL, Berlin, Germany. Pre-diluted cDNA of 2 µl (1:2 to 1:4 dilution) was mixed with 3 µl reaction mix (Table 6). Primer sequences for murine target gene detection are provided in the table 7.

Expression levels of target gene mRNA based on the threshold cycle value ( $C_T$ ) was quantified relative to the expression of the reference housekeeping gene hypoxanthine-guanine phosphoribosyltransferase (*Hprt*)<sup>154,155</sup>.

Component	Volume per sample	Final concentration
10x FastStart DNA Master SYBR Green I	0.50 µl	1x
25 mM MgCl <sub>2</sub>	0.80 µl	3-5 mM
10 µM Primer, forward	0.25 µl	100-500 nM
10 µM Primer, reverse	0.25 µl	100-500 nM
H <sub>2</sub> O, PCR grade	1.20 µl	

**Table 6 Real-time/qPCR reaction mix.**

Gene	Sequence	Base pairs	Product size	Efficiency
<i>FcεR1a</i>	for: accgttcaagacagtggaaa-3' rev: agtagatcaccttgcggaca-3'	21 20	187 bp	2.00
<i>Flg</i>	for: 5'-cactgagcaagaagagctgaa-3' rev: 5'-cgatgtcttggctcatctgga-3'	22 20	81 bp	1.70
<i>Hprt</i>	for: 5'-cgctcgtgattagcagatgatg-3' rev: 5'-aatccagcaggtcagcaaaag-3'	20 20	221 bp	1.80
<i>Ifng</i>	for: 5'-aactattttaactcaagtggcatagat-3' rev: 5'-tgctgttgcgaagaaggtag-3'	27 21	217 bp	1.95
<i>Jag-2</i>	for: 5'-cgagggtcaaggtggaaaacag-3' rev: 5'-ccaccatacgcagataacca-3'	20 20	118 bp	1.80
<i>Krt-14</i>	for: 5'-aacctggaggagaccaaagg-3' rev: 5'-ggatgactgagagccagagg-3'	20 20	261 bp	2.00
<i>Il4</i>	for: 5'-gactctttcgggcttttcg-3' rev: 5'-tgatgctcttaaggcttcca-3'	19 21	105 bp	1.97
<i>IL-10</i>	for: tttaagggttacttggttc-3' rev: agggcttcaagcttctcacc-3'	21 20	137bp	1.86
<i>Lor</i>	for: 5'-tccttcctcactcatcttc-3' rev: 5'-ctctccaccagaggttttc-3'	21 21	126 bp	1.86
<i>TGF-β</i>	for: 5'-gcaacaacgccatctatgag-3' rev: 5'-agacagccactcagcgat-3'	20 20	245 bp	1.79
<i>Tgm-1</i>	21 for: 5'-agacccaaggctcctcaatgc-3' 21 rev: 5'-actgggaaagctgtgactg-3'	21 21	131 bp	1.89

**Table 7 Primers for real-time/qPCR**

### 5.2.7. Statistical analyses

Statistical analyses were performed using GraphPad Prism software. Assumed significance of differences between the independent groups for sample values with non-Gaussian distribution was analyzed by non-parametric Mann-Whitney t-test method. Each data points represented in the graph are shown as either a dot or box plot with the median given as bar which include mean±SEM. A p-value of <0.05 for all tests was considered significant.

## 6. RESULTS

### 6.1. Clinical severity remained unchanged upon bortezomib treatment in an atopic eczema mouse

In a mouse model of atopic eczema associated with increased IgE, bortezomib (Bz) was applied to test for its potential clinical efficacy. Here, a previously established mouse model of allergen induced eczema was used expressing typical features of human AD<sup>144</sup>. After the second patch (as indicated in Figure 8), Bz was injected in mice intravenously on day 36. The severity symptom score from OVA-induced eczematous skin lesions remained stable upon treatment with Bz (Figure 9)<sup>147</sup>. This experiment indicates that Bz is not clinically efficacious at the level of skin.

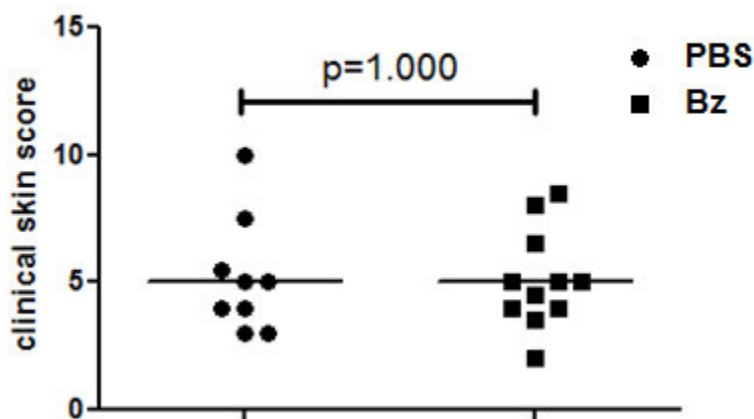
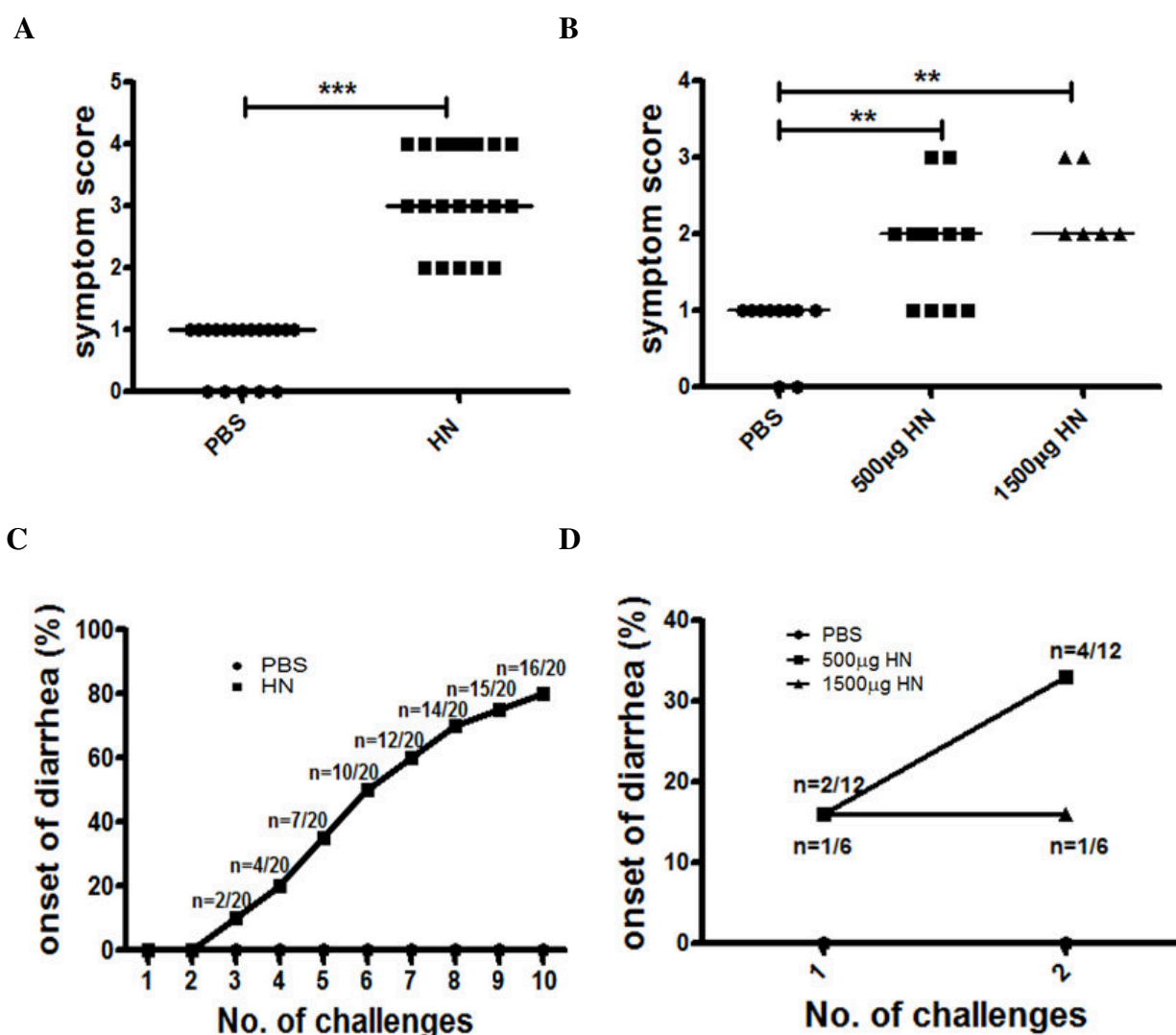


**Figure 9<sup>147</sup>** Proteasome inhibitor Bz application *in vivo* showed no clinical efficacy in mouse with atopic skin eczema. The severity of skin eczema was evaluated on day 71, as described in method section. Values from individual mice are shown as a dot plot with the median given as bar.

### 6.2 Establishment of oral-induced intestinal anaphylaxis in mice

Initially it was aimed to establish a hazelnut (HN) induced intestinal FA mouse model with clinical signs and symptoms of human anaphylaxis. HN was chosen as a sensitizing allergen as it is a major cause of food allergy in children and adults<sup>156-158</sup>. For that purpose two mouse models based on our own experience<sup>159</sup> and the literature<sup>105,107</sup> were examined. We observed a significant onset of local symptoms measured by diarrhea frequency at day 55 and 64 in both the models (Figure 10A-D). However, the immediate drop of rectal temperature as a parameter of systemic effect after HN antigen provocation, was more pronounced in the HN-alum model ( $p < 0.0001$ ; Figure 10E), but not in the HN-SEB model (Figure 10F). According to these clinical observations higher HN specific IgE (sIgE) concentrations were measured in the HN-alum

(Figure 10G) in comparison to the HN-SEB model (Figure 10H). In the non-sensitized PBS group sIgE was not detectable. Overall the HN-SEB model showed a weaker humoral immune response to HN compared to HN-alum model. The correlation analysis shows a moderate association between the clinical severity versus sIgE towards HN in the HN-alum model (Figure 11,  $p=0.0022$ ;  $r=0.6445$ ). A systemic increase of mucosal mast cell derived protease mMCP-1 was detected (Figure 10I,J), although higher levels were measured in the HN-alum model (Figure 10I;  $p=0.0022$ ). Taken together, these data indicate a higher clinical severity and a more pronounced humoral IgE response in the HN-alum model in comparison to the HN-SEB model.



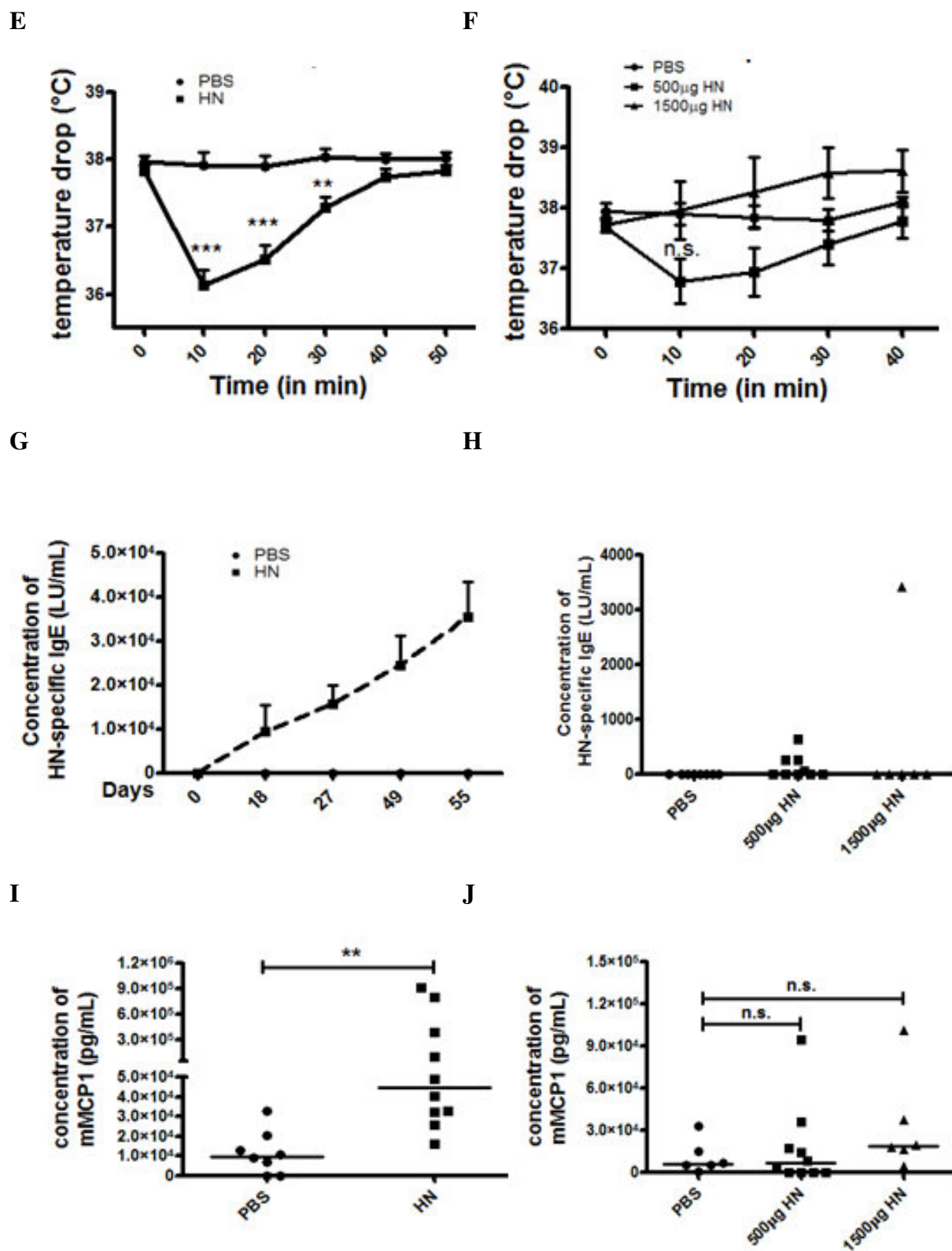


**Figure 10 Comparative analysis of the two investigated food allergy models.** 10 A/C/E/G/I shows data from intraperitoneal sensitization with HN/alum followed by intragastrical HN challenge. 10 B/D/F/H/J

shows the data from the intragastrical sensitization with HN/SEB followed by HN challenge. Each mouse are shown as a dot plot with the median given as bar with mean  $\pm$ SEM. \*\*  $p < 0.01$ , \*\*\*  $p < 0.001$ .

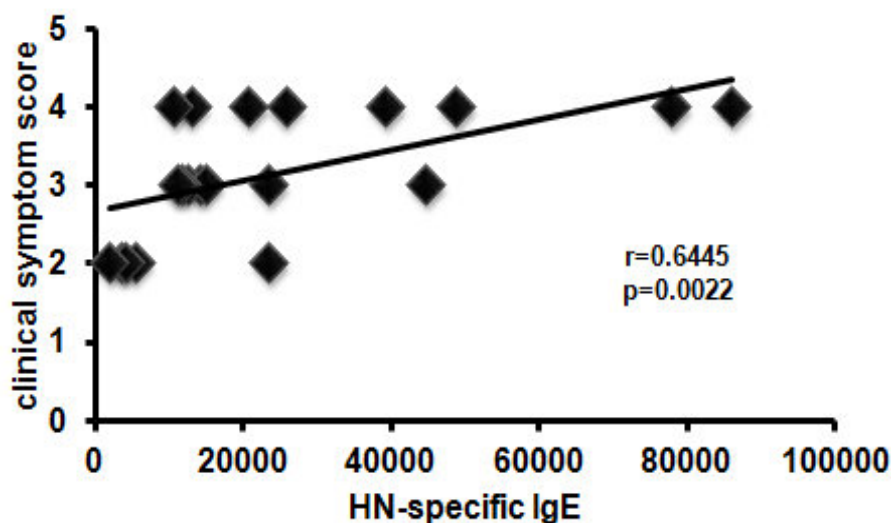
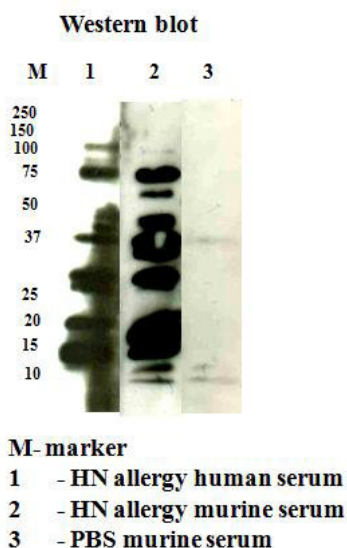


Figure 11 Correlation between clinical symptoms vs hazelnut sIgE.

### 6.3. Comparative analysis of IgE-binding patterns from human and mouse serum

As allergen-sIgE was analyzed in the HN-alum model, next IgE-binding profiles were determined using HN allergic human and mouse sera by western blot. The transferred HN proteins were probed for IgE-binding to allergens from sera of HN allergic human and mouse. A stronger IgE reactivity of to similar HN proteins/allergens was determined (Figure 12A). These allergenic reactivity based on their relative molecular weight was compared between sera from human and mouse (Figure 12A) and are summarized in the table 8 (B) according to their binding reactivity.

A



B

Sl. No	Hazelnut allergen	Molecular weight (kDa)	Allergen reactivity to mice serum	Allergen reactivity to human serum
1	Cora1 (PR-10 like protein, Betv2 homologue)	17-18	+++	+++
2	Cora2 (Profilin, Betv2 homologue)	14	+++	+++
3	Cora8 (Lipid transfer protein)	9.5	++	++
4	Cora9 (11S globulin-like protein)	40	+	+
5	Cora11 (7S Vicilin-like globulin)	48	-	-
6	2S albumin	32	+++	+++
7	Legumin	35	+++	+++

**Figure 12 Detection of HN-specific IgE by western blot analysis.** A. HN allergic sera obtained from human and mice were subjected to probe for specific IgE-binding proteins from HN extract by immunoblotting technique. In each lane 10  $\mu$ g of total protein extract was loaded. B. Table 8 shows comparison of specific allergen reactivity based on their relative molecular weight in human and mouse allergic sera. +++higher, ++medium, +low and -no reactivity to allergens, respectively.

#### 6.4. Bortezomib treatment ameliorates hazelnut-induced intestinal anaphylaxis in mice.

Specific therapeutic treatments to cure FA are limited. In this regard, it was investigated whether Bz drug administration *in vivo* dampens the clinical severity of intestinal anaphylaxis and the specific humoral immune response (Figure 10). After development of clinical symptoms towards HN, Bz was administered intravenously. Interestingly, clinical severity (Figure 13A;  $p=0.0014$ ), the onset of diarrhea (Figure 13B) and the drop of rectal temperature (Figure 13C;  $p<0.0001$ ) was reduced on day 55.

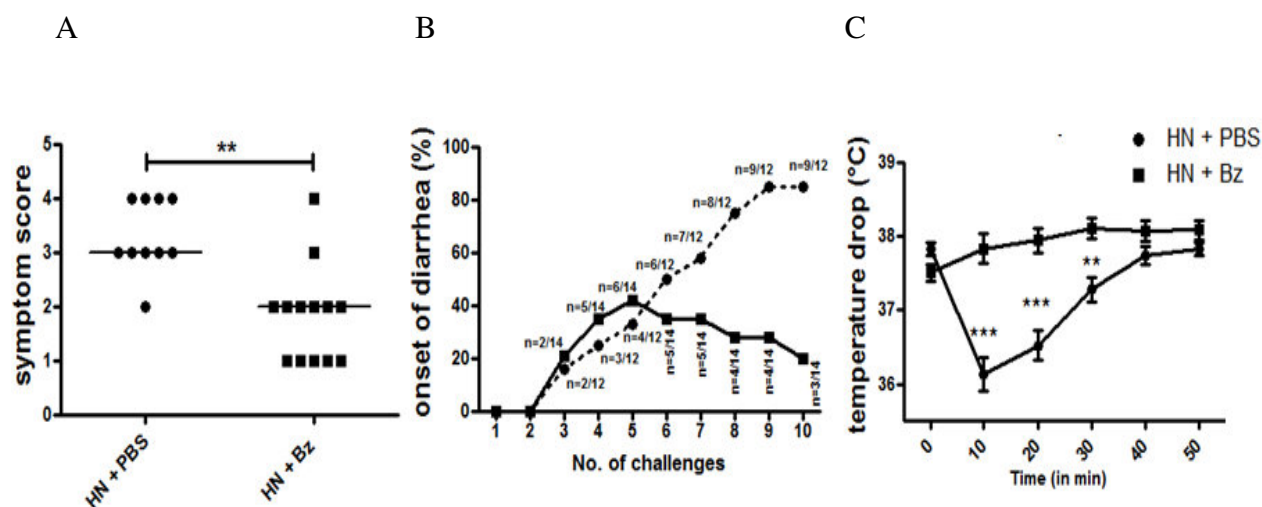


**Figure 13 Bz treatment improves clinical symptoms in mice with intestinal anaphylaxis.** A. Clinical symptoms observed with or without Bz treatment on day 55. B. Diarrhea onset in the HN+PBS group (n=12) compared to HN+Bz (n=14). C. Rectal temperature measurement between the two groups. Mean  $\pm$ SEM are shown. \*\* p < 0.01, \*\*\* p < 0.001.

### 6.5. Reduction of plasma cells by proteasome inhibitor in AD and FA murine models

To investigate in more detail why the clinical severity upon the *in vivo* treatment with Bz in AD<sup>147</sup> and HN-alum FA mice was diminished, it was investigated next whether the proportion of plasma cells is affected due to the treatment (Figure 14A,B). Bz has been previously shown to affect plasma cell survival<sup>129</sup>. Flow cytometric analysis showed that Bz reduced significantly the total number per spleen of the IgG1-specific plasma cell subset (B220<sup>low</sup> IgG1<sup>high</sup> CD138<sup>+</sup>) by 70% (Figure 14B; p=0.0185) and even more potently the OVA-specific IgG1<sup>hi</sup> cell subset (identified as B220<sup>low</sup> IgG1<sup>high</sup> CD138<sup>+</sup> OVA<sup>+</sup>) by 82% in the AD model<sup>147</sup> (Figure 14B; p=0.0276).

Likewise, a reduction of 59% in the population of plasma cells (B220<sup>low</sup> IgG1<sup>high</sup> CD138<sup>+</sup>  $\kappa/\lambda$ ) was observed in the HN-alum model (Figure 14C,D; p=0.0316). Here, the cells expressing IgG1<sup>hi</sup> subsets are relatively more abundant than the small IgE<sup>hi</sup> plasma cell subset. Therefore, B220<sup>low</sup> IgG1<sup>hi</sup> subset on plasma cells was used to analyze low abundance of OVA-specific plasma cells.

Taken together, plasma cells were diminished by Bz upon *in-vivo* treatment in both allergen driven mouse models of atopic eczema and intestinal anaphylaxis.

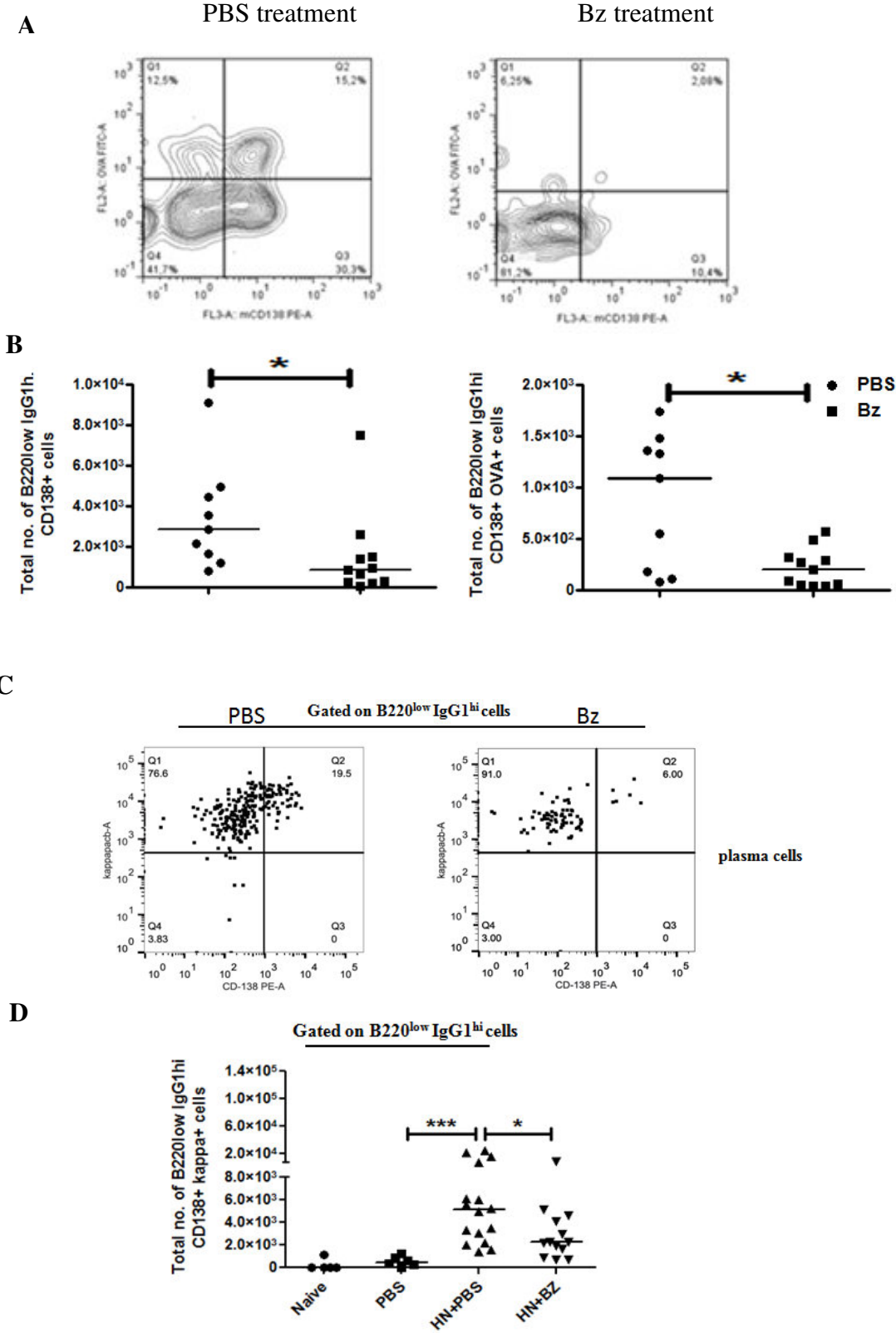
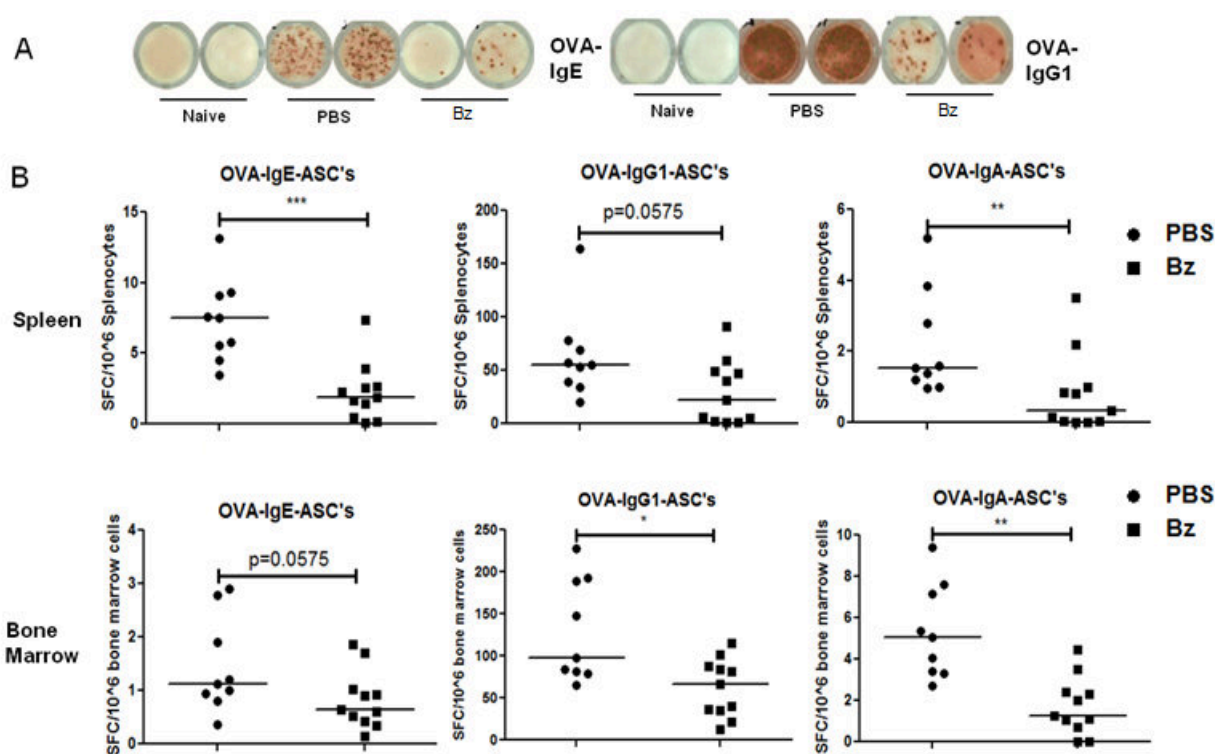


Figure 14 Bz treatment *in vivo* reduces plasma cell numbers in the spleen of AD and FA mice. A. Flow cytometry picture represents reduction of OVA-specific plasma cells in the spleen of AD mice upon

Bz treatment<sup>147</sup>. B. Total and OVA-specific plasma cells from individual mice are shown as a dot plot with the median as bar<sup>147</sup>. C. Representative picture showing Bz suppresses plasma cells in HN-alum FA mice. D. Plasma cell numbers from each mouse are shown as a dot plot with the median as bar. \*  $p < 0.05$ ; \*\*\*  $p < 0.001$ .

ELISpot assay was used to further confirm the frequencies of antibody-secreting cells (ASC's) *ex vivo*<sup>147</sup>. This assay revealed that Bz treatment abolished the number of cells secreting antigen-specific antibodies<sup>147</sup> (Figure 15A,B). Reduction in the percentage of antigen-specific ASC's from spleen and bone marrow are provided in the table 9.



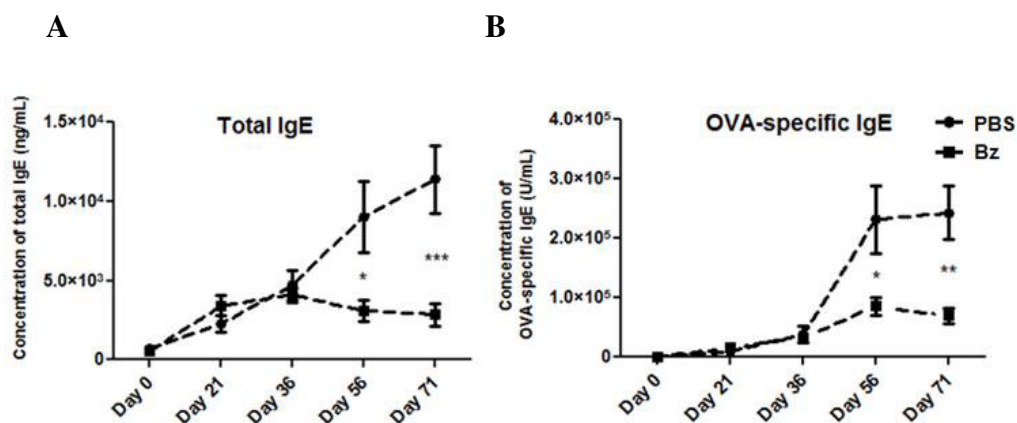
**Figure 15 Reduction in the number of antigen specific antibody secreting cells after Bz treatment in mice with AD analyzed by ELISPOT<sup>147</sup>.** (A) Representative pictures reflect the effect of Bz on OVA-IgE, and OVA-IgG1-specific antibody secreting cells in the spleen on day 71. (b) Overall decrease in the ASC's producing OVA-specific immunoglobulin subtypes – IgE, IgG1 and IgA in the spleen and bone marrow cells, respectively. Values from individual mice are shown as a dot plot with the median given as bar. \*  $p < 0.05$ , \*\*  $p < 0.01$ , \*\*\*  $p < 0.001$ . (Published data<sup>147</sup>)

OVA-specific immunoglobulin's	Reduction of ASC's (%)	Significance
<u>Spleen</u>		
OVA-IgE	75%	P=0.0008
OVA-IgG1	59%	P=0.0575
OVA-IgA	78%	P=0.0098
<u>Bone marrow</u>		
OVA-IgE	43%	P=0.0575
OVA-IgG1	32%	P=0.0014
OVA-IgA	68%	P=0.0334

**Table 9 OVA-specific ASC's in the spleen and bone marrow of AD mice upon Bz treatment at day 71<sup>147</sup>**

### 6.6. Reduction of humoral immune response upon bortezomib treatment

Next, the humoral immune response upon Bz treatment was investigated in the both allergy models. A strong reduction of the antibody levels in serum of mice from both models was measured. Serum obtained from AD mice at different intervals was subjected for determining total and allergen specific immunoglobulin subtypes such as IgE, IgG1, IgA, and IgM (Figure 16 A-H)<sup>147</sup>. Before Bz treatment in this model, Ig titers remained comparable (on days 0, 21, 36) between the PBS vs Bz groups whereas a strong reduction was observed on days 56 and 71 (i.e. after bz treatment). Interestingly, the rapid reduction in immunoglobulin concentrations was observed after 4 days of the first Bz injection (Figure 16). By contrast, the IgG2a isotype was not affected in both groups (data not shown). The decrease in the total and allergen-specific immunoglobulins is depicted in table 10.



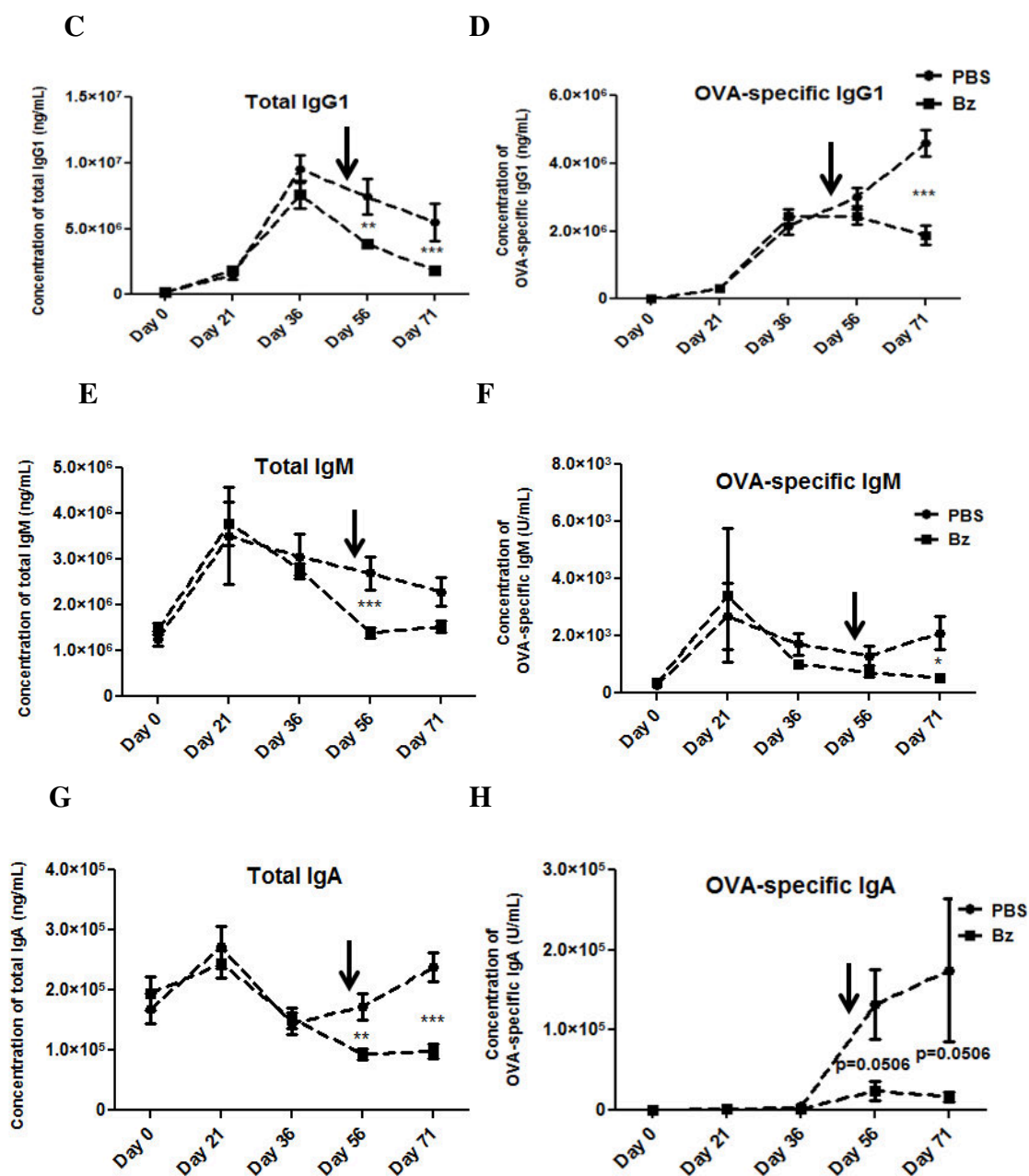


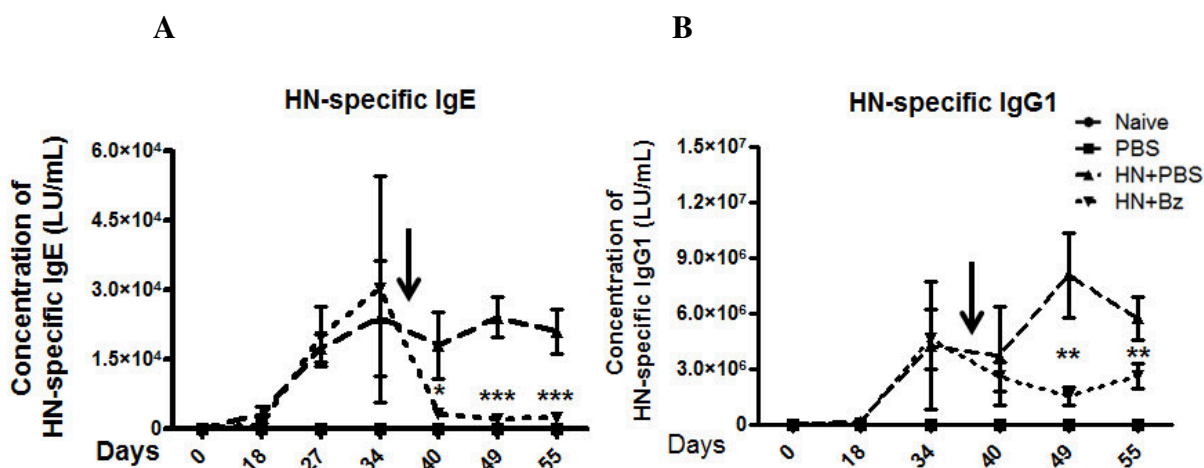
**Figure 16 Reduction of total and OVA-specific immunoglobulin subtypes after Bz treatment in AD mice<sup>147</sup>.** A-H. Total and OVA-specific IgE, IgG1, IgM and IgA were analyzed by ELISA from murine sera at the time intervals as indicated. Graph shows mean+SEM from 9-11 mice, respectively. '↓' - arrow sign in the graph represents the first injection of the Bz (i.e. on day 52). \* p < 0.05, \*\* p < 0.01, \*\*\* p < 0.001

Immunoglobulin's	Reduction (%)	Significance
<b><u>OVA-specific Ig's</u></b>		
IgE	79%	P=0.0014
IgG1	60%	P=0.0003
IgM	67%	P=0.0317
IgA	82%	P=0.0506
<b><u>Total Ig's</u></b>		
IgE	72%	p=0.0008
IgG1	42%	p=0.0002
IgM	29%	p=0.0575
IgA	65%	p=0.0004

**Table 10 Percentage of antibody reduction among the isotypes and p values from sera of AD treatment at day 71<sup>147</sup>**

HN-specific IgE, IgG1 and IgA were determined from HN-alum food allergy mouse model before and after treatment with Bz as well. As evidenced by ELISA measurements, there was a rapid reduction of the allergen-specific antibody concentration in the serum (Figure 17 A-C). The percentages in reduction as well as p values are provided in table 11.

Taken together, Bz suppressed all isotypes, but IgE most pronounced compared to other immunoglobulins in both the allergy models.



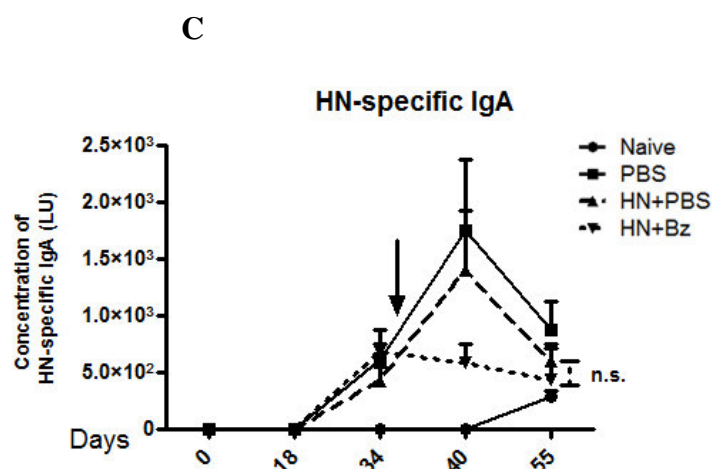


**Figure 17 Reduction of HN-specific immunoglobulins upon Bz treatment in HN-alum FA mouse.** A. ELISA measurement of HN-specific IgE, IgG1 and IgA from FA mice serum at the time points indicated in the figure 8. Graph shows mean+SEM from 14-16 mice, respectively. '↓' - arrow sign in the graph represents the first injection of the Bz (i.e. on day 36). \*  $p < 0.05$ , \*\*  $p < 0.01$ , \*\*\*  $p < 0.001$ . n.s.=not significant.

HN-specific Ig's	Reduction (%)	Significance
IgE	89%	$p < 0.0001$
IgG1	55%	$p = 0.0025$
IgA	n.a.*	n.s.**

**Table 11 Reduction of HN-specific immunoglobulins in the serum of HN-alum FA mice upon Bz treatment.** \*n.a.=not applicable \*\*n.s.=not significant

### 6.7. T- and B- cell subsets upon treatment with bortezomib

As plasma cells were decreased by Bz treatment, next the proportion of T- and B-cell distribution in both models was analyzed. First, the examination of the T cell subsets from spleen, axillary and inguinal draining lymph nodes from the AD model showed a reduction in the proportion of  $CD4^+$  (Figure. 18A;  $p = 0.0303$ ) and transiently  $CD8^+$  T cells (Figure. 18B;  $p = 0.125$ ) in the axillary lymph node after Bz application, but that no changes were observed in the spleen or inguinal lymph node (data not shown)<sup>147</sup>. Further,  $CD4^+$  and  $CD8^+$  memory T cell ( $CD44^+$   $CD62L^-$ ) subsets remained unchanged (Figure 18C,D) including naïve  $CD4^+$  and  $CD8^+$  T cells (data not shown)<sup>147</sup>. Furthermore, Bz did not affect the proportion of  $CD19^+$  B cells (Figure 18E),

marginal zone B cells ( $CD19^+ CD21^{high} CD23^{low}$ ; Figure 18F) and follicular zone B cells ( $CD19^+ CD21^{low} CD23^{high}$ ; data not shown) in the spleen, axillary and inguinal lymph nodes, respectively<sup>147</sup>. Besides the reduction of T cells in the axillary lymph nodes, the subsets of T- and B-cells remained largely stable in the spleen and inguinal lymph nodes to Bz treatment in this model.

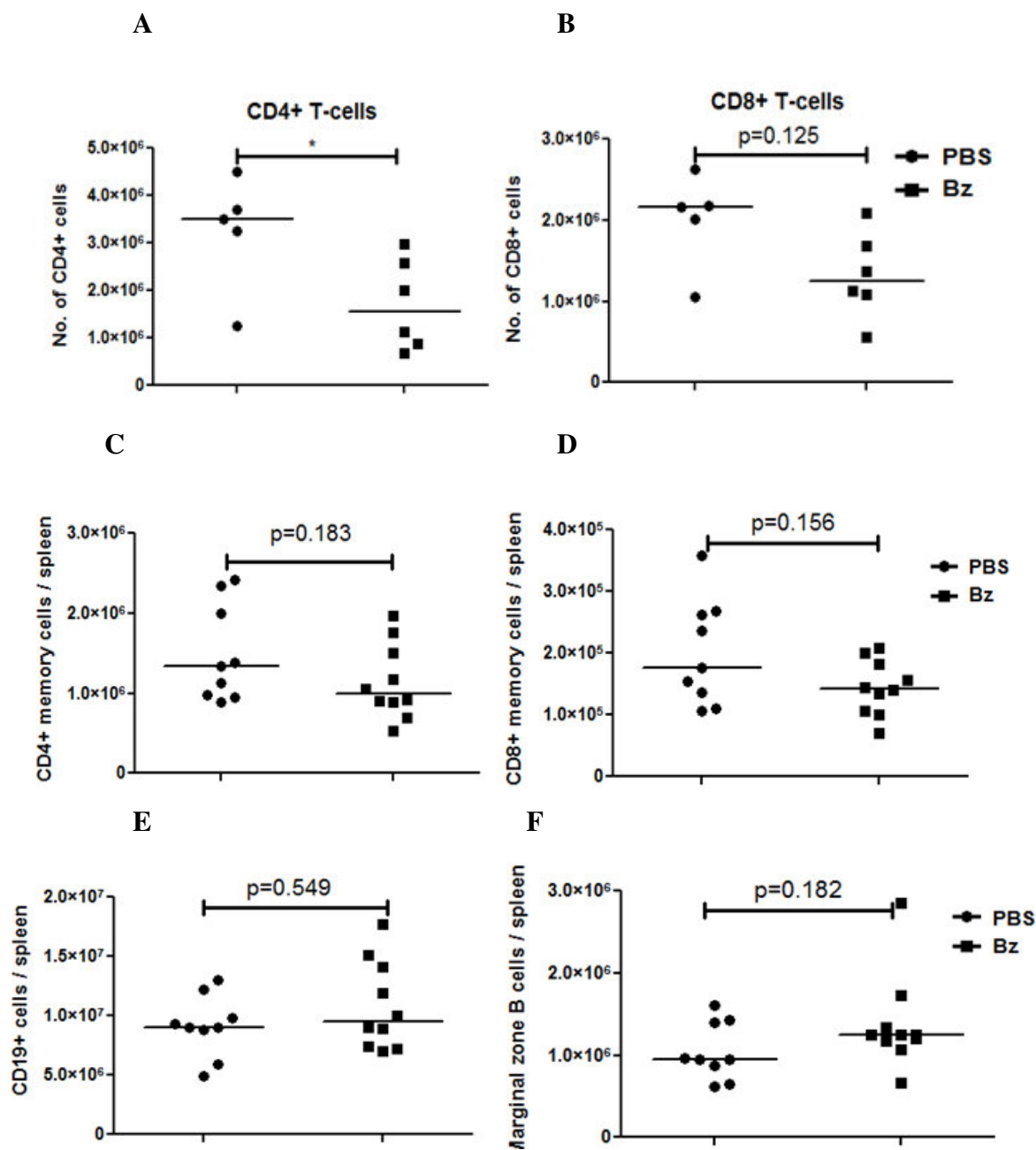


**Figure 18 Reduction of T cell numbers upon Bz treatment in the axillary lymph node of mice with AD<sup>147</sup>.** A-B. CD4<sup>+</sup> and CD8<sup>+</sup> T cells in the axillary lymph nodes (required cell numbers were obtained by

pooling two lymph nodes together from the same group). C-D. Analysis of CD4<sup>+</sup> and CD8<sup>+</sup> memory T-cell numbers in the spleen. E-F. Total number of CD19<sup>+</sup> and marginal zone B cells. The data are shown as a dot plot with the median given as bar. \*  $p < 0.05$

In the HN-alum FA mice model, we observed a significant increase of CD19<sup>+</sup> B cells (Figure 19A;  $p=0.0400$ ) as well as follicular zone B cells (CD19<sup>+</sup> CD21<sup>low</sup> CD23<sup>high</sup>; Figure 19B;  $p=0.0193$ ) towards allergen provocation in HN+PBS group compared to PBS control. Interestingly, these B-cell subsets were reduced by Bz in this model (Figure 19A,B), although no changes occurred in the T cell compartment (data not shown). The decrease in tendency in the proportions of CD19<sup>+</sup> B cells (Figure 19B;  $p=0.0508$ ) and also significant reduction of follicular zone B cells (Figure 19B;  $p=0.0378$ ) was observed, but marginal zone B cells (CD19<sup>+</sup> CD21<sup>high</sup> CD23<sup>low</sup>; data not shown) remained unchanged. Thus, Bz directly targets B-cells subset of in the FA model.

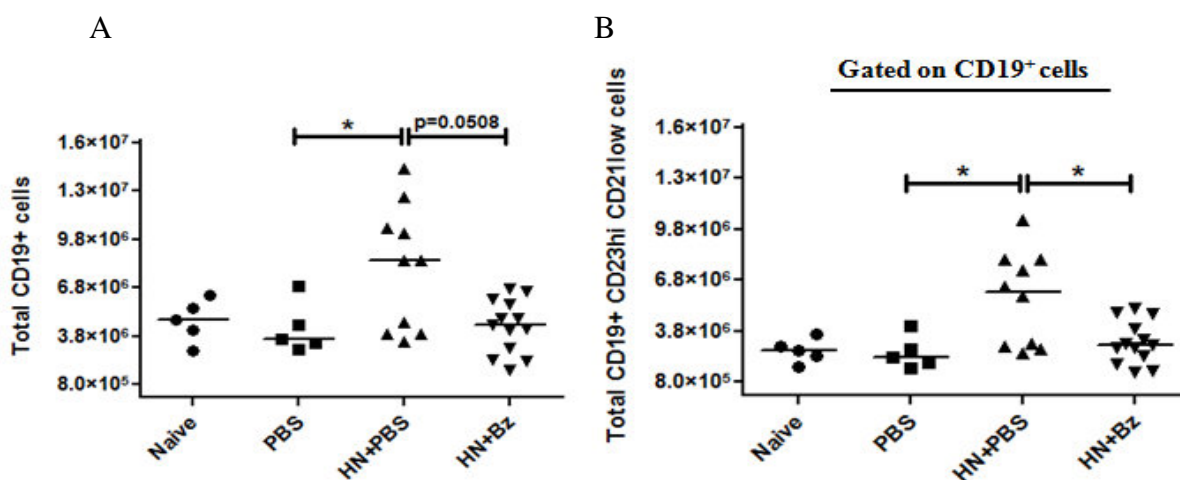


**Figure 19 Bz suppress B cells in the spleen of mice with gastrointestinal FA.** A-B. Analysis of total number of CD19<sup>+</sup> and follicular B-cells (CD19<sup>+</sup> CD23<sup>hi</sup> CD21<sup>low</sup>) by flow cytometry. The data are shown as a dot plot with the median given as bar. \*  $p < 0.05$ , \*\*  $p < 0.01$ , \*\*\*  $p < 0.001$

### 6.8. Interference with the local inflammatory cells

Atopic diseases are often manifested by locally infiltrating cells<sup>20,144,160,161</sup>. Therefore, the local inflammatory response in lesional skin (AD) and the jejunum (FA) mice, respectively was investigated by immunohistochemistry.

Mice treated with Bz show a subsequent reduction of CD4<sup>+</sup> (Figure 20A,B; decrease by 66%;  $p=0.0095$ ) and CD8<sup>+</sup> T cells (Figure 20B; decrease by 67%;  $p=0.0095$ ) in their skin lesions<sup>147</sup>. CD11c<sup>+</sup> and mast cell numbers remained comparable between the groups (data not shown).

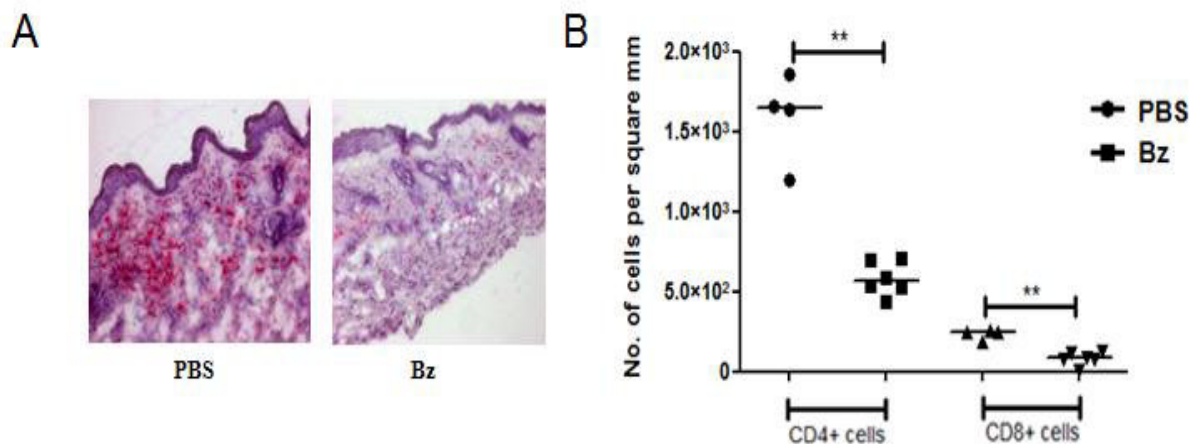


**Figure 20 Bz interferes with infiltrating T cells in to the lesional skin of AD mouse<sup>147</sup>.** (A) Representative picture of the skin sections stained for CD4<sup>+</sup> T cells in AD skin of Bz-treated versus PBS-treated control mice. (B) Analysis of CD4<sup>+</sup> and CD8<sup>+</sup> T cells in the skin of AD mice. The data are shown as a dot plot with the median given as bar. \*\*  $p < 0.01$

The analysis of the jejunum from the mouse intestine after repetitive HN challenge revealed that the frequency of mast cells remained stable (Figure 21C). An increase of eosinophils in the HN/PBS group (Figure 21A,D;  $p=0.0480$ ) compared to control group was determined, which was reduced by Bz group without reaching statistical significance (Figure 21D;  $p=0.0630$ ). Interestingly, the frequency of eosinophils correlated with the clinical severity score (Figure 22;  $p=0.0002$ ;  $r=0.7256$ ). By contrast, B220<sup>+</sup> cells (Figure 21B,F;  $p=0.0265$ ), but not T cells were largely reduced (Figure 21E) after the Bz treatment compared to the control group (PBS). Collectively, local infiltrating eosinophils and B220<sup>+</sup> cells were suppressed by Bz in both the mice models.

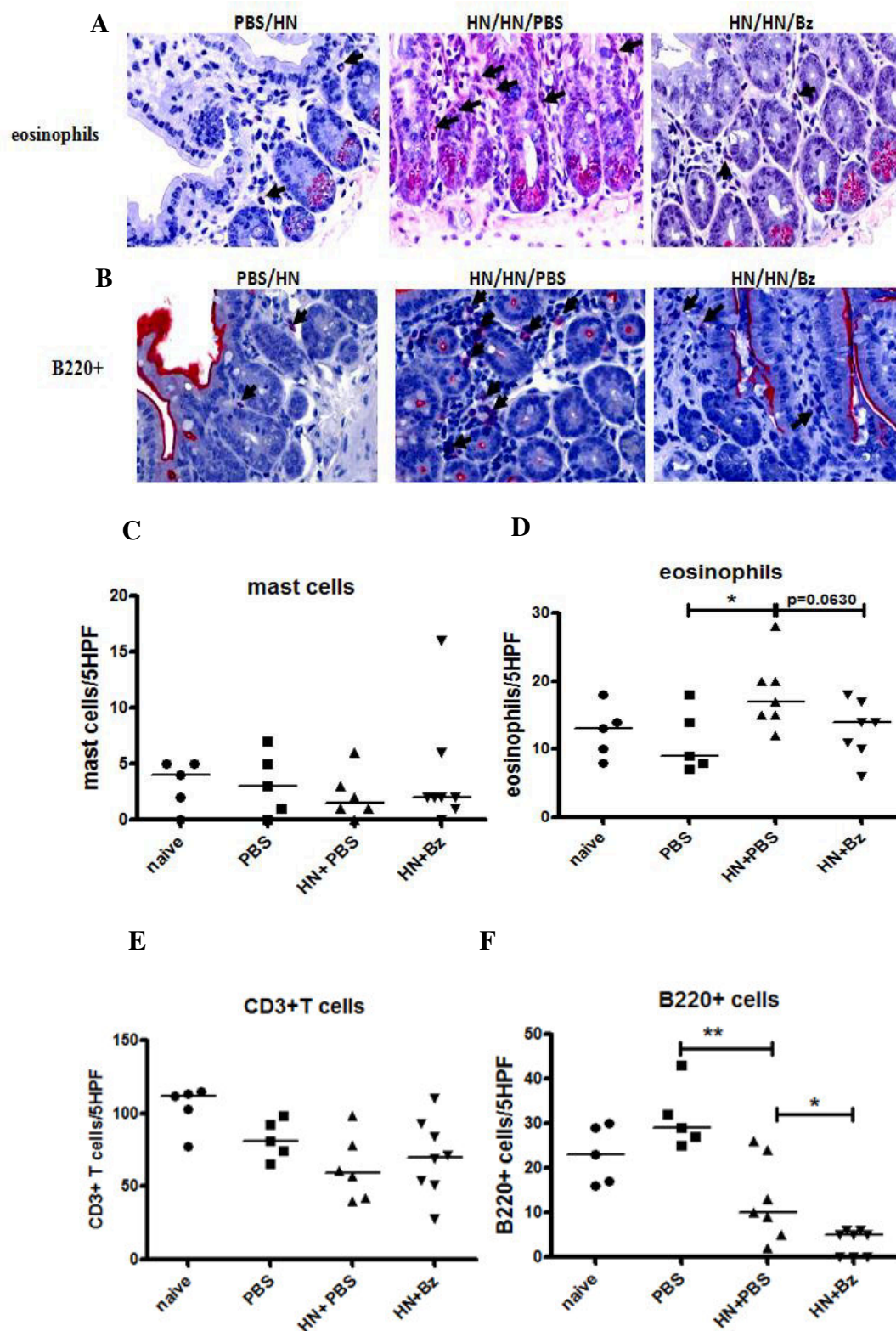


**Figure 21 Regulation of infiltrating inflammatory cells into the gut after Bz treatment. A.** Representative photographs of eosinophils and B. B220<sup>+</sup> cell staining in the jejunum of mouse intestine

by immunohistochemistry. C-F. Numbers of mast cells, eosinophils, CD3<sup>+</sup> T- and B220<sup>+</sup> B-cells per 5 high power field (HPF). The data are shown as a dot plot with the median given as bar. \*  $p < 0.05$ , \*\*  $p < 0.01$ .

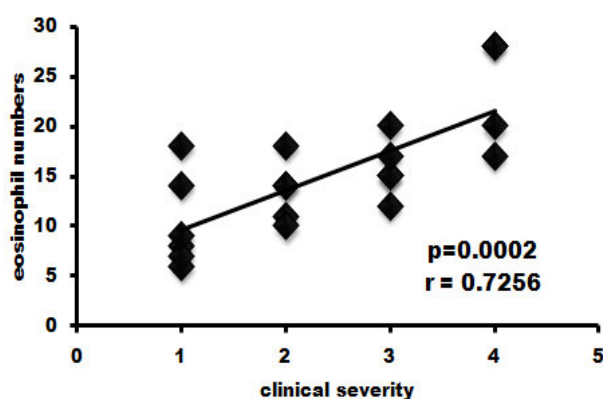
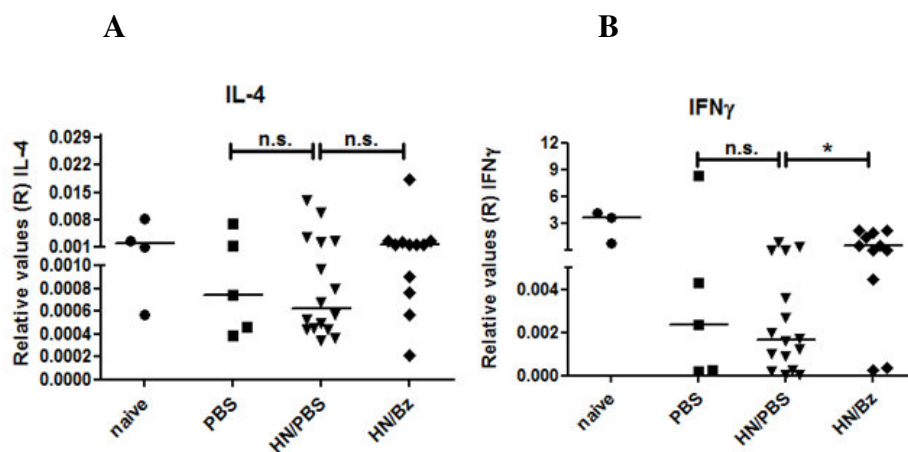
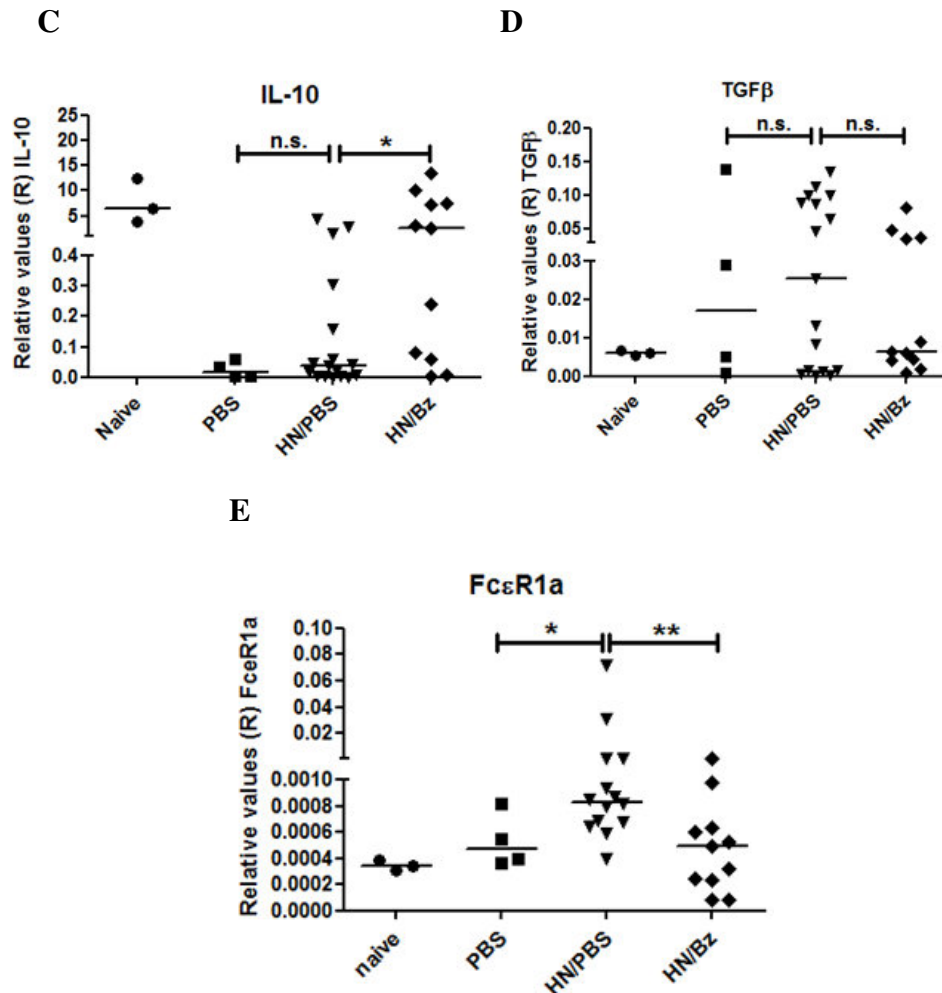


Figure 22 Correlation between the clinical symptoms vs eosinophils.

### 6.9. Altered expression of genes in intestinal jejunum of FA mouse upon bortezomib treatment

To get more insight into the local inflammatory milieu of the jejunum, the expression of a panel of cytokines and receptors which are known to be of importance in the context of allergic gut inflammation was analyzed<sup>105,109,112</sup>. Our data shows no major alterations of T<sub>H</sub>1-T<sub>H</sub>2-cytokine expression profile including IL-4 and IFN- $\gamma$  in the gut neither in sensitised nor in non-sensitised mice (Figure 23A,B). Interestingly, Bz treatment increased the expression of IFN- $\gamma$  (Figure 23B) but, no changes in the IL-4 expression were observed (Figure 23B). Further, IL-10 expression was significantly increased in Bz treated mice ( $p=0.0102$ ; Figure 23C), but not TGF- $\beta$  expression (Figure 23D). Further, the high affinity IgE receptor, Fc $\epsilon$ RI $\alpha$  expression was enhanced in the positive control group (HN/PBS), which was significantly decreased in the HN/Bz group (Figure 23E).





**Figure 23 Modulation of different cytokines and receptors in the intestine of HN-alum FA mouse after Bz application.** A-E. Analysis of IL-4, IFN- $\gamma$ , IL-10, TGF- $\beta$  and Fc $\epsilon$ R1 expression in the biopsies of jejunum by RT-PCR. The expressions of these values were normalized to *Hprt*. The data are shown as a dot plot with the median given as bar. \*  $p < 0.05$ , \*\*  $p < 0.01$ .

### 6.10. Abolished skin barrier genes expression

As the skin symptoms remained unchanged between the PBS vs Bz groups, the impact of Bz on the skin in organ-cultures was analyzed. In a dose-dependent manner, the expression of pro-filaggrin, loricrin (tendency) and, strongly, transglutaminase-1 (Figure 24) were reduced<sup>147</sup>. IL-1 $\beta$  is a pro-inflammatory molecule and mimics the inflammatory microenvironment in the skin<sup>151</sup>. Therefore in the presence of IL-1 $\beta$ , there was much stronger effect in the skin barrier genes expression (Figure 24). It has been shown that IL-1 $\beta$  increases proteins turnover and adaptation of the proteolytic activity of the proteasome<sup>151</sup>. However, in the presence or absence of IL-1 $\beta$ , transglutaminase-1 was largely affected. Also, keratin-14 and jagged-2 were two other

genes, which are highly expressed in the skin and show no effect or elevated expression in the skin (Figure 24). These findings implicate that not all the genes expressed in the skin are susceptible towards proteasome inhibition.

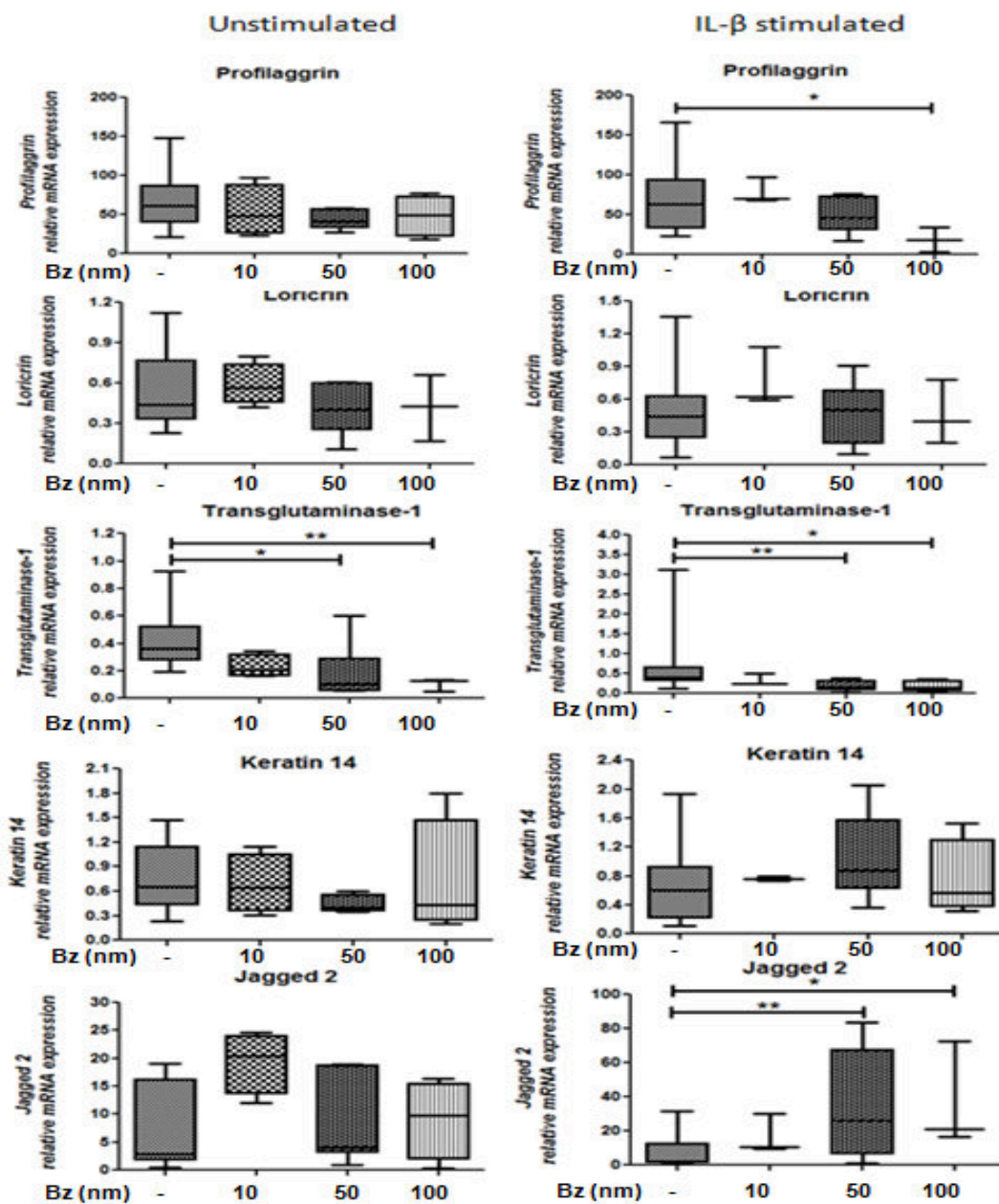


**Figure 24** Expression of skin barrier genes upon Bortezomib treatment<sup>147</sup>. *Ex vivo* skin organ cultures in the absence (left hand side) or presence of IL- $\beta$  (right hand side) along with Bz at different concentrations as mentioned. For RNA extraction, biopsies were snap frozen in liquid nitrogen and stored at  $-80^{\circ}\text{C}$ . Quantitative RT-PCR was performed for profilaggrin, loricrin, transglutaminase-1, keratin-14 and jagged-2 genes. Values are normalized to hprt. Each values are shown as columns with mean +SEM. \* p < 0.05; \*\* p < 0.01.

## 7. DISCUSSION

### 7.1. Bortezomib interferes with the immune response but not the skin eczema

Immunoglobulin-E secreting plasma cells are key cells for the development of an allergic manifestation<sup>162,163</sup>. These plasma cells are terminally differentiated B cell or short-lived and/or resident long-lived<sup>162</sup>. They can be triggered by repetitive antigen exposure<sup>159</sup>. Several reports indicate that total IgE and also allergen-specific IgE are elevated in the majority of patients with AD<sup>164-166</sup>. Previous data from our group suggested that long-lived antigen-specific plasma cells can contribute to the development of IgE-associated manifestations like allergic lung inflammation in mice<sup>159</sup>. However, the contribution of IgE as well as plasma cells in the context of allergen-induced eczema in a mouse model is poorly understood. Previous data obtained from a lupus model revealed that long-lived plasma cells can be targeted by proteasome directed inhibition<sup>129</sup>. The efficacy of the proteasome inhibitor Bz investigated in murine models of lupus, arthritis and myasthenia gravis indicated an improvement in disease severity<sup>129,142,143</sup>. Contrarily, a recent publication showed that long-term proteasome inhibitor Bz treatment suppressed IgE, but failed to encounter changes in the plasma cells in a OVA-induced chronic asthma mouse model which was associated with no clinical improvement<sup>143</sup>. On the other hand, recent reports have indicated a CD20 directed and potential efficacy of IgE therapies in subgroups of AD patients<sup>57,167</sup>.

Therefore the question was addressed whether depletion of plasma cells and consecutively allergen-specific IgE have an impact on the outcome of allergen-induced eczema in mice. To target plasma cells, the proteasome inhibitor Bz was applied *in vivo* in an allergen-triggered eczema mouse model<sup>147</sup>. The data show that the treatment with a proteasome inhibitor resulted in less allergen-specific IgE production but also in less specific immunoglobulins of the other isotypes<sup>147</sup>. Circulating IgE was reduced already after 4 days upon the first treatment with bortezomib and remained low until the end of the experiment. This was accompanied by reduced numbers of immunoglobulin-producing cells in the spleen and also the bone marrow. Nevertheless, the outcome of the allergen-induced eczema was comparable between the treatment versus the control group<sup>147</sup>.

Although plasma cells and consecutively IgE were strongly reduced by the proteasome inhibitor, no clinical improvement of the eczematous skin lesions was observed<sup>147</sup>. This suggests that allergen-specific IgE is not the major driving force for the outcome of eczema in this model.

However, it is still possible that allergen-specific IgE can trigger exacerbation of the disease e.g. during intense allergen exposure during pollen season, which has been demonstrated to occur in allergic patients<sup>168</sup>. Moreover, proteasome inhibition primarily targets plasma cells, but not the memory or naïve compartment of B cells<sup>129</sup>. Therefore, B cells might be involved in various ways in AD onset: 1) by producing IgE and other immunoglobulins, which cause an interaction with the allergen, activating mast cells and other effector cells, 2) on the local production of immunoglobulins in the skin itself, and 3) by other local functions such as antigen presentation in the inflamed skin with subsequent T cell activation or mediation of immunomodulatory effects, such as the production of certain cytokines.

More recently, a publication showed that B cells (expressing CD19) are important to regulate the onset of disease severity in a mouse model of AD<sup>59</sup>. On the other hand, B cell-deficient mice have shown to develop AD-like symptoms<sup>169</sup>, suggesting a negligible role of B cells in the pathophysiology of AD. By contrast, other recent data indicate that immunoglobulin receptor (FcR $\gamma$ ) is essential for AD development using a similar mouse model<sup>58</sup>. The FcR $\gamma$  receptor in which  $\gamma$ -chain acts an essential signal-transducing component of both the high-affinity IgE receptor Fc $\gamma$ RI and the low-affinity IgG receptor i.e. CD16<sup>58</sup>. Here, skin inflammation was reduced after complete fragment crystal (Fc)-ablation. Therefore, the role of antibody producing B cells in AD is still not resolved.

However, published data have shown another important pathway of B cell activation, namely by BAFF (B cell activating factor) and APRIL (a proliferation-inducing ligand). Mice lacking BAFF have a profound peripheral B cell deficiency<sup>170</sup>. APRIL, which binds like BAFF to the receptors BCMA (B cell maturation antigen) and TACI (transmembrane activator and calcium modulator and cyclophilin ligand interactor), promotes plasma cell survival and triggers B cell function at the level of antigen presentation<sup>171</sup>. Although these factors seem to be essential for the development and survival of antibody-producing B cells<sup>172</sup>, their role in AD pathogenesis has not been defined properly. Hence, BAFF and APRIL blockade in the context of AD might be another approach to target distinct B cell functions in this complex skin disease. In fact, interference with these factors by TACI-Ig successfully inhibited allergic asthma in a mouse model<sup>173</sup>. Increased APRIL levels have been reported in AD patients, which correlated with IgE levels and were normalised upon successful AD treatment<sup>174</sup>.

Besides the decrease of allergen-specific IgE upon proteasome inhibition, a significant reduction of CD4<sup>+</sup> and CD8<sup>+</sup> T cell subsets in allergen-induced skin lesions was observed<sup>147</sup>. Here, it was found that approximately one third of T cell infiltrates were reduced compared to that of the control PBS group<sup>147</sup>. The increase of T cells is a hallmark of lesional AD skin and they are believed to play a major role for the associated inflammation<sup>22,58,144,160,161</sup>. However, this specific reduction of T cells in lesional skin of AD fits together with the previously published data by Yanaba *et al.*<sup>175</sup>. Regardless of the fact that this allergen-induced eczema mouse model<sup>147</sup> has several differences in the protocol to their hapten-sensitized contact hypersensitivity model<sup>175</sup> [e.g. prior application of Bz before hapten sensitization], both of these two models show a reduction in T cell infiltration in lesional skin upon Bz treatment. It has also been shown previously by our group that a reduction of T cells in lesional skin is associated with an improvement of the eczema outcome<sup>144,176-179</sup>. However, although a reduction of T cells in the AD-like skin lesions was found, surprisingly no improvement of clinical symptoms was determined. Several explanations may account for this observation. First, the diminished T cell population may not only comprise effector T cells, but also regulatory T cells, which have been shown to counteract dermatitis<sup>180</sup>. Second, counter-regulatory effects of the proteasome inhibitor on other cells in the skin itself may have accounted for the missing clinical efficacy.

In accordance with the data from the skin less activated T cells in the axillary lymph nodes were observed. These results are in line with already published data from another group wherein infiltrating T cells were decreased in the draining lymph nodes upon Bz treatment in a model of contact dermatitis<sup>175</sup>. As there was no clear and significant reduction of either naïve or memory T cells in the spleen, it can be speculated that proteasome inhibition may not alter T cell function in the spleen, but rather interferes with their migration. Whether the skin homing phenotype is directly targeted by proteasome inhibition will need be determined in future investigations.

Disruption of the epidermal skin barrier function is a predisposing factor for AD inducing dry skin along with increased sensitivity to harmful microbes and chemical irritants<sup>20-22,27-29</sup>. Several reports show that structural proteins such as filaggrin, loricrin, transglutaminases and involucrin, are important for the formation of the cornified envelope, and are altered in AD skin<sup>20-22,26-29,37-42,181</sup>. Moreover, loss-of-function mutations within the filaggrin gene have been reported in AD<sup>20-22,37-42</sup> and similarly, loricrin has been described to be down-regulated in AD skin<sup>48</sup>. Furthermore, T cells and T<sub>H</sub>2 cytokines have been shown to interfere with skin barrier protein expression and

function<sup>43,182,183</sup>, thereby contributing to AD. Due to a lack of clinical efficacy at the level of skin lesions in our model, we further investigated whether Bz exerts a direct activity on resident cells of the skin. Therefore, Bz was applied directly onto skin biopsies to analyze its ability to alter the expression of relevant keratinocyte-specific (KCs) genes. The obtained results show that the cultured skin biopsies were sensitive to Bz and the genes involved in barrier function were selectively down-regulated<sup>147</sup>. The effective Bz concentration used in these settings was below the peak plasma concentration<sup>137</sup>. In a previous study it has been shown that *in vitro* cultures of multiple myeloma cells are highly susceptible when the concentration range used here was applied<sup>184,185</sup>. Nevertheless, Bz reduced the expression of KCs genes associated with the cornified envelope formation<sup>26</sup>, whereas other genes highly expressed by keratinocytes were either not much affected (krt14, expressed predominantly to maintain shape of epidermal cell<sup>26</sup>) or even exhibited an up-regulation (jagged-2, highly expressed in the basal cells<sup>186</sup>).

In fact, a recent report demonstrated a topical application of this proteasome inhibitor was associated with the onset of eczematous skin lesions in a murine model of psoriasis<sup>187</sup>. Following these reports, dry skin has been reported as an adverse event upon treatment with the proteasome inhibitor in humans<sup>188</sup>. Accordingly, 60% of patients receiving Bz treatment encounter cutaneous side effects<sup>189</sup>. In conclusion, this work demonstrates the susceptibility of keratinocytes to proteasome function, and for the first time, shows an impairment of barrier genes in inflamed skin as a direct consequence of proteasome inhibition.

In summary, proteasome inhibition leads to pronounced reduction of plasma cells and consecutively the total and antigen-specific antibody secretion in an allergen-dependent eczema mouse model. Although the systemic humoral immune response was substantially suppressed, no improvement of the skin in this murine allergen-induced eczema model was observed. However, neither the plasma cells nor the allergen-specific IgE (in the skin) seem to contribute substantially to the severity of atopic eczema in this model. As proteasome inhibition may exert direct negative effects on keratinocytes, the severity of eczema might have been promoted at the level of the resident skin cells, although resulting in an ameliorated immunological disease outcome.

Taken together, proteasome inhibition of plasma cells may be a favourable therapeutic strategy to treat IgE-dependent allergic diseases, but its usage is most likely not efficacious in skin diseases characterized by a defective barrier function.

## 7.2. Bortezomib treatment ameliorates hazelnut allergen-induced intestinal anaphylaxis in mice

Plasma cells can be effectively targeted by proteasomal inhibition, thereby strongly suppressing IgE and to a lesser extent other immunoglobulins in the context of AD<sup>147</sup>. Based on these findings from a mouse model of allergen-induced atopic eczema, the aim was to investigate the relevance of B cell subsets and IgE in a mouse model of food-induced intestinal anaphylaxis. AD is a complex disease which involves multiple factors as discussed before. In contrast, FA is commonly associated with IgE-mediated type-1 hypersensitivity reactions. The latter disease is often manifested with mild but also fatal reactions. The onset of clinical symptoms includes vomiting, diarrhea, respiratory and cardiovascular impairment<sup>84,105,108</sup>. The knowledge about the pathophysiological role of IgE-secreting B cell subsets in the pathogenesis of food allergy is limited. Therefore, the primary task was to establish a mouse model of food-induced intestinal anaphylaxis which is characterized by hypothermia, diarrhea and displays specific IgE upon hazelnut (*Corylus avellana*) provocation. The second task was to determine whether a depletion of B cells and consecutively allergen-specific IgE by proteasome inhibitor will impact the outcome of hazelnut-induced intestinal anaphylaxis. In addition, hazelnut extract was chosen as an allergen due to its potency in causing serious allergic reactions among sensitized individuals<sup>156-158</sup>, and the suggested high prevalence in the European population<sup>156-158,190-193</sup> (0.1 to 0.5% )<sup>156</sup>.

Two mouse models of hazelnut-induced intestinal allergy were applied. In the first model, mice were sensitized via intragastrical route with lower amounts of hazelnut allergen in the presence of adjuvant SEB followed by challenges of higher amounts of hazelnut. This model was adapted from Ganeshan et al. (2009)<sup>107</sup> by introducing few changes into our protocol. In the second model, hazelnut was systemically injected with alum in mice followed by intragastrical allergen provocation. This model was associated with the development of immediate clinical symptoms including the onset of diarrhea and hypothermia upon hazelnut provocation. The analyses of the serum samples from sensitized mice show elevated concentrations of hazelnut-specific IgE (sIgE) and mMCP-1 levels. Accordingly, an infiltration of eosinophils in the jejunum of mouse intestine was detected. The clinical symptoms of intestinal anaphylaxis in mice display similar signs of food-aggravated anaphylaxis in humans<sup>194</sup>. This established mouse model with anaphylactic symptoms shows also similarities to other intestinal anaphylaxis murine models of

food allergy reported so far<sup>105</sup>. By contrast, hazelnut sensitization in the presence of SEB as an adjuvant showed a weaker response after hazelnut challenge. This may be related to the applied dose of allergen. Due to the high responder rate, the systemic sensitization model (hazelnut plus alum) was selected for further experiments.

The IgE binding patterns to hazelnut-proteins from sera obtained from hazelnut-allergic humans and sensitized mice were determined. Upon probing a similar IgE binding profile to hazelnut allergens, being highly comparable between the species based on the relative molecular weight, was detected. According to the molecular size of the bands known allergens like Cor a1 (17-18 kDa; pathogenesis related protein-10)<sup>157,195</sup>, Cor a2 (14 kDa; profilin)<sup>157,195</sup>, Cor a14 (32 kDa; 2S albumin)<sup>196,197</sup> and legumin (35k Da) were highly reactive to IgE from human and mice, whereas a moderate reactivity was seen to Cor a8 (9-10 kDa; lipid transfer protein)<sup>157,198</sup> and Cor a9 (40 kDa; 11S globulin like protein)<sup>198</sup>. However, only by specific blocking experiments e.g. with peptides or recombinant proteins the proveniences of these allergens can be proven. These hazelnut allergens have been characterized as described above and can promote mild to severe systemic allergic responses in sensitized individuals<sup>192-200</sup>. The correlation between elevated HN-specific IgE and the clinical symptom score show a modest association. Thus, the heterogeneity of hazelnut allergens in the extract may lead to a diversified IgE response.

Mast cell numbers in the intestine and mMCP-1 levels in the serum have been shown previously to be associated with IgE-mediated intestinal anaphylaxis in murine models<sup>105</sup>. Contrarily, mast cell hyperplasia was not present in our mouse model of hazelnut allergy although there was a significant systemic increase in the mucosal mast cell protease-1. The diversity of the hazelnut allergens in the extract may induce various IgE binding epitopes, which diversities of allergen binding to sIgE on the surface of mast cells in the mucosa and may have attributed this observation. Additional factors might be differences in mouse strains and dosages of the allergen<sup>108</sup>. Accordingly, the analysis of mice sensitized with OVA and alum indeed showed elevated mast cell numbers in the jejunum after repetitive OVA application. Following this line, an increase of approximately 30-fold higher mMCP-1 levels compared to the hazelnut-induced allergy model was observed. Such results have been reported elsewhere<sup>105</sup>. Therefore, the allergenic potential of an individual allergen seems to be critically important in inducing mast cell-dependent allergic immune responses.

Apart from mast cells, the intestinal eosinophil numbers were increased in the hazelnut-induced intestinal anaphylaxis model. It has been previously shown that eosinophils are recruited to the site of inflammation in food-induced intestinal anaphylaxis<sup>105,201</sup>. Further, eosinophils have been associated with gastrointestinal disorders causing diarrhea<sup>202,203</sup>. They can be attracted to the site of inflammation by mediators released by mast cells such as histamine, eicosanoids, and cytokines<sup>204</sup>. Analysis of the jejunum showed an increased expression of TGF- $\beta$  in hazelnut-induced intestinal anaphylaxis model. TGF- $\beta$  has been reported to be the common mediator for epithelial growth, tissue remodelling and fibrosis<sup>205</sup>. Another report suggests that the release of cytotoxic mediators from eosinophils contribute to the late phase IgE-dependent immune response<sup>206,207</sup>. Therefore, it is possible that eosinophils release TGF- $\beta$  during the onset of a food allergic reaction and thereby promote gastrointestinal diarrhea.

B cells secrete IgE, which is associated with type-1 mediated hypersensitivity reactions towards harmless food allergens<sup>162,163</sup>. Accordingly, an anti-IgE antibody (omalizumab) based therapy in patients with peanut allergy has been shown to be effective<sup>208</sup>. Another possibility is to target antibody-secreting plasma cells as they produce immunoglobulins including IgE. They can be targeted by proteasome inhibition and this has been shown to ameliorate the outcome of autoimmune and allergic diseases<sup>129,141-143,147</sup>.

With this background, the proteasome inhibitor Bz was administered in mice with hazelnut-induced intestinal anaphylaxis to determine whether clinical efficacy can be achieved. In line with these observations plasma cells and allergen-specific IgE including to a lesser extent IgG1 was diminished. We observed a robust decrease of allergen-specific IgE- (88% reduction) and IgG1- isotype (54% reduction), but not the IgA isotype. This pattern of reduction in immunoglobulin isotypes might be related to the half-life of IgE, IgG1 and IgA as bortezomib targets antibody secreting cells. IgE has a shorter half-life of about 12 h compared to IgG1 (7 days) and IgA (19h)<sup>209</sup>.

The analysis of B cell subsets in our model show that plasma cells (B220<sup>-</sup> IgG1<sup>hi</sup> CD138<sup>+</sup> kappa<sup>+</sup>) and CD19<sup>+</sup> and CD23<sup>hi</sup> follicular B cell (CD19<sup>+</sup> CD23<sup>hi</sup> CD21<sup>low</sup>) numbers in the spleen were increased after repetitive hazelnut allergen challenge. These observations are in line with previous published data from our group in which allergen-specific antibody secreting cells in the spleen were elevated after respiratory mucosal allergen challenge<sup>159</sup>. Upon treatment with Bz *in vivo* the total number of antibody secreting plasma cells as well as CD19<sup>+</sup> and follicular B cell

subsets were reduced. Most likely activated or proliferating B cells are targeted as this show a high proteasomal activity. CD23, the low affinity IgE receptor is expressed on antigen-stimulated B cells<sup>210</sup>. Several other reports indicate IgE/CD23 as a complex mediates transepithelial allergen transport in the intestine of allergen sensitized mice<sup>211-215</sup>. Accordingly, blocking with anti-CD23 antibody completely abolished antigen uptake in sensitized mice and similar results were obtained from sensitized CD23<sup>-/-</sup> mice<sup>213,214</sup>. Nevertheless, the role of CD23 expression during allergen uptake in the intestine of hazelnut challenged mice needs to be explored further.

The frequency of marginal zone B cells (CD19<sup>+</sup> CD21<sup>hi</sup> CD23<sup>low</sup>), which are activated independently from T cells, was not affected by proteasome inhibition in our model. Published data show that marginal zone B cells *in vivo* can remain resistant to proteasome inhibition<sup>216</sup>. Proteasome inhibition has been also shown to impair effector T cells in an antigen-dependent manner<sup>217,218</sup>. Moreover, effector T cells and T<sub>H</sub>2 cytokines are important for the induction of the allergic immune response in murine models of intestinal anaphylaxis<sup>77,105,108-112</sup>.

The analysis of infiltrating cells in the jejunum of hazelnut-challenged mice after bortezomib treatment show reduced eosinophils and B220<sup>+</sup> cells. It has been shown previously that eosinophils are sensitive to proteasome inhibitor PS-519 treatment in a mouse model of allergen-induced pulmonary eosinophilia<sup>219</sup>. Another report demonstrated that eosinophil numbers were reduced in the BAL fluid upon short-term Bz treatment in a chronic experimental asthma model without improving the disease severity<sup>143</sup>. These findings can be related to direct but also an indirect activity of proteasome inhibition and will need to be clarified in future studies. The evidence suggests that B220<sup>+</sup> is not only expressed on B-cells, but also on T-cells, dendritic cells and natural killer cells<sup>220</sup>. Therefore, further studies are currently underway to determine the type of cells expressing the B220<sup>+</sup> phenotype in the gut from the allergic mice. In contrast, other cell types such as CD3<sup>+</sup> T cells and mast cells remained stable upon Bz treatment in the jejunum of the intestinal anaphylaxis mice. Taken together, the reduction of eosinophil infiltration in the intestine may have possibly attributed to the reduced allergic diarrhea in mice with intestinal anaphylaxis.

In summary, a mouse model of oral food-induced intestinal anaphylaxis was established without using mucosal adjuvants or genetic modifications. Hazelnut was used as it is known to be a potential allergen in causing a wide range of allergic symptoms in humans. *In vivo* treatment with the proteasome inhibitor bortezomib in this model improved the clinical severity including

diarrhea and hypothermia. Additionally, bortezomib abolished allergen-specific IgE and to a lesser extent IgG1 due to reduced antibody-producing B cell subsets. Thus, targeting IgE and antibody-secreting B cells in the context of IgE-mediated allergy by proteasome inhibition may be a promising therapeutic approach for food allergy in the future.

## 8. BIBLIOGRAPHY

1. Silverstein, A.M., Clemens Freiherr von Pirquet: explaining immune complex disease in 1906. *Nat Immunol*, **2000**. 1(6): p. 453-455.
2. Coca, A., and Cooke, R., On the classification of the phenomena of hypersensitiveness. *J Immunol*, **1923**. 8: p. 163-183.
3. Galli, S.J., Tsai, M., and Piliponsky, A.M., The development of allergic inflammation. *Nature*, **2008**. 454(7203): p. 445-454.
4. Johansson, S.G., Bieber, T., Dahl, R., *et al.*, Revised nomenclature for allergy for global use: Report of the Nomenclature Review Committee of the World Allergy Organization. *J Allergy Clin Immunol*, **2004**. 113: p. 832–836.
5. Cookson, W., The immunogenetics of asthma and eczema: a new focus on the epithelium. *Nat Rev Immunol*, **2004**. 4(12): p. 978-988.
6. Vercelli, D., Discovering susceptibility genes for asthma and allergy. *Nat Rev Immunol*, **2008**. 8(3): p. 169-182.
7. Kuriakose, J.S. and Miller, R.L., Environmental epigenetics and allergic diseases: recent advances. *Clin Exp Allergy*, **2010**. 40(11): p. 1602-1610.
8. Martino, D.J. and Prescott, S.L., Silent mysteries: epigenetic paradigms could hold the key to conquering the epidemic of allergy and immune disease. *Allergy*, **2010**. 65(1): p. 7-15.
9. Okada, H., Kuhn, C., Feillet, H., *et al.*, The ‘hygiene hypothesis’ for autoimmune and allergic diseases: an update. *Clin Exp Immunol*, **2010**. 160(1): p. 1-9.
10. Fleischer, D.M., Spergel, J.M., Assa'ad, A.H., *et al.*, Primary prevention of allergic diseases through nutritional interventions. *J Allergy Clin Immunol Pract.*, **2013**. 1(1): p. 29-36.
11. Kubo, A., Nagao, K., Amagai, M., *et al.*, Epidermal barrier dysfunction and cutaneous sensitization in atopic diseases. *J Clin Invest*, **2012**. 122(2): p. 440-447.
12. Spergel, J.M., Epidemiology of atopic dermatitis and atopic march in children. *Immunol Allergy Clin North Am*, **2010**. 30: p. 269–280.
13. Papadopoulos, N.G., Agache, I., Bavbek, S., *et al.*, Research needs in allergy: an EAACI position paper, in collaboration with EFA. *Clin Transl Allergy*, **2012**. 2(1): p. 21.
14. Zheng, T., Yu, J., Oh M.H., *et al.*, The Atopic March: Progression from Atopic Dermatitis to Allergic Rhinitis and Asthma. *Allergy Asthma Immunol Res*, **2011**. 3(2): p. 67–73.
15. Breiteneder, H., and Mills, E.N., Molecular properties of food allergens. *J Allergy Clin Immunol*, **2005**. 115(1): p. 14-23.
16. Uzzaman, A., and Cho, S.H., Chapter 28: Classification of hypersensitivity reactions. *Allergy Asthma Proc*, **2012**. 33(1): p. S96-9.
17. Akdis, M., and Akdis, C.A., Therapeutic manipulation of immune tolerance in allergic disease. *Nat Rev Drug Discov*, **2009**. 8(8): p. 645-660.
18. Galli, S.J., and Tsai, M., IgE and mast cells in allergic disease. *Nat Med*, **2012**. 18(5): p. 693-704.

19. Geha, R.S., Jabara, H.H., and Brodeur, S.R., The regulation of immunoglobulin E class-switch recombination. *Nat Rev Immunol*, **2003**. 3(9): p. 721-732.
20. Bieber, T., Atopic Dermatitis. *N Engl J Med*, **2008**. 358(14): p. 1483-1494.
21. Leung, D.Y.M., Boguniewicz, M., Howell, M.D., *et al.*, New insights into atopic dermatitis. *J Clin Invest*, **2004**. 113(5): p. 651-657.
22. Bieber, T., Atopic dermatitis. *Ann Dermatol*, **2010**. 22(2): p. 125-137.
23. Wüthrich, B., and Schmid-Grendelmeier, P., The atopic eczema/dermatitis syndrome. Epidemiology, natural course, and immunology of the IgE-associated ("extrinsic") and the nonallergic ("intrinsic") AEDS. *J Invest Allergol Clin Immunol*, **2003**. 13(1): p. 1-5.
24. Tokura, Y., Extrinsic and intrinsic types of atopic dermatitis. *J Dermatol Sci*, **2010**. 58(1): p. 1-7.
25. Suárez-Fariñas, M., Dhingra, N., Gittler, J., *et al.*, Intrinsic atopic dermatitis shows similar TH2 and higher TH17 immune activation compared with extrinsic atopic dermatitis. *J Allergy Clin Immunol*, **2013**. 132(2): p. 361-370.
26. Candi, E., Schmidt, R., and Melino, G., The cornified envelope: a model of cell death in the skin. *Nat Rev Mol Cell Biol*, **2005**. 6(4): p. 328-340.
27. Hitomi, K., Transglutaminases in skin epidermis. *Eur J Dermatol*, **2005**. 15(5): p. 313-319.
28. Oyoshi, M.K., He, R., Kumar, L., *et al.*, Cellular and Molecular Mechanisms in Atopic Dermatitis, in *Adv Immunol*, **2009**. Academic Press. p. 135-226.
29. Elias, P.M., and Steinhoff, M., "Outside-to-inside" (and now back to "outside") pathogenic mechanisms in atopic dermatitis. *J Invest Dermatol*, **2008**. 128(5): p. 1067-1070.
30. Gittler, J.K., Shemer, A., Suárez-Fariñas, M., *et al.*, Progressive activation of TH2/TH22 cytokines and selective epidermal proteins characterizes acute and chronic atopic dermatitis. *J Allergy Clin Immunol*, **2012**. 130: p. 1344-1354.
31. Wüthrich, B., Cozzio, A., Roll, A., *et al.*, Atopic eczema: genetics or environment? *Ann Agric Environ Med*, **2007**. 14(2): p. 195-201.
32. Kuo, I., Yoshida, T., De Benedetto, A., *et al.*, The cutaneous innate immune response in patients with atopic dermatitis. *J Allergy Clin Immunol*, **2013**. 131: p. 266-278.
33. Broccardo, C.J., Mahaffey, S., Schwarz, J., *et al.*, Comparative proteomic profiling of patients with atopic dermatitis based on history of eczema herpeticum infection and *Staphylococcus aureus* colonization. *J Allergy Clin Immunol*, **2011**. 127: p. 186-193.
34. Imokawa, G., A possible mechanism underlying the ceramide deficiency in atopic dermatitis: expression of a deacylase enzyme that cleaves the N-acyl linkage of sphingomyelin and glucosylceramide. *J Dermatol Sci*, **2009**. 55(1): p. 1-9.
35. Scharschmidt, T.C., Man, M.Q., Hatano, Y., *et al.*, Filaggrin deficiency confers a paracellular barrier abnormality that reduces inflammatory thresholds to irritants and haptens. *J Allergy Clin Immunol*, **2009**. 124(3): p. 496-506.
36. Ong, P.Y., Ohtake, T., Brandt, C., *et al.*, Endogenous antimicrobial peptides and skin infections in atopic dermatitis. *N Engl J Med*, **2002**. 347: p. 1151-1160.

37. Palmer, C.N.A., Irvine, A.D., Terron-Kwiatkowski, A., *et al.*, Common loss-of-function variants of the epidermal barrier protein filaggrin are a major predisposing factor for atopic dermatitis. *Nat Genet*, **2006**. 38(4): p. 441-446.
38. Weidinger, S., Illig, T., Baurecht, H., *et al.*, Loss-of-function variations within the filaggrin gene predispose for atopic dermatitis with allergic sensitizations. *J Allergy Clin Immunol*, **2006**. 118(1): p. 214-219.
39. O'Regan, G.M., and Irvine, A.D., The role of filaggrin loss-of-function mutations in atopic dermatitis. *Curr Opin Allergy Clin Immunol*, **2008**. 8(5): p. 406-410.
40. McAleer, M.A., Irvine, A.D., The multifunctional role of filaggrin in allergic skin disease. *J Allergy Clin Immunol*, **2013**. 131: p. 280-291.
41. Böhme, M., Söderhöll, C., Kull, I., *et al.*, Filaggrin mutations increase the risk for persistent dry skin and eczema independent of sensitization. *J Allergy Clin Immunol*, **2012**. 129: p. 1153-1155
42. Kawasaki, H., Nagao, K., Kubo, A., *et al.*, Altered stratum corneum barrier and enhanced percutaneous immune responses in filaggrin-null mice. *J Allergy Clin Immunol*, **2012**. 129: p. 1538-1546.
43. Howell, M.D., Kim, B.E., Gao, P., *et al.*, Cytokine modulation of atopic dermatitis filaggrin skin expression. *J Allergy Clin Immunol*, **2007**. 120: p. 150-155.
44. Kim, B.E., Howell, M.D., Guttman, E., *et al.*, TNF-alpha down-regulates filaggrin and loricrin through c-Jun N-terminal kinase: Role for TNF-alpha antagonists to improve skin barrier. *J Invest Dermatol*, **2011**. 131: p. 1272-1279.
45. Deleuran, M., Hvid, M., Kemp, K., *et al.*, IL-25 induces both inflammation and skin barrier dysfunction in atopic dermatitis. *Chem Immunol Allergy*, **2012**. 96: p. 45-49.
46. Furuse, M., Hata, M., Furuse, K., *et al.*, Claudin-based tight junctions are crucial for the mammalian epidermal barrier: a lesson from claudin-1-deficient mice. *J Cell Biol*, **2002**. 156: p. 1099-1111.
47. De Benedetto, A., Rafaels, N.M., McGirt, L.Y., *et al.*, Tight junction defects in patients with atopic dermatitis. *J Allergy Clin Immunol*, **2011**. 127: p. 773-786.
48. Suarez-Farinas, M., Tintle, S.J., Shemer, A., *et al.*, Nonlesional atopic dermatitis skin is characterized by broad terminal differentiation defects and variable immune abnormalities. *J Allergy Clin Immunol*, **2011**. 127: p. 954-964.
49. Jin, H., He, R., Oyoshi, M., *et al.*, Animal models of atopic dermatitis. *J Invest Dermatol*, **2009**. 129(1): p. 31-40.
50. Nomura, I., Goleva, E., Howell, M.D., *et al.*, Cytokine milieu of atopic dermatitis, as compared to psoriasis, skin prevents induction of innate immune response genes. *J Immunol*, **2003**. 171: p. 3262-3269.
51. Nakajima, S., Kitoh, A., Egawa, G., *et al.*, IL-17A as an Inducer for Th2 Immune Responses in Murine Atopic Dermatitis Models. *J Invest Dermatol*, **2014**. (ahead of print).
52. Herz, U., Daser, A., Renz, H., The humanized (Hu-PBMC) SCID mouse as an in vivo model for human IgE production and allergic inflammation of the skin. *Int Arch Allergy Immunol*, **1997**. 113(1-3): p. 150-152.

53. Carballido, J.M., Biedermann, T., Schwärzler, C., *et al.*, The SCID-hu Skin mouse as a model to investigate selective chemokine mediated homing of human T-lymphocytes to the skin in vivo. *J Immunol Methods*, **2003**. 273(1-2): p. 125-135.
54. Ashcroft, D.M., Dimmock, P., Garside, R., *et al.*, Efficacy and tolerability of topical pimecrolimus and tacrolimus in the treatment of atopic dermatitis: meta-analysis of randomised controlled trials. *BMJ*, **2005**. 330(7490): p. 516.
55. Simpson, D., and Noble, S., Tacrolimus ointment: a review of its use in atopic dermatitis and its clinical potential in other inflammatory skin conditions. *Drugs*, **2005**. 65(6): p. 827-858.
56. Lugović, L., Lipozencić, J., Jakić-Razumović, J., Prominent involvement of activated Th1-subset of T-cells and increased expression of receptor for IFN-gamma on keratinocytes in atopic dermatitis acute skin lesions. *Int Arch Allergy Immunol*, **2005**. 137(2): p.125-133.
57. Simon, D., Hösli, S., Kostylina, G., *et al.*, Anti-CD20 (rituximab) treatment improves atopic eczema. *J Allergy Clin Immunol*, **2008**. 121(1): p. 122-128.
58. Abboud, G., Staumont-Sallé, D., Kanda, A., *et al.*, Fc(epsilon)RI and FcgammaRIII/CD16 differentially regulate atopic dermatitis in mice. *J Immunol*, **2009**. 182: p. 6517-6526.
59. Yanaba, K., Kamata, M., Asano, Y., *et al.*, CD19 expression in B cells regulates atopic dermatitis in a mouse model. *Am J Pathol*, **2013**. 182: p. 2214-2222.
60. Akhavan, A., Rudikoff, D., Atopic dermatitis: systemic immunosuppressive therapy. *Semin Cutan Med Surg*, **2008**. 27: p. 151-155.
61. Chang, T.W., Wu, P.C., Hsu, C.L., *et al.*, Anti-IgE antibodies for the treatment of IgE-mediated allergic diseases. *Adv Immunol*, **2007**. 93: p. 63-119.
62. Heil, P.M., Maurer, D., Klein, B., *et al.*, Omalizumab therapy in atopic dermatitis: depletion of IgE does not improve the clinical course – a randomized, placebo-controlled and double blind pilot study. *J Dtsch Dermatol Ges*, **2010**. 8: p. 990–998.
63. Spergel, J.M., Mizoguchi, E., Brewer, J., *et al.*, Epicutaneous sensitization with protein antigen induces localized allergic dermatitis and hyperresponsiveness to metacholine after single exposure to aerosolized antigen in mice. *J Clin Invest*, **1998**. 101: p. 1614–1622.
64. Spergel, J.M., Mizoguchi, E., Oettgen, H., *et al.*, Roles of TH1 and TH2 cytokines in a murine model of allergic dermatitis. *J Clin Invest*, **1999**. 103:1103–1111.
65. Laouini, D., Alenius, H., Bryce, P., *et al.*, IL-10 is critical for Th2 responses in a murine model of allergic dermatitis. *J Clin Invest*, **2003**. 112: p. 1058–1066.
66. Ma, W., Bryce, P., Humbles, A.A., *et al.*, CCR3 is essential for skin eosinophilia and airway hyperresponsiveness in a murine model of allergic skin inflammation. *J Clin Invest*, **2002**. 109: p. 621–628.
67. Bussmann, C., Bockenhoff, A., Henke, *et al.*, Does allergen-specific immunotherapy represent a therapeutic option for patients with atopic dermatitis? *J Allergy Clin Immunol*, **2006**. 118: p. 1292–1298.
68. Huang, C.H., Kuo, I.C., Xu, H., *et al.*, Mite allergen induces allergic dermatitis with concomitant neurogenic inflammation in mouse. *J Invest Dermatol*, **2003**. 121: p. 289–293.

69. Laouini, D., Kawamoto, S., Yalcindag, A., *et al.*, Epicutaneous sensitization with superantigen induces allergic skin inflammation. *J Allergy Clin Immunol*, **2003**. 112: p. 981–987.
70. Chan, L.S., Robinson, N., Xu, L., Expression of interleukin-4 in the epidermis of transgenic mice results in a pruritic inflammatory skin disease: an experimental animal model to study atopic dermatitis. *J Invest Dermatol*, **2001**. 117: p. 977–983.
71. Dillon, S.R., Sprecher, C., Hammond, A., *et al.*, Interleukin 31, a cytokine produced by activated T cells, induces dermatitis in mice. *Nat Immunol*, **2004**. 5: p. 752–760.
72. Yoo, J., Omori, M., Gyarmati, D., *et al.*, Spontaneous atopic dermatitis in mice expressing an inducible thymic stromal lymphopoietin transgene specifically in the skin. *J Exp Med*, **2005**. 202: p. 541–549.
73. Yamanaka, K., Tanaka, M., Tsutsui, H., *et al.*, Skin-specific caspase-1-transgenic mice show cutaneous apoptosis and pre-endotoxin shock condition with a high serum level of IL-18. *J Immunol*, **2000**. 165: p. 997–1003.
74. Nakanishi, K., Yoshimoto, T., Tsutsui, H., Interleukin-18 regulates both Th1 and Th2 responses. *Annu Rev Immunol*, **2001**. 19: p. 423–474.
75. Konishi, H., Tsutsui, H., Murakami, T., *et al.*, IL-18 contributes to the spontaneous development of atopic dermatitis-like inflammatory skin lesion independently of IgE/stat6 under specific pathogen-free conditions. *Proc Natl Acad Sci USA*, **2002**. 99: p. 11340–11345.
76. Sampson, H.A., Update on food allergy. *J Allergy Clin Immunol*, **2004**. 113(5): p. 805-819.
77. Sicherer, S.H., and, Sampson, H.A., Food allergy: Epidemiology, pathogenesis, diagnosis, and treatment. *J Allergy Clin Immunol*, **2014**. 133(2): p. 291-307.
78. Huang, H.-W., Hsu, C.-P., Yang, B. B., *et al.*, Potential Utility of High-Pressure Processing to Address the Risk of Food Allergen Concerns. *Comprehensive Reviews in Food Science and Food Safety*, **2014**. 13: p. 78–90.
79. Brandtzaeg, P., Food allergy: separating the science from the mythology. *Nat Rev Gastroenterol Hepatol*, **2010**. 7(7): p. 380-400.
80. Chehade, M., and, Mayer, L., Oral tolerance and its relation to food hypersensitivities. *J Allergy Clin Immunol*, **2005**. 115(1): p. 3-12.
81. Macpherson, A.J., and, Smith, K., Mesenteric lymph nodes at the center of immune anatomy. *J Exp Med*, **2006**. 203(3): p. 497-500.
82. Mucida, D., Kutchukhidze, N., Erazo, A., *et al.*, Oral tolerance in the absence of naturally occurring Tregs. *J Clin Invest*, **2005**. 115(7): p. 1923-1933.
83. Astwood, J.D., Leach, J.N., Fuchs, R.L., Stability of food allergens to digestion in vitro. *Nat Biotechnol*, **1996**. 14(10):1269-1273.
84. Wang, J., and, Sampson, H.A., Food anaphylaxis. *Clin Exp Allergy*, **2007**. 37(5): p. 651-60.
85. Berin, M.C., and, Sampson, H.A., Mucosal Immunology of Food Allergy. *Curr Biol*, **2013**. 23(9): p. R389-400.
86. Jones, S.M., Pons, L., Roberts, J.L., *et al.*, Clinical efficacy and immune regulation with peanut oral immunotherapy. *J Allergy Clin Immunol*, **2009**. 124(2): p. 292-300.

87. Chatila, T.A., Role of regulatory T cells in human diseases. *J Allergy Clin Immunol*, **2005**. 116(5): p. 949-959.
88. King, N., Helm, R., Stanley, J.S., *et al.*, Allergenic characteristics of a modified peanut allergen. *Mol Nutr Food Res*, **2005**. 49(10): p. 963-971.
89. Bannon, G.A., Cockrell, G., Connaughton, C., *et al.*, Engineering, characterization and in vitro efficacy of the major peanut allergens for use in immunotherapy. *Int Arch Allergy Immunol*, **2001**. 124(1-3): p. 70-72.
90. Li, X.M., Srivastava, K., Grishin, A., *et al.*, Persistent protective effect of heat-killed *Escherichia coli* producing "engineered", recombinant peanut proteins in a murine model of peanut allergy. *J Allergy Clin Immunol*, **2003**. 112(1): p. 159-167.
91. Li, S., Li, X.M., Burks, A.W., *et al.*, Modulation of peanut allergy by peptide-based immunotherapy. *J Allergy Clin Immunol*, **2001**. 107: p. S233.
92. Horner, A.A., Nguyen, M.D., Ronaghy, A., *et al.*, DNA-based vaccination reduces the risk of lethal anaphylactic hypersensitivity in mice. *J Allergy Clin Immunol*, **2000**. 106: p. 349-356.
93. Srivastava, K., Li, X.M., Bannon, G.A., *et al.*, Investigation of the use of Iss-linked Ara h2 for the treatment of peanut-induced allergy. *J Allergy Clin Immunol*, **2001**. 107: p. S233.
94. Roy, K., Mao, H.Q., Huang, S.K., *et al.*, Oral gene delivery with chitosan-DNA nanoparticles generates immunologic protection in a murine model of peanut allergy. *Nat Med*, **1999**. 5: p. 387-391.
95. Leung, D.Y., Sampson, H.A., Yunginger, J.W., *et al.*, Longitudinal Study of Parents and Children Study Team. Effect of anti-IgE therapy in patients with peanut allergy. *N Engl J Med*, **2003**. 348: p. 986-993.
96. Casale, T.B., Busse, W.W., Kline, J.N., *et al.*, Immune Tolerance Network Group. Omalizumab pretreatment decreases acute reactions after rush immunotherapy for ragweed-induced seasonal allergic rhinitis. *J Allergy Clin Immunol*, **2006**. 117: p. 134-140.
97. Sampson, H.A., A phase II, randomized, double-blind, parallel group, placebo-controlled oral food challenge trial of Xolair (omalizumab) in peanut allergy. *J Allergy Clin Immunol*, **2007**. 119: p. S117.
98. Srivastava, K.D., Kattan, J.D., Zou, Z.M., *et al.*, The Chinese herbal medicine formula FAHF-2 completely blocks anaphylactic reactions in a murine model of peanut allergy. *J Allergy Clin Immunol*, **2005**. 115: p. 171-178.
99. Srivastava, K.D., Zhang, T., Qu, C., *et al.*, Silencing peanut allergy: A Chinese Herbal Formula, Fahf-2, completely blocks peanut-induced anaphylaxis for up to 6 months following therapy in a murine model of peanut allergy. *J Allergy Clin Immunol*, **2006**. 117: p. S328.
100. Srivastava, K.D., Sampson, H.A., Li, X.M., The traditional Chinese medicine formula FAHF-2 provides complete protection from anaphylaxis in a murine model of multiple food allergy. *J Allergy Clin Immunol*, **2009**. 123: p. S151.
101. Ko, J., Busse, P.J., Shek, L., Effect of Chinese herbal formulas on T-cell responses in patients with peanut allergy or asthma [abstract]. *J Allergy Clin Immunol*, **2005**. 115: p. S34.

102. Bowman, C.C., and, Selgrade, M.K., Utility of rodent models for evaluating protein allergenicity. *Regul Toxicol Pharmacol*, **2009**. 54(3): p. S58-61.
103. McClain, S., and, Bannon, G. A., Animal models of food allergy: opportunities and barriers. *Current Allergy and Asthma Reports*, **2006**. 6(2): p. 141–144.
104. Van Gramberg, J.L., de Veer, M.J., O'Hehir, R.E., *et al.*, Use of animal models to investigate major allergens associated with food allergy. *J Allergy (Cairo)*, **2013**. P. 635-695.
105. Brandt, E.B., Strait, R.T., Hershko, D., *et al.*, Mast cells are required for experimental oral allergen-induced diarrhea. *J Clin Invest*, **2003**. 112(11): p. 1666-1677.
106. Morafo, V., Srivastava, K., Huang, C. K., *et al.*, Genetic susceptibility to food allergy is linked to differential TH2-TH1 responses in C3H/HeJ and BALB/c mice. *J Allergy Clin Immunol*, **2003**. 111(5): p. 1122–1128.
107. Ganeshan, K., Neilsen, C.V., Hadsaitong, A., *et al.*, Impairing oral tolerance promotes allergy and anaphylaxis: a new murine food allergy model. *J Allergy Clin Immunol*, **2009**. 123(1): p. 231-238.
108. Finkelman, F.D., Anaphylaxis: lessons from mouse models. *J. Allergy Clin. Immunol.* **2007**. 120: p. 506–515.
109. Brandt, E.B., Munitz, A., Orekov, T., *et al.*, Targeting IL-4/IL-13 signaling to alleviate oral allergen-induced diarrhea. *J Allergy Clin Immunol*, **2009**. 123(1): p. 53-58.
110. Cardoso, C.R., Provinciatto, P.R., Godoi, D.F., *et al.*, IL-4 regulates susceptibility to intestinal inflammation in murine food allergy. *Am J Physiol Gastrointest Liver Physiol*, **2009**. 296(3): p. G593-600.
111. Knight, A.K., Blázquez, A.B., Zhang, S., *et al.*, CD4 T cells activated in the mesenteric lymph node mediate gastrointestinal food allergy in mice. *Am J Physiol Gastrointest Liver Physiol*, **2007**. 293(6): p. G1234-1243.
112. Forbes, E.E., Groschwitz, K., Abonia, J.P., *et al.*, IL-9- and mast cell-mediated intestinal permeability predisposes to oral antigen hypersensitivity. *J Exp Med*, **2008**. 205(4): p. 897-913.
113. Tsujimura, Y., Obata, K., Mukai, K., *et al.*, Basophils play a pivotal role in immunoglobulin-G-mediated but not immunoglobulin-E-mediated systemic anaphylaxis. *Immunity*, **2008**. 28(4): p. 581-589.
114. Sudo, N., Sawamura, S., Tanaka, K., *et al.*, The requirement of intestinal bacterial flora for the development of an IgE production system fully susceptible to oral tolerance induction. *J Immunol*, **1997**. 159(4): p. 1739-1745.
115. Cahenzli, J., Köller, Y., Wyss, M., *et al.*, Intestinal microbial diversity during early-life colonization shapes long-term IgE levels. *Cell Host Microbe*, **2013**. 14(5): p. 559-5570.
116. Bashir, M.E., Louie, S., Shi, H.N., *et al.*, Toll-like receptor 4 signaling by intestinal microbes influences susceptibility to food allergy. *J Immunol*, **2004**. 172(11): p. 6978-6987.
117. Berin, M.C., Zheng, Y., Domaradzki, M., *et al.*, Role of TLR4 in allergic sensitization to food proteins in mice. *Allergy*, **2006**. 61(1): p. 64-71.
118. Li, X.M., Schofield, B.H., Huang, C.K., *et al.*, A murine model of IgE-mediated cow's milk hypersensitivity. *J Allergy Clin Immunol*, **1999**. 103(2): p. 206-214.

119. Sun, J., Arias, K., Alvarez, D., *et al.*, Impact of CD40 ligand, B cells, and mast cells in peanut-induced anaphylactic responses. *J Immunol*, **2007**. 179(10): p. 6696-6703.
120. Berin, M.C., Kiliaan, A.J., Yang, P.C., *et al.*, The influence of mast cells on pathways of transepithelial antigen transport in rat intestine. *J. Immunol*, **1998**. 161, 2561–2566.
121. Perdue, M.H., Masson, S., Wershil, B.K. *et al.*, Role of mast cells in ion transport abnormalities associated with intestinal anaphylaxis. Correction of the diminished secretory response in genetically mast cell-deficient W/W<sup>v</sup> mice by bone marrow transplantation. *J. Clin. Invest*, **1991**. 87, 687–693.
122. Takayama, N., Igarashi, O., Kweon, M. N., *et al.*, Regulatory role of Peyer's patches for the inhibition of OVA-induced allergic diarrhea. *Clin. Immunol*, **2007**. 123: 199 – 208.
123. Saeki, Y., Toh-E, A., Kudo, T., *et al.*, Multiple proteasome-interacting proteins assist the assembly of the yeast 19S regulatory particle. *Cell*, **2009**. 137(5): p. 900-913.
124. Murata, S., Yashiroda, H., Tanaka, K., Molecular mechanisms of proteasome assembly. *Nat Rev Mol Cell Biol*, **2009**. 10(2): p. 104-115.
125. Saeki, Y., and Tanaka, K., Assembly and function of the proteasome. *Methods Mol Biol*, **2012**. 832: p. 315-337.
126. Xie, Y., Structure, assembly and homeostatic regulation of the 26S proteasome. *J Mol Cell Biol*, **2010**. 2(6): p. 308-317.
127. DeMartino, G.N., and Gillette, T.G., Proteasomes: Machines for All Reasons. *Cell*, **2007**. 129(4): p. 659-662.
128. Daulny, A., and Tansey, W.P., Damage control: DNA repair, transcription, and the ubiquitin-proteasome system. *DNA Repair (Amst)*, **2009**. 8(4): p. 444-448.
129. Neubert, K., Meister, S., Moser, K., *et al.*, The proteasome inhibitor bortezomib depletes plasma cells and protects mice with lupus-like disease from nephritis. *Nat Med*, **2008**. 14: p. 748-755.
130. Gomez, A.M., Willcox, N., Molenaar, P.C., *et al.*, Targeting plasma cells with proteasome inhibitors: possible roles in treating myasthenia gravis? *Ann N Y Acad Sci*, **2012**. 1274: p. 48–59.
131. Gass, J.N., Gifford, N.M., Brewer, J.W., Activation of an unfolded protein response during differentiation of antibody-secreting B cells. *J Biol Chem*, **2002**. 277(50): p. 49047-4954
132. Kim, R., Emi, M., Tanabe, K., *et al.*, Role of the unfolded protein response in cell death. *Apoptosis*, **2006**. 11(1): p. 5-13.
133. Oliva, L., and Cenci, S., Autophagy in Plasma Cell Pathophysiology. *Front Immunol*, **2014**. 5: p. 103.
134. Curran, M.P., and McKeage, K., Bortezomib: a review of its use in patients with multiple myeloma. *Drugs*, **2009**. 69: p. 859-888.
135. Blackburn, C., Gigstad, K.M., Hales, P., *et al.*, Characterization of a new series of non-covalent proteasome inhibitors with exquisite potency and selectivity for the 20S beta5-subunit. *Biochem J*, **2010**. 431(3): p. 433.

136. Mateos, M.V., and, San Miguel, J.F., Bortezomib in multiple myeloma. *Best Pract Res Clin Haematol*, **2007**. 20: p. 701-715.
137. Levêque, D., Carvalho, M.C., Maloisel, F., Review. Clinical pharmacokinetics of bortezomib. *In Vivo*, **2007**. 21(2): p. 273-278.
138. Nencioni, A., Grünebach, F., Patrone, F., *et al.*, Proteasome inhibitors: antitumor effects and beyond. *Leukemia*, **2007**. 21: p. 30–36.
139. Cenci, S., Oliva, L., Cerruti, F., *et al.*, Pivotal Advance: Protein synthesis modulates responsiveness of differentiating and malignant plasma cells to proteasome inhibitors. *J Leukoc Biol*, **2012**. 92(5): p. 921-931.
140. Cenci, S., Mezghrani, A., Cascio, P., *et al.*, Progressively impaired proteasomal capacity during terminal plasma cell differentiation. *EMBO J*, **2006**. 25(5): p. 1104-1113.
141. Lee, S.W., Kim, J.H., Park, Y.B., *et al.*, Bortezomib attenuates murine collagen-induced arthritis. *Ann Rheum Dis*, **2009**. 68: p. 1761-1767.
142. Gomez, A.M., Vrolix, K., Martínez-Martínez, P., *et al.*, Proteasome inhibition with bortezomib depletes plasma cells and autoantibodies in experimental autoimmune myasthenia gravis. *J Immunol*, **2011**. 186: p. 2503-2513.
143. Wegmann, M., Lunding, L., Orinska, Z., *et al.*, Long-term bortezomib treatment reduces allergen-specific IgE but fails to ameliorate chronic asthma in mice. *Int Arch Allergy Immunol*, **2012**. 158: p. 43-53.
144. Dahten, A., Koch, C., Ernst, D., *et al.*, Systemic PPARgamma ligation inhibits allergic immune response in the skin. *J Invest Dermatol*, **2008**. 128: p. 2211-2218.
145. Mine, Y., and, Yang, M., Epitope characterization of ovalbumin in BALB/c mice using different entry routes. *Biochim Biophys Acta*, **2007**. 1774(2): p. 200-212.
146. Kool, M., Soullie, T., van Nimwegen, M., *et al.*, Alum adjuvant boosts adaptive immunity by inducing uric acid and activating inflammatory dendritic cells. *J Exp Med*, **2008**. 205(4): p. 869-882.
147. Mudnakudu Nagaraju, K.K., Babina, M., Worm, M., Opposing effects on immune function and skin barrier regulation by the proteasome inhibitor bortezomib in an allergen-induced eczema model. *Exp Dermatol*, **2013**. 22(11): p. 742-747.
148. Li, X.M., Serebrisky, D., Lee, S.Y., *et al.*, A murine model of peanut anaphylaxis: T- and B-cell responses to a major peanut allergen mimic human responses. *J Allergy Clin Immunol*, **2000**. 106(1): p. 150-158.
149. Wang, M., Okamoto, M., Domenico, J., *et al.*, Inhibition of Pim1 kinase prevents peanut allergy by enhancing Runx3 expression and suppressing T(H)2 and T(H)17 T-cell differentiation. *J Allergy Clin Immunol*, **2012**. 130(4): p. 932-944.
150. Bradford, M.M., A rapid and sensitive method for the quantitation of microgram quantities of protein utilizing the principle of protein-dye binding. *Anal Biochem*, **1976**. 72: p. 248-254.

151. Voigt, A., Rahnefeld, A., Kloetzel, P.M., *et al.*, Cytokine-induced oxidative stress in cardiac inflammation and heart failure-how the ubiquitin proteasome system targets this vicious cycle. *Front Physiol*, **2013**. 4(42): p. 1-6.
152. Rozen, S., and, Skaletsky, H.J., Primer3 on the WWW for general users and for biologist programmers., in Krawetz S, Misener S (eds) *Bioinformatics Methods and Protocols: Methods in Molecular Biology*. Humana Press, Totowa, NJ, **2000**. p. 365-386.
153. Nolan, T., Hands, R.E., Bustin, S.A., Quantification of mRNA using real-time RT-PCR. *Nat Protocols*, **2006**. 1(3): p. 1559-1582.
154. Schmittgen, T.D. and Livak, K.J., Analyzing real-time PCR data by the comparative CT method. *Nat Protocols*, **2008**. 3(6): p. 1101-1108.
155. Pfaffl, M.W., A new mathematical model for relative quantification in real-time RT-PCR. *Nucleic Acids Res*, **2001**. 29(9): p. e45.
156. Tariq, S.M., Stevens, M., Matthews, S., Cohort study of peanut and tree nut sensitisation by age of 4 years. *BMJ*, **1996**. 313(7056): p. 514-517.
157. Hansen, K.S., Ballmer-Weber, B.K., Sastre, J., Component-resolved in vitro diagnosis of hazelnut allergy in Europe. *J Allergy Clin Immunol*, **2009**. 123(5): p. 1134-1141.
158. Worm, M., Hompes, S., Fiedler, E.M., *et al.*, Impact of native, heat-processed and encapsulated hazelnuts on the allergic response in hazelnut-allergic patients. *Clin Exp Allergy*, **2009**. 39(1): p. 159-166.
159. Luger, E.O., Fokuhl, V., Wegmann, M., *et al.*, Induction of long-lived allergen-specific plasma cells by mucosal allergen challenge. *J Allergy Clin Immunol*, **2009**. 124: p. 819-826.
160. Hennino, A., Vocanson, M., Toussaint, Y., *et al.*, Skin-infiltrating CD8+ T cells initiate atopic dermatitis lesions. *J Immunol*, **2007**. 178(9): p.5571-5577.
161. Oflazoglu, E., Simpson, E.L., Takiguchi, R., *et al.*, CD30 expression on CD1a+ and CD8+ cells in atopic dermatitis and correlation with disease severity. *Eur J Dermatol*, **2008**. 18(1): p.41-49.
162. Luger, E.O., Wegmann, M., Achatz, G., *et al.*, Allergy for a lifetime? *Allergol Int*, **2010**. 59(1): p. 1-8.
163. Radbruch, A., Muehlinghaus, G., Luger, E.O., *et al.* Competence and competition: the challenge of becoming a long-lived plasma cell. *Nat Rev Immunol*, **2006**. 6: p. 741-750.
164. Platts-Mills, T.A., Mitchell, E.B., Rowntree, S., *et al.*, The role of dust mite allergens in atopic dermatitis. *Clin Exp Dermatol*, **1983**. 8: p. 233-247.
165. King, C.L., Poindexter, R.W., Raganathan, J., *et al.*, Frequency analysis of IgE-secreting B lymphocytes in persons with normal or elevated serum IgE levels. *J Immunol*, **1991**. 146: p. 1478-1483.
166. Schmid-Grendelmeier, P., Simon, D., Simon, H.U., *et al.*, Epidemiology, clinical features, and immunology of the "intrinsic" (non-IgE-mediated) type of atopic dermatitis (constitutional dermatitis). *Allergy*, **2001**. 56: p. 841-849.

167. Sheinkopf, L.E., Rafi, A.W., Do, L.T., *et al.*, Efficacy of omalizumab in the treatment of atopic dermatitis: a pilot study. *Allergy Asthma Proc*, **2008**. 29: p. 530-537.
168. Kuehr, J., Brauburger, J., Zielen, S., *et al.*, Efficacy of combination treatment with anti-IgE plus specific immunotherapy in polysensitized children and adolescents with seasonal allergic rhinitis. *J Allergy Clin Immunol*, **2002**. 109: p. 274-280.
169. Woodward, A.L., Spregel, J.M., Alenius, H., *et al.*, An obligate role for T-cell receptor alphabeta+ T cells but not T-cell receptor gammadelta+ T cells, B cells or CD40/CD40L interactions in a mouse model of atopic dermatitis. *J Allergy Clin Immunol*, **2001**. 107: p. 359-366.
170. Gross, J.A., Dillon, S.R., Mudri, S., *et al.*, TACI-Ig neutralizes molecules critical for B cell development and autoimmune disease. impaired B cell maturation in mice lacking BLyS. *Immunity*, **2001**. 15: p. 289-302.
171. Dillon, S.R., Gross, J.A., Ansell, S.M., *et al.*, An APRIL to remember: novel TNF ligands as therapeutic targets. *Nat Rev Drug Discov*, **2006**. 5: p. 235-246.
172. Benson, M.J., Dillon, S.R., Castigli, E., *et al.*, Cutting edge: the dependence of plasma cells and independence of memory B cells on BAFF and APRIL. *J Immunol*, **2008**. 180: p. 3655-3659.
173. Bilborough, J., Chadwick, E., Mudri, S., *et al.*, TACI-Ig prevents the development of airway hyperresponsiveness in a murine model of asthma. *Clin Exp Allergy*, **2008**. 38: p. 1959-1968.
174. Matsushita, T., Fujimoto, M., Echigo, T., *et al.*, Elevated serum levels of APRIL, but not BAFF, in patients with atopic dermatitis. *Exp Dermatol*, **2008**. 17: p. 197-202.
175. Yanaba, K., Yoshizaki, A., Muroi, E., *et al.*, The proteasome inhibitor bortezomib inhibits T cell-dependent inflammatory responses. *J Leukoc Biol*, **2010**. 88: p. 117-122.
176. Babina, M., Kirn, F., Hoser, D., *et al.*, Tamoxifen counteracts the allergic immune response and improves allergen-induced dermatitis in mice. *Clin Exp Allergy*, **2010**. 40: p. 1256-1265.
177. Weise, C., Zhu, Y., Ernst, D., *et al.*, Oral administration of Escherichia coli Nissle 1917 prevents allergen-induced dermatitis in mice. *Exp Dermatol*. **2011**. 20: p. 805-809.
178. Hartmann, B., Riedel, R., Jörss, K., *et al.*, Vitamin D receptor activation improves allergen-triggered eczema in mice. *J Invest Dermatol*, **2012**. 132: p. 330-336.
179. Weise, C., Ernst, D., van Tol, E.A., *et al.*, Dietary polyunsaturated fatty acids and non-digestible oligosaccharides reduce dermatitis in mice. *Pediatr Allergy Immunol*, **2013**. 24: p. 361-367.
180. Fyhrquist, N., Lehtimäki, S., Lahl, K., *et al.*, Foxp3+ cells control Th2 responses in a murine model of atopic dermatitis. *J Invest Dermatol*, **2012**. 132: p. 1672-1680.
181. Sevilla, L.M., Nachat, R., Groot, K.R., *et al.*, Mice deficient in involucrin, envoplakin, and periplakin have a defective epidermal barrier. *J Cell Biol*, **2007**. 179(7): p. 1599-1612.
182. Hänel, K.H., Cornelissen, C., Lüscher, B., *et al.*, Cytokines and the skin barrier. *Int J Mol Sci*, **2013**. 14: p. 6720-6745.
183. Gutowska-Owsiak, D., and Ogg, G.S., Cytokine regulation of the epidermal barrier. *Clin Exp Allergy*, **2013**. 43(6): p. 586-598.

184. Hideshima, T., Richardson, P., Chauhan, D., *et al.*, The proteasome inhibitor PS-341 inhibits growth, induces apoptosis, and overcomes drug resistance in human multiple myeloma cells. *Cancer Res*, **2001**. 61(7): p. 3071-3076.
185. Davenport, E.L., Moore, H.E., Dunlop, A.S., *et al.*, Heat shock protein inhibition is associated with activation of the unfolded protein response pathway in myeloma plasma cells. *Blood*, **2007**. 110(7): p. 2641-2649.
186. Powell, B.C., Passmore, E.A., Nesci, A., *et al.*, The Notch signalling pathway in hair growth. *Mech Dev*, **1998**. 78: p. 189-192.
187. Tung, D., Cheung, P.H., Kaur, P., *et al.*, Anti-inflammatory and immunomodulatory effects of bortezomib in various in vivo models. *Pharmacology*, **2011**. 88: p. 100-113.
188. Ozcan, M.A., Alacacioglu, I., Piskin, O., *et al.*, Bortezomib-induced skin lesion. *Acta Haematol*, **2006**. 116: p. 226-227.
189. Patrizi, A., Venturi, M., Dika, E., *et al.*, Cutaneous adverse reactions linked to targeted anticancer therapies bortezomib and lenalidomide for multiple myeloma: new drugs, old side effects. *Cutan Ocul Toxicol*, **2014**. 33(1): p. 1-6.
190. Flinterman, A.E., Akkerdaas, J.H., Knulst, A.C., *et al.*, Hazelnut allergy: from pollen-associated mild allergy to severe anaphylactic reactions. *Curr Opin Allergy Clin Immunol*, **2008**. 8(3): p. 261-265.
191. de Groot, H., de Jong, N.W., Vuijk, M.H., *et al.*, Birch pollinosis and atopy caused by apple, peach, and hazelnut; comparison of three extraction procedures with two apple strains. *Allergy*, **1996**. 51(10): p. 712-718.
192. Burney, P.G., Potts, J., Kummeling, I., *et al.*, The prevalence and distribution of food sensitization in European adults. *Allergy*, **2014**. 69(3): p. 365-371.
193. Schocker, F., Lüttkopf, D., Müller, U., *et al.*, IgE binding to unique hazelnut allergens: identification of non pollen-related and heat-stable hazelnut allergens eliciting severe allergic reactions. *Eur J Nutr*, **2000**. 39(4): p. 172-180.
194. Ben-Shoshan, M., and, Clarke, A.E., Food-induced anaphylaxis: Clinical highlights and knowledge gaps. *Paediatr Child Health*. **2012**. 17(1): p. 29-30.
195. International Union of Immunological Societies Allergen Nomenclature: IUIS official list <http://www.allergen.org>. Accessed **2013** (June).
196. Garino, C., Zuidmeer, L., Marsh, J., *et al.*, Isolation, cloning, and characterization of the 2S albumin: a new allergen from hazelnut. *Mol Nutr Food Res*, **2010**. 54(9): p. 1257-1265.
197. Masthoff, L.J., Mattsson, L., Zuidmeer-Jongejan, L., *et al.*, Sensitization to Cor a 9 and Cor a 14 is highly specific for a hazelnut allergy with objective symptoms in Dutch children and adults. *J Allergy Clin Immunol*, **2013**. 132(2): p. 393-399.
198. Schocker, F., Lüttkopf, D., Scheurer, S., *et al.*, Recombinant lipid transfer protein Cor a 8 from hazelnut: a new tool for in vitro diagnosis of potentially severe hazelnut allergy. *J Allergy Clin Immunol*, **2004**. 113(1): p. 141-147.

199. Wensing, M., Koppelman, S.J., Penninks, A.H., *et al.*, Hidden hazelnut is a threat to allergic patients. *Allergy*, **2001**. 56(2): p. 191-192.
200. Hansen, K.S., Ballmer-Weber, B.K., Luttkopf, D., *et al.*, Roasted hazelnuts-allergenic activity evaluated by double-blind, placebo-controlled food challenge. *Allergy*, **2003**. 58(2): p. 132-138.
201. Wang, M., Takeda, K., Shiraishi, Y., *et al.*, Peanut-induced intestinal allergy is mediated through a mast cell-IgE-FcεRI-IL-13 pathway. *J Allergy Clin Immunol*, **2010**. 126: p. 306-316.
202. Rothenberg, M.E., Mishra, A., Collins, M.H., *et al.*, Pathogenesis and clinical features of eosinophilic esophagitis. *J Allergy Clin Immunol*, **2001**. 108(6): p. 891-894.
203. Kweon, M.N., and, Kiyono, H., Eosinophilic gastroenteritis: a problem of the mucosal immune system? *Curr Allergy Asthma Rep*, **2003**. 3(1): p. 79-85.
204. Minai-Fleminger, Y., and, Levi-Schaffer, F., Mast cells and eosinophils: the two key effector cells in allergic inflammation. *Inflamm Res*, **2009**. 58: p. 631-638.
205. Roman, S., Savarino, E., Savarino, V., *et al.*, Eosinophilic oesophagitis: from physiopathology to treatment. *Dig Liver Dis*, **2013**. 45: p. 871-878.
206. Wahn, U., Niggemann, B., Kleinau, I., *et al.*, Monitoring of inflammation during challenge tests in children. *Allergy*, **1993**. 48: p. 107-109.
207. Dainese, R., Galliani, E.A., De Lazzari, F., *et al.*, Role of serological markers of activated eosinophils in inflammatory bowel diseases. *Eur J Gastroenterol Hepatol*, **2012**. 24: p. 393-397.
208. Eller, E., and, Bindslev-Jensen, C., Clinical value of component-resolved diagnostics in peanut-allergic patients. *Allergy* **2013**. 68: p. 190-194.
209. Vieira, P., and, Rajewsky, K., The half-lives of serum immunoglobulins in adult mice. *Eur J Immunol* **1988**. 18: p. 313-316.
210. Yoshida, H., Satoh, K., Koyama, M., *et al.*, Deficiency of plasma platelet-activating factor acetylhydrolase: roles of blood cells. *Am J Hematol*, **1996**. 53: p. 158-164.
211. Gould, H.J., Sutton, B.J., Beavil, A.J., *et al.*, The biology of IGE and the basis of allergic disease. *Annu Rev Immunol*, **2003**. 21: p. 579-628.
212. Yang, P.C., Berin, M.C., Yu, L.C.H., *et al.*, Enhanced intestinal transepithelial antigen transport in allergic rats is mediated by IgE and CD23 (FcεRII). *J Clin Invest*, **2000**. 106(7): p. 879-886.
213. Yu, L.C. H., Yang, P.C., Berin, M.C., *et al.*, Enhanced transepithelial antigen transport in intestine of allergic mice is mediated by IgE/CD23 and regulated by interleukin-4. *Gastroenterology*, **2001**. 121(2) p. 370-381.
214. Yu, L.C.H., Montagnac, G., Yang, P.C., *et al.*, Intestinal epithelial CD23 mediates enhanced antigen transport in allergy: evidence for novel splice forms. *Am J Physiol*, **2003**. 285(1): p. G223-G234.
215. Bevilacqua, C., Montagnac, G., Benmerah, A., *et al.*, Food allergens are protected from degradation during CD23-mediated transepithelial transport. *Int Arch Allergy Immunol*, **2004**. 135(2): p. 108-116.

216. Lang, V.R., Mielenz, D., Neubert, K., *et al.*, The early marginal zone B cell-initiated T-independent type 2 response resists the proteasome inhibitor bortezomib. *J Immunol*, **2010**. 185: p. 5637-5647.
217. Blanco, B., Perez-Simon, J.A., Sanchez-Abarca, L.I., *et al.*, Treatment with bortezomib of human CD4+ T cells preserves natural regulatory T cells and allows the emergence of a distinct suppressor T-cell population. *Haematologica*, **2009**. 94: p. 975-983.
218. Weng, J., Lai, P., Lv, M., *et al.*, Bortezomib modulates regulatory T cell subpopulations in the process of acute graft-versus-host disease. *Clin Lab*, **2013**. 59: p. 51-58.
219. Elliott, P.J., Pien, C.S., McCormack, T.A., *et al.*, Proteasome inhibition: A novel mechanism to combat asthma. *J Allergy Clin Immunol*, **1999**. 104(2): p. 294-300.
220. Blasius, A.L., Barchet, W., Cella, M., *et al.*, Development and function of murine B220+CD11c+NK1.1+ cells identify them as a subset of NK cells. *J Exp Med*, **2007**. 204: p. 2561-2568.

## 9. ACKNOWLEDGEMENT

Words are inadequate to express deep sense of gratitude to my promoter Prof. Dr. med. M Worm, Department of Allergology and Dermatology, Charite, Berlin for her valuable advice, meticulous guidance, critical suggestions, helpful discussion and constant encouragement in bringing out this thesis work to its zenith. I would also thank cordially for providing me the financial support during my stay.

I extend my sincere thanks to Prof. Dr. rer. nat. Roderich Süßmuth, Rudolf-Wiechert-Professor für Biologische Chemie, Technische Universität Berlin, Institut für Chemie, for providing me an opportunity to pursue doctoral studies under his guidance.

I am extremely grateful to Dr. rer. nat. Magda Babina, Department of Allergology and Dermatology, Charite, Berlin, for her invaluable guidance and excellent supervision during entire course of my doctoral work and helping me in writing publication. I also take this opportunity to thank Dr. rer. nat. Christin Weise, for her support in writing publication. Further, I also thank Dr. rer. medic. Anja Kühl for histochemical stainings.

My gratitude is also extended to all my teachers, who are immense supporters in successful completion of my thesis work.

I express my sincere thanks to all the lab mates, Dr. med. Guido Heine, Dr. rer. nat. Bernhard, Dr. rer. nat. Gennadiy Drozdenko, Dr. rer. medic. Sabine Dolle, Maria Nassiri, Vandana Kumari, Juliane Lindner, Tim Hollstein, Caroline Hobe, Lauer for their co operation and support during my stay. I also thank previous lab colleagues, Dr. rer. nat. Björn Hartmann and Dr. rer. nat. Kerstin Geldmeyer-Hilt for their help in experiments.

Further I would extend my deepest thankfulness to Dennis Ernst for helping me in the animal and lab work.

I would also wish to thank my research scholars and friends, for their valuable help and enthusiastic encouragement.

Last but not the least, I am very much grateful to my beloved parents Shri. M.V. Nagaraju and Smt. Premanagaraju, brother Shri. Mahesh and eternal gratefulness to my lovely wife Smt. Lavanya Kiran for their cooperation and moral support.

Kiran Kumar M.N.

**10. PUBLICATIONS**

**Kiran Kumar Mudnakudu N**, Harish babu BN, and Venkatesh YP. Higher Histamine Sensitivity In Non-atopic Subjects By Skin Prick Test May Result in Misdiagnosis of Eggplant Allergy. *Immunological Investigations*. **2009**; 38(1): p. 93-103

**Kiran Kumar Mudnakudu N** and Saluja Rohit. Impact of Genetically Modified Food On Allergenicity. *Res. J. Biotech*. **2013**. 17: p. 1-2. (Editorial)

**Kiran Kumar Mudnakudu N**, Magda Babina and Margitta Worm. Opposing Effects On Immune Function and Skin Barrier Regulation By The Proteasome Inhibitor Bortezomib In An Allergen-Induced Eczema Model. *Exp Dermatol*. **2013**. 22: p. 742-747